UNIVERSITAT POLITÈCNICA DE VALÈNCIA

PhD Thesis

Wave overtopping and crown wall stability of cube and Cubipod-armored mound breakwaters

AUTHOR:

Jorge Molines Llodrá

SUPERVISED BY:

Dr. Josep Ramon Medina Folgado

Date: January 2016

A mi familia y amigos

Agradecimientos

Tras varios años de trabajo presento esta tesis doctoral, que no habría sido posible sin el apoyo de las personas que me rodean. Ha habido momentos fáciles y otros menos fáciles pero todos ellos forman parte de esta tesis. A todas las personas que han participado de ellos están destinadas estas líneas.

A mis padres y mi hermano: siempre conmigo al pie del cañón para tenderme una mano amiga o un comentario agradable en momentos en los que se torcían algunas cosas.

A mis amigos, con quienes en muchas ocasiones no he podido pasar todo el tiempo que desearía.

A la gran familia formada en el Laboratorio de Puertos y Costas, con quienes he compartido este largo viaje de principio a fin. Quique y Vicente, ¿aún recordáis aquél día que como buenos estudiantes íbamos preguntando por PFC y terminamos en el despacho de Josep? Ahí empezó nuestra andadura por el LPC y la época en la que íbamos en pack indivisible por la escuela y fuera de ella. Gracias Tomás y Guille por regalarme muy buenos momentos, donde una simple carcajada aliviaba la tensión de todo un día. Y por supuesto a Ainoha, Gloria y Cesar, quienes me habéis sufrido durante la última etapa de la tesis y con los que comparto mi día a día.

A Mapi, gracias por todos los ánimos y apoyo diario ininterrumpido. He recorrido contigo todo el camino y definitivamente, “juntos mola más”.

A mi director de tesis, Josep, quién me ha inculcado su pasión por la ingeniería marítima y con quién he pasado largos y buenos momentos contrastando resultados y opiniones. Junto con él, al resto de compañeros de la unidad de ingeniería marítima y a Pepe Andreu, Ana y Debra.

A mis compañeros de SATO, donde estuve poco tiempo pero compartimos muchas experiencias.

Agradezco el apoyo del Ministerio de Educación, Cultura y Deporte por la financiación brindada conforme al marco del Programa de Formación del Profesorado Universitario (AP2010-4366), que me ha permitido llevar a cabo esta tesis.

Finalmente, agradezco el apoyo del Ministerio de Ciencia e Innovación en el proyecto ESCOLIF (BIA2012-33967). También agradezco el apoyo de CDTi y SATO-OHL prestado durante el proyecto CUBIPOD.

Resumen

La influencia del tipo de elemento del manto sobre el rebase de diques en talud se caracteriza habitualmente mediante el factor de rugosidad (γ_f). Sin embargo, en la literatura existen diferentes valores del factor de rugosidad para el mismo tipo de elemento. El factor de rugosidad no depende solo del tipo de elemento, número de capas y permeabilidad del núcleo sino también de la formulación y de la base de datos empleada. En la presente tesis se desarrolla y aplica una nueva metodología basada en técnicas de *bootstrapping* para caracterizar estadísticamente el factor de rugosidad de diferentes elementos (entre ellos el Cubípodo) sobre diferentes formulaciones de rebase. Se observan diferencias de hasta el 20% entre los factores de rugosidad óptimos y los que se proporcionan en la literatura. La porosidad del manto afecta notablemente al factor de rugosidad pero también a la estabilidad del manto; mayores porosidades proporcionan menor rebase pero también menor estabilidad hidráulica. Por ello, las porosidades de diseño recomendadas deben emplearse para evitar daños durante la vida útil.

Fórmulas con pocas variables de entrada son sencillas de emplear pero absorben a través del factor de rugosidad toda la información que no se incluye explícitamente en las variables de entrada. En cambio, la red neuronal de CLASH evita en gran medida estos inconvenientes y al mismo tiempo proporciona excelentes resultados para estimar el rebase sobre diques en talud convencionales. En la presente tesis se ha desarrollado una fórmula explícita que permite emular el comportamiento de la red neuronal de CLASH. La nueva fórmula posee 16 parámetros, seis variables de entrada (R_c/H_{m0}, $\xi_{0,-1}$, R_c/h, G_c/H_{m0}, A_c/R_c y una variable para representar a la berma de pie basada en R_c/h) y dos factores de reducción (γ_f y γ_β). La nueva fórmula se construye en base a simulaciones controladas empleando la red neuronal de CLASH y proporciona el menor error en la predicción de rebase sobre diques en talud de entre los estimadores estudiados.

Una de las maneras más efectivas de disminuir el rebase sobre diques en talud es incrementar la cota de coronación mediante un espaldón de hormigón. Estas estructuras sufren el impacto del oleaje y deben ser diseñadas para resistirlo. En la presente tesis se han empleado ensayos de laboratorio de cubos y Cubípodos para desarrollar una nueva fórmula que permita calcular las fuerzas horizontales y verticales del oleaje sobre el espaldón. Las nuevas fórmulas incluyen la influencia de cuatro variables adimensionales (γ_f $R_{u0.1\%}/R_c$, $(R_c\text{-}A_c)/C_h$, $\sqrt{L_m/G_c}$ y F_c/C_h) y de la geometría del espaldón. Incluyen la influencia del tipo de elemento mediante el factor de rugosidad al igual que las fórmulas de rebase. Las fuerzas verticales disminuyen significativamente con el aumento de la cota de cimentación. Las nuevas fórmulas proporcionan el menor error de predicción sobre los registros de laboratorio analizados.

Resum

La influència del tipus d'element del mantell principal en l'ultrapassament dics en talús és caracteritza habitualment mitjançant el factor de rugositat (γ_f). En canvi, en la literatura existeixen diferents valors del factor de rugositat per al mateix tipus d'element. Així doncs, el factor de rugositat no depèn només del tipus d'element, nombre de capes i permeabilitat del nucli però també de la formulació i de la base de dades utilitzada. En la present tesi es desenvolupa i aplica una nova metodologia basada en tècniques de *bootstrapping* per a caracteritzar estadísticament el factor de rugositat de diferent elements (entre ells el Cubípode) utilitzant diferents formulacions d'ultrapassament. S'observen diferències fins al 20% entre els factors de rugositat òptims i els que apareixen en la literatura. La porositat del mantell afecta notablement el factor de rugositat però també a l'estabilitat del mantell; majors porositats proporcionen menor ultrapassament però també menor estabilitat hidràulica. Per això, les porositats de disseny recomanades deuen emprar-se per a evitar danys durant la vida útil.

Formules amb poques variables d'entrada són senzilles d'utilitzar però absorbeixen mitjançant el factor del factor de rugositat tota la informació que no s'inclou de manera explícita en les variables d'entrada. D'altra banda, la xarxa neuronal de CLASH evita en gran mesura aquests inconvenients i al mateix temps proporciona excel·lents resultats per a estimar l'ultrapassament sobre els dics en talús convencionals. En la present tesi s'ha desenvolupat una formulació explícita que permet emular el comportament de la xarxa neuronal de CLASH. La nova formulació té 16 paràmetres, sis variables d'entrada (R_c/H_{m0}, $\xi_{0,-1}$, R_c/h, G_c/H_{m0}, A_c/R_c i una variable per a representar la berma de peu basada en R_c/h) i dos factors de reducció (γ_f y γ_β). La nova fórmula es construeix mitjançant simulacions controlades amb la xarxa neuronal de CLASH i proporciona el menor error en la predicció de l'ultrapassament sobre dics en talús de entre els estimadors analitzats.

Una de les maneres més efectives de disminuir l'ultrapassament sobre dics en talús és incrementar la cota de coronació mitjançant un espatller de formigó. Aquestes estructures sofreixen l'impacte de les ones i deuen ser dissenyades per a resistir. En la present tesi, s'utilitzen assajos de laboratori de cubs i Cubípodes per a desenvolupar una nova formulació per a calcular les forces horitzontals i verticals causades per l'onatge en l'espatller. Les noves fórmules inclouen la influència de quatre variables adimensionals (γ_f $R_{u0.1\%}/R_c$, $(R_c\text{-}A_c)/C_h$, $\sqrt{L_m/G_c}$ y F_c/C_h) i de la geometria de l'espatller. Inclouen la influència del tipus d'element mitjançant el factor de rugositat al igual que les fórmules d'ultrapassament. Les forces verticals disminueixen significativament amb l'augment de la cota de cimentació. Les noves fórmules proporcionen el menor error en la predicció sobre els registres de laboratori analitzats.

Abstract

The influence of the type of armor on wave overtopping on mound breakwaters is usually represented by the roughness factor. However, different values of roughness factor for the same armor unit are given in the literature. Thus, the roughness factor depends not only on the type of armor, number of layers and permeability but also on the formula and database considered. In the present thesis, a new methodology based on bootstrapping techniques is developed and applied to characterize the roughness factors for different armor units. Differences up to 20% appeared when comparing the optimum roughness factors with those given in the literature. Armor porosity greatly affects the roughness factor and the armor stability: higher armor porosities reduce wave overtopping as well as hydraulic stability. Therefore, armor porosity values usually recommended in the literature should be used to avoid damage during lifetime.

Formulas with few variables are easy to apply but they allow the roughness factor to absorb the information not explicitly included in the formula. However, the CLASH neural network avoids this problem and gives excellent estimation for wave overtopping on mound breakwaters. In this thesis, a new formula which emulates the behavior of the CLASH neural network is developed. The new formula has 16 parameters, six dimensionless input variables (R_c/H_{m0}, $\xi_{0,-1}$, R_c/h, G_c/H_{m0}, A_c/R_c and a toe berm variable based on R_c/h) and two reduction factors (γ_f and γ_β). The new formula is built-up after systematic simulations using the CLASH neural network and provides the lowest prediction error.

Wave overtopping on mound breakwaters can be minimized by increasing the crest freeboard, usually with a concrete crown wall. Crown walls must resist wave loads and armor earth pressure to be stable. In the present study, small-scale test results with cube- and Cubipod-armored mound breakwaters are used to develop a new estimator for calculating horizontal and up-lift forces from waves. The new formulas include four dimensionless input variables (γ_f $R_{u0.1\%}/R_c$, $(R_c\text{-}A_c)/C_h$, $\sqrt{L_m/G_c}$ and F_c/C_h) and the crown wall geometry. The roughness factor selected for overtopping prediction is used to consider the type of armor. Up-lift forces decreased sharply with increasing foundation levels. The new formulas provide the lowest error when predicting wave forces on crown walls.

Table of contents

Chapter 1. Introduction

Climate change is a vital factor to keep in mind in coastal protection projects. Sea level rises associated with more severe wind and wave storms are expected to increase in the coming years. Climate change will increase the risk of flooding in low lying areas, accelerate erosion of exposed beaches and cause damage to existing coastal structures. The design of new coastal structures as well as the upgrade of existing ones must be adapted to the challenges facing coastal engineers.

The Panel on Climate Change IPCC (2013) predicted sea level rises at least in the range 0.26m-0.55m with a mean value of 0.40m by the end of the 21st century. Chini and Stansby (2012) pointed out that wave overtopping and flooding will be severely affected by rising sea levels. These authors found that mean overtopping discharge with a 100-year return period will increase up to 10 times for a sea level rise of 1m. In shallow waters, higher water levels will be associated with higher wave heights since wave breaking is less severe. Isobe (2013) analyzed the influence of increasing sea water levels and wind speeds on wave run-up, wave overtopping, armor stability and caisson stability in shallow waters. This author described a strategy to adapt coastal structures to climate change considering the sea water level and wave height at the beginning of each lifetime. Nørgaard (2013) analyzed the performance of existing structures especially in shallow waters, providing design tools for dikes and mound breakwaters. Burcharth et al. (2014) applied different solutions to upgrade a rock-armored revetment by modifying the structure profile and adding structure elements. These authors conducted a cost-effective analysis of the solutions and concluded that structures can be upgraded at moderate costs.

The performance of rubble mound breakwaters will be affected by climate change. Mound breakwaters consist in many layers of rock material usually protected by concrete armor units. Dupray and Roberts (2009) illustrated many types of armor units from simple cubes to those with specific geometries such as Dolos (see Figure 1-1). The Cubipod is an armor unit developed in the *Universitat Politècnica de València* by Professor Josep R. Medina and Doctor Esther Gómez-Martín and is used in part of this thesis.

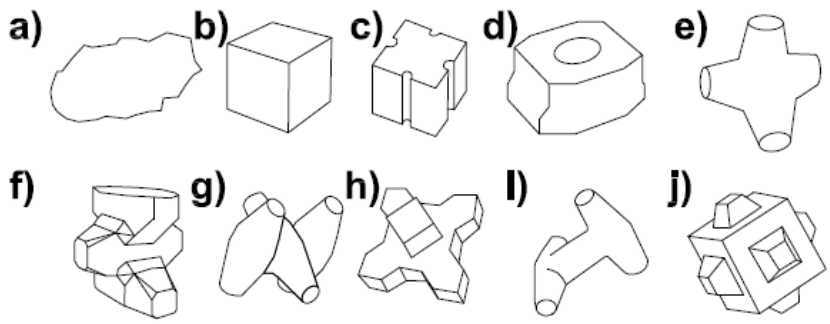

Figure 1-1. Concrete armor units: (a) rock; (b) cube; (c) Antifer; (d) Haro; (e) Tetrapod; (f) Accropode; (g) Core-loc; (h) Xbloc; (i) Dolos and (j) Cubipod.

The present thesis focuses on crown wall stability and wave overtopping on mound breakwaters. New design formulas are proposed to give better insights to how specific structural and wave variables affect crown behavior.

1.1 Focus of the study

Several formulas exist to evaluate forces on crown walls (see Nørgaard, 2013) and wave overtopping on armored mound breakwaters (see EurOtop, 2007). However, the influence of the type of armor on both phenomena is complex and only a few studies are available in the literature (see Pearson et al., 2004).

The need for guidance to understand forces on crown walls and wave overtopping on Cubipod-armored breakwaters is the motivation for the present thesis. The main objective of this thesis was to provide new design formulas that include the effect of Cubipod armors on both crown wall stability and wave overtopping in non-breaking conditions. To this end, parametric studies of the variables that may influence both phenomena were conducted using small-scale tests as well as neural network tools.

1.2 Background for the research

The present thesis is the result of a research process conducted by the author and funded through the FPU program (*Formación del Profesorado Universitario*, Grant AP2010-4366) by the Spanish *Ministerio de Educación, Cultura y Deporte*. Part of the

thesis results are based on research projects related to Cubipod-armored mound breakwaters:

- *Convenio de Colaboración entre la Sociedad Anónima Trabajos y Obras (SATO) y la Universidad Politécnica de Valencia (UPV) para la realización de Investigaciones relativas a los Ensayos Físicos Desarrollo del Cubípodo* (CUBIPOD, 2007-2009). Funded by SATO, *Sociedad Anónima Trabajos y Obras.*
- *Convenio de Colaboración entre la Sociedad Anónima Trabajos y Obras (SATO) y la Universidad Politécnica de Valencia para los Experimentos de Construcción, Estabilidad y Rebase de Mantos de Cubípodos (CUBIPOD2).* (CUBIPOD2, 2010). Funded by SATO, *Sociedad Anónima Trabajos y Obras*.

The results of the thesis have been previously published in the following:

Molines, J. and Medina, J.R., 2010. Overtopping and Wave Forces on Crown Walls of Cube and Cubipod Armoured Breakwaters, Proceedings 3rd International Conference on the Application of Physical Modelling to Port and Coastal Protection, p. 8 Paper No. 24/ structures, Barcelona (SPAIN).

Molines, J., Ripoll, E., Pardo, V., Zarranz, G. and Medina J.R., 2011. Influencia de la Porosidad del Manto Principal de Cubos y Cubípodos sobre los Caudales de Rebase, XI Jornadas Españolas de Ingeniería de Costas y Puertos (in Spanish).

Molines J., 2011. Stability of Mound Breakwater Crown Walls armoured with Cubes and Cubipods, PIANC e-Magazine On Course 143, 29-41.

The author was awarded in 2010 by the Modesto Vigueras Award given by the ATPYC (Spanish division of PIANC) for his work “Estabilidad de los espaldones de diques en talud con mantos de cubos y Cubípodos”. The publication in 2011 in the PIANC magazine summarizes that study.

Molines, J., Pérez, T.J., Zarranz, G. and Medina, J.R., 2012. Influence of cube and Cubipod armor porosities on overtopping. Proceedings 33rd International Conference on Coastal Engineering, ASCE, Paper No. 43/structures (Online).

Molines, J. and Medina, J.R., 2013. Estimación del rebase de diques en talud de cubos y Cubípodos mediante la red neuronal de CLASH. XII Jornadas Españolas de Ingeniería de Costas y Puertos (in Spanish).

Molines, J. and Medina, J.R., 2015. Calibration of overtopping roughness factors for concrete armor units in non-breaking conditions using the CLASH database, Coastal Engineering, Elsevier, 96, 62-70.

Molines, J., Argente, G., Herrera, M.P., and Medina, J.R., 2015. Overtopping prediction of cube and Cubipod armored breakwaters using the CLASH neural network. E-proceedings of the 36th IAHR World Congress.

Negro, V., López, J.S., Polvorinos, J.I., Molines, J., 2014. Discussion: Comparative study of breakwater crown wall – calculation methods, Maritime Engineering, Proceedings of the ICE, 154-155.

A paper is accepted for publication in the Journal of Waterway, Port, Coastal and Ocean Engineering:

Molines, J., and Medina, J.R., (accepted). Explicit wave overtopping formula for mound breakwaters with crown walls using CLASH neural network-derived data. Journal of Waterway, Port, Coastal and Ocean Engineering, 10.1061/(ASCE)WW.1943-5460.0000322

1.3 Thesis structure

The thesis has been structured as follows:

- Chapter 2, the literature review of wave loads on crown walls and wave overtopping on mound breakwaters.
- Chapter 3, small-scale tests used for the present thesis.
- Chapter 4, influence of rough slopes on wave overtopping of conventional mound breakwaters
- Chapter 5, new overtopping estimator on conventional mound breakwaters.
- Chapter 6, new formulas to estimate wave forces on crown walls.
- Chapter 7, conclusions and future research.
- Appendix 1 with an application example of the formulas derived within the thesis.

The terms: Cubipod®, Haro® and Xbloc® have all rights reserved. The terms: Accropode™ and Core-loc™ are trademarks. To improve readability, armor units are written without any superscript and symbols and variables are not continuously repeated in the thesis, the reader is invited to consult the notations and acronyms in case of doubt.

Chapter 2.
Literature review

This chapter contains the state-of-the-art regarding the crown wall design and wave overtopping estimation. The most relevant literature related to both issues is reported separately in this chapter.

2.1 Wave overtopping on mound breakwaters

Determining the crest freeboard of coastal structures involves cost, protection, risk and aesthetic factors. Overtopping rates are dependent on wave conditions such as wave height, wave period or angle of wave attack and structure geometry such as slope angle, crest berm width or crown wall freeboard. Figure 2-1 illustrates a common cross-section for mound breakwater that can be defined using eight structural parameters and three wave characteristics.

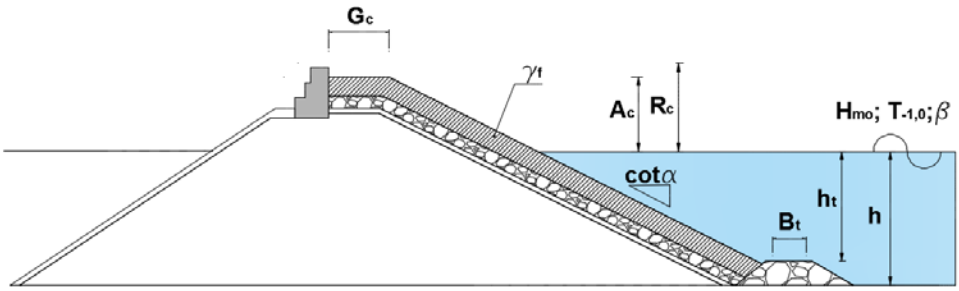

Figure 2-1. Cross-section for conventional mound breakwaters.

The design of coastal structures must ensure lower overtopping discharges than the permitted overtopping discharges due to port activities, structural stability, etc. Table 2-1 presents the tolerable values of the mean overtopping discharge given by USACE (2002), which must be taken as rough guidelines.

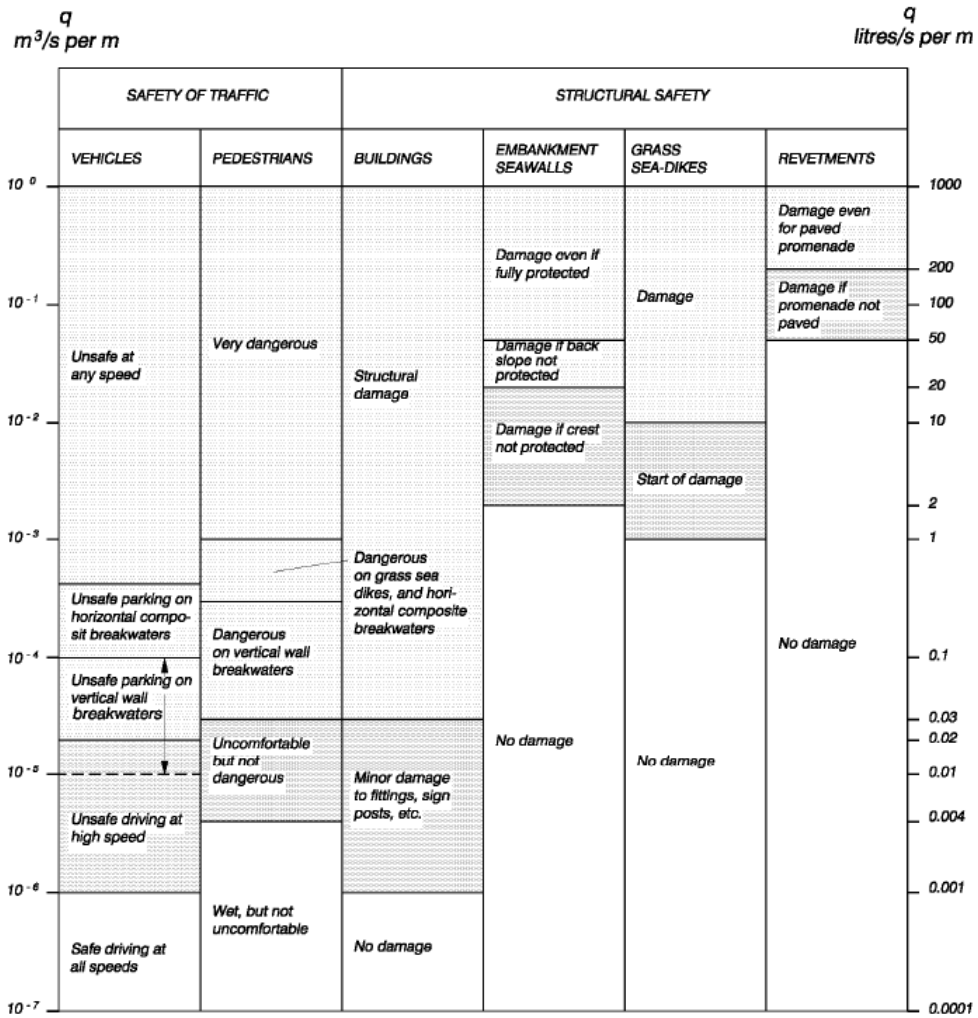

Table 2-1. Critical values for mean overtopping discharges (Source: USACE, 2002).

USACE (2002) listed the numerous overtopping formulas, dimensionless overtopping discharge and dimensionless input variables described in the literature. Mainly two types of overtopping models are used in the literature given by Eq. **2-1** and Eq. **2-2**.

Eq. 2-1 $$\boldsymbol{Q = aexp(-bR)}$$

Eq. 2-2 $$\boldsymbol{Q = a\, R^{-b}}$$

where Q is the dimensionless mean overtopping discharge per meter of structure width, R is the dimensionless crest freeboard and *a*, *b* are fitted coefficients. Overtopping estimators such as those given by Owen (1980), Ahrens and Heimbaugh (1988), and Van der Meer and Janssen (1994) used an Eq. **2-1**-type while estimators such as those given by Bradbury and Allsop (1988), Aminti and Franco (1988) and Pedersen (1996) used an Eq. **2-2**-type.

Owen (1980) conducted an extensive series of small-scale tests to evaluate wave overtopping discharges with irregular waves on seawalls. Eq. **2-3** was based on simple and bermed seawalls, the latter being comparable to embankments.

Eq. 2-3 $$\frac{q}{\sqrt{gH_s^3}}\sqrt{\frac{s_{0m}}{2\pi}} = a_{\text{Eq.2-3}}\, exp\left(-b_{\text{Eq.2-3}}\frac{R_c}{H_s}\sqrt{\frac{s_{0m}}{2\pi}}\frac{1}{\gamma_f}\right)$$

$a_{\text{Eq.2-3}}$ and $b_{\text{Eq.2-3}}$ values depend on the kind of structure (straight or bermed smooth slope) and the slope angle. Owen (1980) considered the roughness factor (γ_f) as the ratio between the run-up of a given wave on a rough slope and the run-up of the same wave on a smooth slope. This author proposed γ_f = 0.50-0.60 for rock slopes and γ_f = 1.00 for smooth slopes. For straight smooth slopes, the coefficients $a_{\text{Eq.2-3}}$, $b_{\text{Eq.2-3}}$ are given in Table 2-2 and the range of application is given in Table 2-3, respectively.

Slope	$a_{\text{Eq.2-3}}$	$b_{\text{Eq.2-3}}$
1:1	0.0079	20.12
1:1.5	0.0102	20.12
1:2	0.0125	22.06
1:2.5	0.0145	26.10
1:3	0.0163	31.90
1:3.5	0.0178	38.90
1:4	0.0192	46.96
1:4.5	0.0215	55.70
1:5	0.0250	65.20

Table 2-2. Coefficients in formula by Owen (1980) for straight slopes.

$0.05 < \frac{R_c}{H_s}\sqrt{\frac{s_{0m}}{2\pi}} < 0.30$
$10^{-6} < \frac{q}{\sqrt{gH_s^3}}\sqrt{\frac{s_{0m}}{2\pi}} < 10^{-2}$
$1.5 < h/H_s < 5.5$
$0.035 < S_{0m} < 0.055$

Table 2-3. Range of application in formula by Owen (1980) for straight slopes.

Ahrens and Heimbaugh (1988) performed overtopping tests on sloping structures and proposed an Eq. **2-1**-type estimator with $Q=q/(gH_s^3)^{0.5}$ and $R=R_c/(H_s^2L_{0p})^{1/3}$. These authors pointed out that small changes in geometry configuration can have a major influence on the overtopping rate, which confirms that care should be taken when applying the developed models to structure types with (even slightly) varying structure characteristics.

Bradbury and Allsop (1988) proposed a model, Eq. 2-4, to describe wave overtopping on rock armored sloping structures with cotα=2 and crown wall based on small-scale tests. These authors included the influence of the width and freeboard of the crest berm.

Eq. 2-4 $$\frac{q}{gH_sT_m} = a_{\text{Eq.2-4}}\left(\frac{R_c^2}{H_sT_m\sqrt{gH_s}}\right)^{-b_{\text{Eq.2-4}}}$$

where $a_{\text{Eq.2-4}}$ and $b_{\text{Eq.2-4}}$ are fitted coefficients depending on the values of G_c/H_s, G_c/R_c and A_c/R_c. The ranges of application are $0.79<G_c/H_s<3.30$, $0.58<G_c/R_c<2.14$ and $0.21<A_c/R_c<1.00$.

Aminti and Franco (1988) used Eq. **2-4** with small-scale tests to derive new coefficients $a_{\text{Eq.2-4}}$ and $b_{\text{Eq.2-4}}$ that fit for rock-, cube- and tetrapod-armored mound breakwaters. These authors tested cotα=1.33 and 2.00 and $1.10< G_c/H_s<2.60$.

Van der Meer (1993) and Van der Meer and Janssen (1994) analyzed wave run-up and wave overtopping on dikes and revetments. These authors gave recommendations on the distribution of overtopping volumes per wave, concluding that the maximum volume of overtopping by the highest wave may be a thousand times larger than the average overtopping discharge. These authors examined wave overtopping of breaking and non-breaking waves and introduced the influence of a berm, a shallow foreshore (depth-limited waves), roughness elements on the slope and obliquely incoming waves, both short-crested and long-crested. The original model given by Van der Meer (1993) has been improved subsequently (TAW, 2002) resulting in the most recent form in EurOtop (2007) for $\xi_{0,-1}<5$, see Eq. **2-5** and Eq. **2-6**.

Eq. 2-5 $$\frac{q}{\sqrt{gH_{m0}^3}} = \frac{0.067}{\sqrt{tan\alpha}}\gamma_b\,\xi_{0,-1}\,exp\left(-4.75\frac{R_c}{H_{m0}}\frac{1}{\xi_{0,-1}\,\gamma_b\gamma_\beta\gamma_f\gamma_v}\right)$$

Eq. 2-6 with a maximum of $\frac{q}{\sqrt{gH_{m0}^3}} = \mathbf{0.2}\boldsymbol{exp}\left(-\mathbf{2.6}\frac{R_c}{H_{m0}}\frac{\mathbf{1}}{\gamma_\beta\gamma_f}\right)$

where γ_b, γ_β, γ_f, and γ_v, are the reduction factors to account for an intermediate berm, oblique wave attack, roughness slope and the presence on a wall, respectively (see EurOtop, 2007). The corresponding ranges of application for the slope angle and relative crest freeboard are $1.0<\cot\alpha<4.0$ and $0.5<R_c/H_{m0}<3.5$. The reliability of Eq. **2-5** is expressed by considering a normally distributed random variable $N(4.75, 0.5^2)$. The reliability of Eq. **2-6** is expressed by considering a normally distributed random variable $N(2.6, 0.35^2)$.

Pedersen (1996) tested rock-, cube- and Dolos-armored breakwaters with irregular waves. This author concluded that wider crest berms reduced wave overtopping and also introduced the effect of the type of armor.

Eq. 2-7 $$\frac{qT_m}{L_{0m}^2} = \mathbf{3.2} * \mathbf{10^{-5}}\frac{H_s^5}{R_c^3 A_c G_c \cot\alpha} * \boldsymbol{f(armor)}$$

where f(rocks)=f(Dolos)=1 and f(cubes)=3. The ranges of application are $1.1<\xi_{0m}<5.1$, $0.5<H_s/A_c<1.7$, $1<R_c/A_c<2.6$, $0.3<A_c/G_c<1.1$ and $1.5<\cot\alpha<3.5$. The reliability of Eq. 2-7 is expressed by considering $N(3.2*10^{-5},(0.3*10^{-5})^2)$.

Hebsgaard et al. (1998) developed an overtopping formula adjusting the coefficients of the formula to obtain the best fit when using a $\gamma_f = 0.55$ for double-layer rock armors, following the γ_f recommended by other authors. Eq. 2-8 is valid for perpendicular and oblique wave attack in non-breaking waves.

Eq. 2-8 $$\frac{q}{\ln(s_{0p})\sqrt{gH_s^3}} = \boldsymbol{a}_{\text{Eq.2-8}}\boldsymbol{exp}\left(\frac{\boldsymbol{b}_{\text{Eq.2-8}}(\mathbf{2}\boldsymbol{R_c}+\mathbf{0.35}\boldsymbol{G_c})}{\boldsymbol{\gamma_f H_s}\sqrt{\boldsymbol{cos\beta}}}\right)$$

where $a_{\text{Eq.2-8}}$=-0.3 and $b_{\text{Eq.2-8}}$=-1.6 are valid for pure rubble mound structures while $a_{\text{Eq.2-8}}$=-0.01 and $b_{\text{Eq.2-8}}$=-1.0 are valid for rubble mound structures with crown walls. This formula includes the effect of the angle of wave attack. These authors proposed γ_f (Dolos, 2Layers)= 0.45, γ_f (rock, 2Layers)= γ_f (Accropode, 1Layer)= 0.55 and γ_f (Antifer, 2Layers)= 0.65.

Besley (1999) reanalyzed overtopping data to derive design techniques for seawalls. Specific tests on rock- and Accropode-armored mound breakwaters with $R_c=A_c$ were conducted to determine the influence of the crest berm width on overtopping discharges. This author proposed a correction factor to be applied on the overtopping discharges given by Eq. 2-9.

Eq. 2-9 $$\mathbf{Cr} = \boldsymbol{a}_{\text{Eq.2-9}}\boldsymbol{exp}\left(\boldsymbol{b}_{\text{Eq.2-9}}\frac{G_c}{H_s}\right)$$

with $a_{\text{Eq.2-9}}$=4.35 and $b_{\text{Eq.2-9}}$=-2.1 for Accropode armor layers and $a_{\text{Eq.2-9}}$=3.06 and $b_{\text{Eq.2-9}}$=-1.5 for rock armor layers. Besley (1999) suggested using results from the rock-

armored structure to take a conservative approach. For rock slopes, no reduction in overtopping was found if $G_c/H_s<0.75$.

The CLASH EU-Project (2001-2003) collected 10,532 wave overtopping data mainly from small-scale tests. To define one test, the CLASH database used 17 structural parameters, 11 hydraulic parameters and 3 general parameters. More detailed information can be found in the CLASH report, in for example, Van der Meer et al. (2009) and Verhaegue (2005). There were two main purposes of the database:

- The CLASH database itself is an inventory of data that can be useful to analyze specific structure types. Data can be extracted to compare with similar structures or conduct new analysis of a specific kind of structures.
- The CLASH database was used to develop a neural network prediction method for mean overtopping discharges on coastal structures, (see Van gent et al., 2007). The CLASH Neural Network (CLASH NN) is able to predict the mean overtopping discharge and the associated confidence intervals for almost any type of coastal structure. Figure 2-1 shows the 15 input parameters that the CLASH NN requires to define a case. The CLASH NN can be used to determine not only a single value but also trends to determine the influence on overtopping of changes on a specific variable. The CLASH NN is routinely used by consultants in the preliminary design stage of breakwaters and by scientists for small-scale experiments.

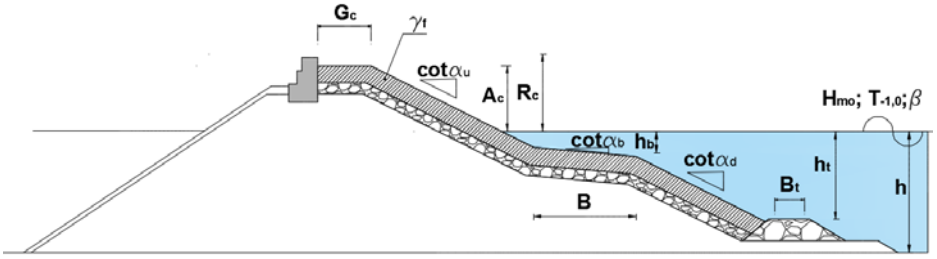

Figure 2-2. CLASH breakwater cross-section considered for the CLASH NN predictor.

Within the CLASH EU-Project, different white spots were detected indicating how additional tests could improve the generic prediction method. The CLASH team considered that the most important points to study were:

- The influence of surface roughness/permeability (see Pearson et al., 2004)
- The effect of obliqueness, short-crested waves and directional spreading (s), (see Lykke-Andersen and Burcharth, 2004).

Pearson et al. (2004) provided a set of roughness factors (γ_f) based on overtopping measurements for different armor units. Those roughness factors were calibrated considering results from a specific cross-section and using the formula given by Van der Meer and Janssen (1994). Pearson et al. (2004) factored all the initial γ_f values, the γ_f

for the smooth slope being $\gamma_f = 1.00$; as γ_f obtained from smooth slope data was $\gamma_f = 1.05$, a 5% reduction was imposed on all values. However, the CLASH NN used the γ_f given by Coeveld et al. (2005), which were different from those derived by Pearson et al. (2004). Recently, the new manual of the CLASH NN (http://nn-overtopping.deltares.nl/helppage.aspx) proposes certain changes to the roughness factors. Bruce et al. (2006) reported specific tests and results from Pearson et al. (2004) and listed γ_f for different armor units which were used in the formulas given by EurOtop (2007). Bruce et al. (2009) reexamined the tests reported by Bruce et al. (2006), proposing changes in the γ_f and calculating the confidence intervals for each γ_f by analyzing variance. Overtopping rates were measured in specific small-scale tests for mound breakwaters without a toe berm ($B_t = 0$); cotα=1:1.5; $R_c=A_c$ and $G_c=3D_n$ (where D_n is the nominal diameter).

Lykke-Andersen and Burcharth (2004) pointed out that γ_f based on run-up measurements may not be adequate to estimate overtopping rates. For rock and cube armor units, Lykke-Andersen and Burcharth (2004) analyzed the correction factor given by Besley (1999) to take into account a permeable crest berm in both Owen's (1980) and Van der Meer and Janssen's (1994) formulas. The correction factor decreased the scatter on the data in both formulas; however, the best corrected formulas required different γ_f for the same armor unit, and in both cases these were different from the roughness factors originally proposed by Owen (1980) and Van der Meer and Janssen (1994).

Table 2-4 summarizes the roughness factors given by different authors.

Type of armor 2L=double-layer 1L=single-layer	Packing density (ϕ)	Owen (1980)	Hebsgaard et al. (1998)	Coeveld et al. (2005) CLASH NN	Pearson et al. (2004) Bruce et al. (2006) EurOtop (2007)	Smolka et al. (2009)	Bruce et al. (2009)	Kortenhaus et al. (2014)	CLASH NN Manual
Smooth	-	1.00	-	1.00	1.00	-	1.00	-	1.00
Rock (2L)	1.38	0.50-0.60	0.55	0.50	0.40	-	0.40	-	0.55
Cube(2L, random)	1.17	-	-	0.50	0.47	0.50	0.47	-	0.40
Cube (2L, flat)	1.17	-	-	-	0.47	-	0.47	-	-
Cube (1L, flat)	0.70	-	-	-	0.50	-	0.49	-	-
Antifer (2L)	1.17	-	0.65	0.50	0.47	-	0.50	-	-
Haro (2L)	-	-	-	0.47	0.47	-	0.47	0.57/0.63	-
Haro (1L)	-	-	-	-	-	-	-	0.57/0.63	-
Tetrapod (2L)	1.04	-	-	0.40	0.38	-	0.38	-	0.40
Accropode (1L)	0.62	-	0.55	0.49	0.46	-	0.46	-	0.40
Core-Loc (1L)	0.56	-	-	0.47	0.44	-	0.44	-	0.40
Xbloc (1L)	0.58	-	-	0.49	0.45	-	0.44	-	-
Dolos (2L)	-	-	0.45	0.43	*0.43*	-	*0.43*	-	0.40
Cubipod (2L)	1.18	-	-	-	-	0.44	-	-	-
Cubipod (1L)	0.61	-	-	-	-	0.46	-	-	-

Table 2-4. Packing densities and roughness factors given in the literature.

Lykke-Andersen and Burcharth (2004, 2009) conducted specific tests on cube and rock armored mound breakwaters with cotα=2:1 to derive an obliquity factor (γ_β) for short-crested (s>0) and long-crested waves (1/s=0). The obliquity factor given by Eq.

2-10 valid for β<60º was created to be applied on Van der Meer and Janssen (1994) estimator for non-breaking waves (Eq. **2-6**), although Lykke-Andersen and Burcharth (2009) proposed a multiplication factor on q to correct different overtopping formulas.

Eq. 2-10

$$\gamma_\beta = 1 - 0.0077|\beta| \text{ for long-crested waves}$$
$$\gamma_\beta = 1 - 0.0058|\beta| \text{ for short-crested waves}$$

Lykke-Andersen and Burcharth (2009) reported that the CLASH NN predicted overtopping of short-crested waves very well in the entire range of obliqueness, but overpredicted overtopping of long-crested waves for β>45° (outside the range of validity of the CLASH NN).

EurOtop (2007) proposed calculating wave overtopping on armored mound breakwaters using the maximum wave overtopping given by Van der Meer and Janssen (1994) for dikes in non-breaking conditions (Eq. 2-6) together with the correction by Besley (1999) to consider the influence of a permeable crest berm (Eq. 2-9).

Smolka et al. (2009) conducted small-scale tests of Cubipod-armored mound breakwaters in non-breaking conditions which are detailed in Chapter 3. For cube- and Cubipod-armored mound breakwater, Smolka et al. (2009) proposed the following overtopping formula:

Eq. 2-11

$$\frac{q}{\sqrt{g \cdot H_{m0}^3}} = 0.2 \cdot \exp\left(0.53 \cdot \xi_{0p} - 3.27 \cdot \frac{A_c}{R_c} - 2.16 \frac{R_c}{H_{m0}} \cdot \frac{1}{\gamma_f}\right)$$

where $\xi_{0p}=\tan\alpha/[2\pi H_{m0}/gT_p^2]^{1/2}$ considering γ_f [cube, 2 Layers randomly-placed] =0.50; γ_f [Cubipod, 1 Layer] =0.46 and γ_f [Cubipod, 2 Layers] =0.44. The ranges of application are as follows: $2.7<\xi_{0p}<7.0$, $\cot\alpha=1.5$, $0.70<A_c/R_c$ [cube, 2 Layers randomly placed]<1.00, $0.40<A_c/R_c$ [Cubipod, 1 Layer]<0.65, $0.58<A_c/R_c$ [Cubipod, 2 Layers]<0.80, and $1.30<R_c/H_{m0}<2.80$.

Molines et al. (2012) studied wave overtopping on sections under construction, when the crown wall freeboard takes on relatively low values. Two formulas similar to Eq. 2-11 were proposed to estimate wave overtopping on cube- and Cubipod-armored breakwaters. The variable R_c/h was statistically significant in both formulas. Armor damage was also a relevant variable for cube-armored breakwaters. This could be understood as changes in armor porosity and the number of layers during wave attack producing variations in the armor roughness.

Victor and Troch (2012) studied wave overtopping on smooth impermeable steep slopes with low crest freeboards, with the aim of increasing the efficiency of wave energy generation. They proposed prediction formulas similar to Eq. 2-6 to consider the effects of slope angle and a small relative crest freeboard in non-breaking conditions.

Jafari and Etemad-Shahidi (2012) used the CLASH database and model tree techniques to develop prediction formulas of wave overtopping on rubble mound

structures. Model trees divide the initial complex problem into small subdomains where multiple linear regression techniques can be applied. The overtopping estimator is given by Eq. 2-12:

$$\boldsymbol{if}\ \frac{R_c}{H_s} > \mathbf{2.08}\ \boldsymbol{and}\ \frac{G_c}{H_s} > \mathbf{1.51}\boldsymbol{:}\ \frac{q}{\sqrt{gH_s^3}} = \boldsymbol{exp}\left(-\mathbf{0.6396}\frac{R_c}{H_s}\frac{1}{\gamma_\beta\gamma_f}\frac{\sqrt{s_{0p}}}{\tan\alpha} - \mathbf{0.7085}\tan\alpha - \mathbf{11.4897}\right)$$

Eq. 2-12 $$\boldsymbol{if}\ \frac{R_c}{H_s}\frac{1}{\gamma_\beta\gamma_f}\frac{\sqrt{s_{0p}}}{\tan\alpha} \le \mathbf{0.86}\boldsymbol{:}\ \frac{q}{\sqrt{gH_s^3}} = \boldsymbol{exp}\left(-\mathbf{6.18}\frac{R_c}{H_s}\frac{1}{\gamma_\beta\gamma_f}\frac{\sqrt{s_{0p}}}{\tan\alpha} - \mathbf{3.21}\right)$$

$$\boldsymbol{if}\ \frac{R_c}{H_s}\frac{1}{\gamma_\beta\gamma_f}\frac{\sqrt{s_{0p}}}{\tan\alpha} > \mathbf{0.86}\boldsymbol{:}\ \frac{q}{\sqrt{gH_s^3}} = \boldsymbol{exp}\left(-\mathbf{3.1}\frac{R_c}{H_s}\frac{1}{\gamma_\beta\gamma_f}\frac{\sqrt{s_{0p}}}{\tan\alpha} - \mathbf{6.05}\tan\alpha - \mathbf{2.63}\right)$$

These authors proposed using the values of γ_f and γ_β given by EurOtop (2007).

Van der Meer and Bruce (2014) proposed modifying the Q_{VMJ} formula to estimate overtopping on sloping structures in non-breaking conditions, valid in a wider range of application, $R_c \geq 0$:

Eq. 2-13
$$\frac{q}{\sqrt{g \cdot H_{m0}^3}} = 0.09 \cdot \exp\left(-\left(1.5 \cdot \frac{R_c}{H_{m0}} \cdot \frac{1}{\gamma_f \gamma_\beta}\right)^{1.3}\right)$$

Van der Meer and Bruce (2014) noted that Eq. 2-13 provides overtopping discharge estimations similar to Eq. **2-6**, but better estimations for low and zero crown wall freeboards (R_c/H_{m0}<0.5). The reliability of Eq. 2-13 is expressed by considering 0.09 as a normally distributed random variable N(0.09, 0.013^2) and 1.5 as N(1.5, 0.15^2).

Kortenhaus et al. (2014) tested single- and double-layer Haro armors. These authors obtained the roughness factors for single- and double-layer Haro armors which best fitted their tests using formulas given by Van der Meer and Janssen (1994) and Van der Meer and Bruce (2014). The former resulted in $\gamma_f = 0.57$ and the latter in $\gamma_f = 0.63$. Their tested model was similar to that analyzed by Pearson et al. (2004) who proposed $\gamma_f = 0.47$; Kortenhaus et al. (2014) suggested that the differences in γ_f values were due to either model or scale effects, and thus the need for a more detailed analysis.

Etemad-Shahidi and Jafari (2014) derived overtopping formulas for inclined structures with smooth impermeable surfaces using model tree techniques similar to Jafari and Etemad-Shahidi (2012). Recently, Van Doorslaer et al. (2015) analyzed the influence of crest modifications to reduce wave overtopping of non-breaking waves over a smooth dike slope, deriving several correction factors to be applied to an Eq. 2-6 type overtopping estimator.

Molines and Medina (2015) described the dependence of the roughness factor not only on the armor porosity and breakwater permeability but also on the overtopping

estimator and database. These authors developed a methodology to calibrate the roughness factors for different overtopping estimators using the CLASH database. The specific results are given in the following Chapters.

2.2 Wave loads on crown walls

Rubble mound breakwaters are usually crowned by a concrete wall to achieve a higher crest freeboard reducing the amount of granular material to be placed. Crown walls are also accessible structures which are useful for surveillance tasks, drainage and electricity pipelines, etc. and in some cases even promenades are placed in their rear part.

The crown wall behavior is very different from the armor behavior. While the armor layer is progressively damaged by wave attack, the crown wall can suddenly collapse due to large unstabilizing forces without any previous damage. Four common types of failure affecting the crown wall can be identified:

- Sliding is the most common failure mode. It happens when the horizontal force is greater than the friction resistance, which can be altered by ascending pressure. The condition to be stable is given by:

  Eq. 2-14 $(W-\Sigma Fv)\mu \geq \Sigma Fh$

  where W is the crown wall weight (buoyancy-reduced when necessary), ΣFv is the total up-lift force on the crown wall base, μ is the friction coefficient between the concrete and rock and ΣFh is the total horizontal force on the vertical wall.

- Overturning happens when the unstabilizing overturning moments are larger than the stabilizing ones. The condition to be stable is given by:

  Eq. 2-15 $M_w \geq \Sigma M_{Fh} + \Sigma M_{Fv}$

  where M_W is the stabilizing overturning moment produced by the crown wall weight (buoyancy-reduced when necessary), ΣM_{Fh} is the total antistabilizing overturning moment due to horizontal forces and ΣM_{Fv} is the total antistabilizing overturning moment due to up-lift forces.
- Cracking refers to the deterioration of the material over its lifetime.
- Geotechnical failure is caused when the load transmitted by the crown wall is higher than the load of collapse of the foundation.

Overturning and cracking can be solved by the proper design of the crown wall geometry. Geotechnical failures are related to the foundation soil rather than to the crown wall design; therefore, sliding is the most typical critical failure as pointed out by other authors such as Pedersen (1996), since it requires building the crown wall with sufficient weight. In some cases, designers should keep in mind that due to constructive process the crown wall may not be monolithic. In that case, the stability of each part of the crown wall should be ensured independently.

Forces on crown walls are the result of waves that reach sufficient run-up to hit the crown wall and even to overtop it. Therefore, crown wall stability will be closely related to the same variables that affect wave overtopping such as the crown wall freeboard, crest berm width or type of armor. Crown wall stability must consider not only wave attack but also the effect of earth armor-layer pressure. The present thesis deals with forces due to waves, only some recommendations being given for earth armor-layer pressure.

Pressure on crown walls has been modeled in the literature similarly to some of the three distributions given by Figure 2-3. Distributions change from a pure hydrostatic pressure to a pure dynamic pressure.

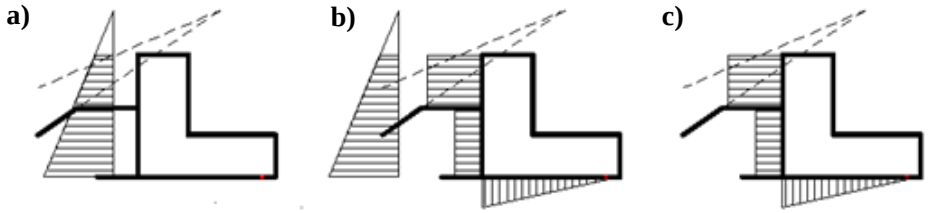

Figure 2-3. Pressure schemes by different authors.

Iribarren and Nogales (1954) proposed triangular distributions similar to Figure 2-3.a. based on the maximum horizontal crest speed after wave breaking on the slope. Jensen (1984) studied the influence of the wave height, wave period and sea water level on the maximum wave force per meter wall for 1000 waves ($Fh_{0.1\%}$). This author concluded that the influence of sea water level variations can be expressed through the crest freeboard, and that the horizontal force is directly proportional to H_s/A_c. The wave period shows a clear trend: when the period increases, the forces increase too. Eq. **2-16**.a and Eq. **2-16**.b estimate the horizontal and vertical wave force, respectively.

Eq. 2-16.a $$\boldsymbol{Fh_{0.1\%}} = \left(\boldsymbol{a}_{\text{Eq.2-16}} + \boldsymbol{b}_{\text{Eq.2-16}}\frac{\mathbf{H_s}}{\boldsymbol{A_c}}\right)\boldsymbol{\rho g C_h L_{0p}}$$

Eq. 2-16.b $$\boldsymbol{Fv_{0.1\%}} = \left(\boldsymbol{a}_{\text{Eq.2-16}} + \boldsymbol{b}_{\text{Eq.2-16}}\frac{\mathbf{H_s}}{\boldsymbol{A_c}}\right)\boldsymbol{\rho g C_b L_{0p}}\mathbf{0.5}$$

where C_h is the crown wall height, C_b is the length of the crown wall base, L_{0p} is the deepwater wavelength associated to T_p, $a_{\text{Eq.2-16}}$ and $b_{\text{Eq.2-16}}$ are fitted coefficients that depend on the slope angle, angle of wave attack, permeability and crown geometry. Jensen's formula is included in USACE (2002).

Günback and Göcke (1984) proposed a method to calculate the pressures based on run-up. They separated the action of the waves on the vertical wall into two simultaneous distributions: a hydrostatic one extended up to the end of the wedge run-up representing the mass of water that hits the wall, and a rectangular one associated with the kinetic

energy of the wave (see Figure 2-3.b.). They proposed a triangular distribution for the up-lift forces.

Bradbury and Allsop (1988) investigated the effect of the slope on the loads over the superstructure, but did not draw clear conclusions about its influence. The results agree with those reported by Jensen (1984), i.e. proportionality between force and wave height and an increase in the forces with the wave period. Bradbury and Allsop (1988) fitted their own coefficients to Eq. **2-16** with good results, but with the drawback that the coefficients are only useful for geometries very close to theirs.

Hamilton and Hall (1992) conducted a parametric research based on small-scale tests mostly under regular waves to determine crown wall stability. These authors concluded that:

- The increase in forces is directly proportional to wave height at moderate overtopping rates: from this point, the increase in forces decreases until approaching an horizontal asymptote.
- Forces increase with the period, but the authors did not provide clear conclusions.
- The gentler the slope, the lower the forces.
- Crown wall stability greatly decreases when placed on the armor layer, because there is no crest berm to dissipate wave energy.
- The use of extended legs in the crown walls increases resistance to sliding compared to crown walls without extended legs; length is not relevant.

Pedersen and Burcharth (1992) studied the influence of certain parameters on the stability of the crown wall. Their conclusions are similar to those of Hamilton and Hall (1992) and Jensen (1984):

- The higher the wave height, the higher the load on the crown wall.
- The longer the period, the greater the actions on the crown wall.
- The H_s/A_c parameter displays a clear linear dependence on the force.
- Non-conclusive results were obtained regarding the influence of the crest berm width.
- Forces on crown walls depend on the area not protected by the crest berm. When the height of the vertical wall is very high, a maximum value that depends only on the sea conditions and the sea level is reached.

Burcharth (1993) presented a formula for force calculation based on the idea of Günback and Göcke (1984) extending the wedge run-up until the imaginary prolongation of the slope is reached. For simplicity, Burcharth (1993) did not separate the force into an impulsive one and a hydrostatic one, but considered it as a fictitious hydrostatic force. Burcharth (1993) concluded that the proposed distribution does not correctly simulate pressures in the area protected by the berm, overestimating the pressures on the base of the crown wall, so that the up-lift forces yield a very conservative value (see Figure 2-3.a).

Martín et al. (1995) proposed a formula to calculate the forces in the case of regular waves. The method is applicable to those crown walls of mound breakwaters that are not affected by impact pressures, i.e. those in which the waves are broken or running up on the slope. The tested cross-section was a model of the Spanish Príncipe de Asturias breakwater in the Port of Gijón with 90 t. cubes in the core and 120 t. cubes in the armor layer, resulting in a much larger permeability than in normal rubble mound breakwaters.

The proposed model is based on the appearance in the pressures laws of two out-of-phase peaks in time. The first peak is attributed to the horizontal deceleration of the water mass, while the second one is caused by the vertical acceleration when the accumulated water descends against the structure. Martin et al. (1995) have suggested two distributions for each pressure peak: for the first one they proposed an almost rectangular distribution, whereas for the second, they presented a nearly hydrostatic distribution (see Figure 2-3.b). These authors proposed calculating the crown wall stability for both pressure peaks separately (Eq. **2**-**18**.a and Eq. **2**-**18**.b) and design the crown wall for the combination with the lowest sliding coefficient.

For the up-lift pressures Martin et al. (1995) proposed a triangular distribution according to the continuity of pressures; thus, the designed crown wall is on the safety side because supposedly the wave impact occurs at the same time both on the vertical wall and on the crown wall base.

Pedersen (1996) conducted a thorough analysis of wave overtopping and crown stability with rock-, cube- and Dolos armored breakwaters. This author reached the following conclusions:

- A linear dependency of the force with wave height existed if there was no overtopping. When overtopping began, the force tended towards an asymptotic value.
- The force was greater with longer wave periods, assuming that the force-wavelength relation is linear.
- There was a clear linear dependency between the horizontal force and $1/A_c$.
- There was a clear linear dependency between the horizontal force and $1/\cot\alpha$.
- The three types of armor units placed randomly (cubes, rocks and Dolos) showed almost identical values for the horizontal force.
- When there was no overtopping, the crown wall height had no influence on the force. However, when overtopping existed, the observed forces were proportional to the square of the crown wall height.
- The influence of the crest berm width was ambiguous. In some tests an increase in wave loads was observed when increasing the crest berm width.

Pedersen's (1996) model of pressures has two rectangular distributions: one for the zone not protected by the crest berm and the other for the protected zone (see Figure 2-3.c.). For the up-lift pressures, Pedersen (1996) proposed a triangular distribution that

satisfies the pressure continuity law. Figure 2-4 and Eq. **2-17** summarize the method used by Pedersen (1996).

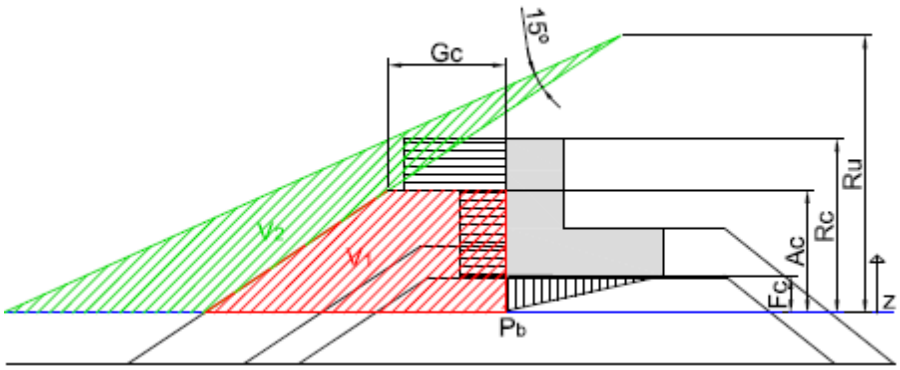

Figure 2-4. Summary of Pedersen's (1996) formula.

Eq. 2-17.a $$\boldsymbol{Fh_{0.1\%}} = \boldsymbol{a}_{\text{Eq.2-17}}\sqrt{\frac{\boldsymbol{L_{0m}}}{\boldsymbol{G_c}}}\left(\boldsymbol{p_m}\cdot\boldsymbol{y_{eff}}\cdot\boldsymbol{b}_{\text{Eq.2-17}} + \frac{\boldsymbol{p_m}}{\boldsymbol{2}}\boldsymbol{V}(\boldsymbol{A_c}-\boldsymbol{F_c})\right)$$

Eq. 2-17.b $$\boldsymbol{Mh_{0.1\%}} = \boldsymbol{c}_{\text{Eq.2-17}}\left((\boldsymbol{A_c}-\boldsymbol{F_c}) + \boldsymbol{y_{eff}}\right)\boldsymbol{Fh_{0.1\%}}$$

Eq. 2-17.c $$\boldsymbol{pb_{0.1\%}} = \boldsymbol{d}_{\text{Eq.2-17}}\boldsymbol{Vp_m}$$

Eq. 2-17.d $$p_m = g\rho_w(R_{u0.1\%} - A_c)$$

Eq. 2-17.e $$V = \begin{cases} {}^{V_2}/_{V_1} & for\ V_2 < V_1 \\ 1 & for\ V_2 \geq V_1 \end{cases}$$

Eq. 2-17.e $$y_{eff} = \min\left(0.5 * \frac{R_{u0.1\%}-A_c}{sin\alpha}\frac{sin15^{\circ}}{\cos(\alpha-15^{\circ})}; (R_c - A_c)\right)$$

Eq. 2-17.f $$\boldsymbol{R_{u0.1\%}} = \begin{cases} \boldsymbol{1.12H_s\xi_{0m}} & \boldsymbol{\xi_{0m} \leq 1.5} \\ \boldsymbol{1.34H_s\xi_{0m}^{0.55}} & \boldsymbol{\xi_{0m} \geq 1.5} \end{cases}$$ with a maximum $\frac{\boldsymbol{R_{u0.1\%}}}{\boldsymbol{H_s}} \leq \boldsymbol{2.58}$

Where $a_{\text{Eq.2-17}} = 0.21$, $b_{\text{Eq.2-17}} = 1.6$, $c_{\text{Eq.2-17}} = 0.55$, $d_{\text{Eq.2-17}} = 1.00$, $\xi_{0m} = tan\alpha/\sqrt{2\pi H_s/(gT_m{}^2)}$ and L_{0m} is the deepwater wavelength associated to T_m. Figure 2-4 illustrates all the variables to be used in Eq. 2-17. If $R_{u0.1\%} < A_c$, then a value of y_{eff}=0 should be used. The range of application of Eq. 2-17 is $1.1 < \xi_{0m} < 4.2$; $0.5 < H_s/A_c < 1.5$; $1 < R_c/A_c < 2.6$; $0.3 < A_c/G_c < 1.1$ and $1.5 < \cot\alpha 3.5$.

Silva et al. (1998) extended the methodology given by Martín et al. (1995) method to irregular waves using the statistical characterization of the run-up. Martín et al. (1999) introduced minor modifications to Martín et al. (1995), mainly in the run-up factor that

directly affects the horizontal pressures related to the dynamic response of the crown wall and in the consideration of the up-lift pressures. For the up-lift pressures, they proposed a trapezial distribution if the foundations are below the sea level, including the hydrostatic pressure corresponding to the foundation level. Figure 2-5 and Eq. **2-18** summarize the method given by Martin et al. (1995 and 1999) for a crown wall above sea water level.

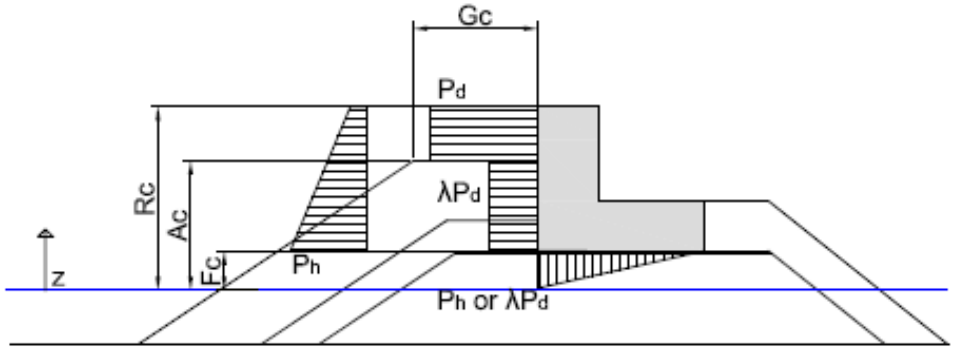

Figure 2-5. Summary of Martin et al.'s (1999) method.

Eq. 2-18.a $$P_d(z) = \begin{cases} P_{so} \;\; for\; z > A_c \\ \lambda P_{so} \;\; for\; F_c < z < A_c \end{cases}$$

Eq. 2-18.b $$P_h(z) = m\rho_w g(s_0 + A_c - z) \;\; for\; F_c < z < A_c + s_0$$

Eq. 2-18.c $$P_{s0} = r\rho_w g s_0$$

Eq. 2-18.d $$r = 2.9\left(\frac{R_u}{H}cos\alpha\right)^2$$

Eq. 2-18.e $$s_0 = H\left(1 - \frac{A_c}{R_u}\right)$$

Eq. 2-18.f $$\lambda = 0.8e^{-10.9\frac{G_c}{L}}$$

Eq. 2-18.g $$m = a_{\text{Eq.2-18}}\, e^{c_{\text{Eq.2-18}}\left(H/L - b_{\text{Eq.2-18}}\right)^2}$$

In Eq. **2-18**, L is the local wavelength, and $a_{\text{Eq.2-18}}$, $b_{\text{Eq.2-18}}$ and $c_{\text{Eq.2-18}}$ are coefficients that depend on the number of units placed on the crest berm. The wave run-up height by Martin et al. (1999) is based on the surf similarity parameter in deep water and two empirical coefficients A_u and B_u which depend on the type of armor unit.

Eq. 2-19 $$\frac{R_u}{H} = A_u\left(1 - e^{B_u\xi_0}\right) \text{ with } \xi_0 = \frac{tan\alpha}{\sqrt{2\pi H/(gT^2)}}$$

Martin et al. (1995 and 1999) suggested extending the method to irregular waves assuming the hypothesis of equivalence given by Saville (1962). They proposed

performing a zero-crossing analysis to obtain individual H and T from a synthetic surface elevation time series based on a spectrum with Hs and Tp. The breaking criterion by Miche was suggested to be applied to each individual wave in the time series. The method is applicable to waves that do not directly break on the crown wall; these authors proposed a diagram depending on A_c/H and G_c/H to evaluate the region of application.

Camus and Flores (2004) evaluated the formulas by Günback and Göcke (1984), Jensen (1984), Bradbury and Allsop (1988), Pedersen (1996) and Martín et al. (1999). They concluded that Pedersen's (1996) method was the approach that best represented the maximum horizontal forces, whereas the methodology by Martín et al. (1999) best represented the physical phenomenon of wave impact on the crown wall.

Berenguer and Baonza (2006) introduced a formula to calculate the maximum forces on the crown wall for non-breaking waves based on laboratory tests. This formula considers the influence of the foundation level on the wave loads on the crown wall. They did not propose any distribution for the horizontal pressures, only a triangular distribution for the up-lift pressures. Some blocks in the armor layer were deliberately placed in the tests with a certain position to simulate the armor damage. These authors compared the performance of this experimental formulation to 201 real Spanish breakwaters, obtaining a good agreement between the real crown wall weight and the calculated weight strictly not to slide.

if $Ru_{2\%} > R_c$:

Eq. 2-20.a $$Fx = \rho_w g C_h^{0.5} L_p^{1.5} \left(a1_{\text{Eq.2-20}} \frac{Ru_{2\%}}{A_c^{2/3} G_c^{1/3}} + b1_{\text{Eq.2-20}} \right)$$

Eq. 2-20.b $$Fy = \rho_w g C_h^{0.5} L_p^{1.5} \left(a2_{\text{Eq.2-20}} \frac{Ru_{2\%} - \mathrm{F_c}}{A_c^{2/3} G_c^{1/3}} + b2_{\text{Eq.2-20}} \right)$$

Eq. 2-20.c $$Mx = \rho_w g C_h \; L_p^2 \left(a3_{\text{Eq.2-20}} \frac{F_{\mathrm{x}}}{\rho_w g C_h^{0.5} L_p^{1.5}} + b3_{\text{Eq.2-20}} \right)$$

Eq. 2-20.d $$My = \mathrm{Fy}\left(\mathrm{C_b} - 0.018\mathrm{L_p}\right) + (\mathrm{Fyt} - \mathrm{Fy}) \left(\frac{0.046\mathrm{L_p} - 0.217\mathrm{C_b}}{0.102\mathrm{L_p} - 0.651\mathrm{C_b}} \right) \left(\mathrm{C_b} - 0.043\mathrm{L_p}\right)$$

if $Ru_{2\%} \leq R_c$;

Eq. 2-20.e $$Fx = \rho_w g (Ru_{2\%} - F_c)^{0.5} L_p^{1.5} \left(a1_{\text{Eq.2-20}} \frac{Ru_{2\%}}{A_c^{2/3} G_c^{1/3}} + b1_{\text{Eq.2-20}} \right)$$

Eq. 2-20.f $$Fy = \rho_w g (Ru_{2\%} - F_c)^{0.5} L_p^{1.5} \left(a2_{\text{Eq.2-20}} \frac{Ru_{2\%} - \mathrm{F_c}}{A_c^{2/3} G_c^{1/3}} + b2_{\text{Eq.2-20}} \right)$$

Eq. 2-20.g $$Mx = \rho_w g (Ru_{2\%} - \mathrm{F_c}) L_p^2 \left(a3_{\text{Eq.2-20}} \frac{F_{\mathrm{x}}}{\rho_w g (Ru_{2\%} - \mathrm{F_c})^{0.5} L_p^{1.5}} + b3_{\text{Eq.2-20}} \right)$$

Eq. 2-20.h $$My = \mathrm{Fy}\left(\mathrm{C_b} - 0.018\mathrm{L_p}\right) + (\mathrm{Fyt} - \mathrm{Fy}) \left(\frac{0.046\mathrm{L_p} - 0.217\mathrm{C_b}}{0.102\mathrm{L_p} - 0.651\mathrm{C_b}} \right) \left(\mathrm{C_b} - 0.043\mathrm{L_p}\right)$$

In both cases:

Eq. 2-20.i $$Fyt = \mathrm{Fy} + \left(0.017\mathrm{L_p} - 0.109\mathrm{C_b}\right)\left(\mathrm{C_b} - 0.043\mathrm{L_p}\right)$$

Eq. 2-20.j $$Ru_{2\%} = 0.86\xi_p^{0.54}H_s$$

where $a1_{\text{Eq.2-20}}$, $a2_{\text{Eq.2-20}}$, $a3_{\text{Eq.2-20}}$, $b1_{\text{Eq.2-20}}$, $b2_{\text{Eq.2-20}}$, $b3_{\text{Eq.2-20}}$ depend on the force calculation, type of armor, Iribarren number and level of damage, L_p is the local wavelength at the breakwater toe, ξ_p is Iribarren's number using L_p, *Mx* is the overturning moment caused by horizontal forces and *My* is the overturning moment caused by up-lift forces. The range of application is $2.0 < \xi_p < 8.5$, $0.7 < H_s/A_c < 1.7$, $1.0 < R_c/A_c < 3.1$, $0.4 < A_c/G_c < 1.0$, $\cot\alpha = 1.5\text{-}2.0$.

Molines (2010 and 2011) measured wave forces on crown walls and on cube and Cubipod-armored breakwaters. Test characteristics are given in Chapter 3 and data are reanalyzed and discussed in Chapter 6.

Nørgaard et al. (2012) conducted small-scale tests to evaluate the validity of simple models and Finite-Element models to calculate the displacement of monolithic rubble-mound breakwaters crown walls. These authors used the analytical one-dimensional model by Burcharth et al. (2008) for caisson breakwaters and modified it to obtain almost equal measured and estimated displacements.

Nørgaard et al. (2013) later adapted Pedersen's formula for shallow water conditions by modifying the term of wave run-up. These authors considered the results of Kobayashi et al. (2008), *i.e.* if the incident irregular wave heights are Rayleigh-distributed then the wave run-up can also be assumed to be Rayleigh distributed. Nørgaard et al. (2013) proposed using $H_{0.1\%}$ both in shallow and deep water conditions to represent the run-up exceeded by 0.1% waves on Pedersen's formula. These authors proposed calculating $R_{u0.1\%}$ given by Eq. **2-17** using $H_s/H_{0.1\%}=0.538$ given by the Rayleigh distribution rather than H_s. They also suggested that $H_{0.1\%}$ can be estimated using the distribution given by Battjes and Groenendijk (2000). These authors noticed that pressure gauges used by Pedersen (1996) could have been affected by dynamic amplifications, thus they proposed a correction to the fitted coefficient of $b_{\text{Eq.2-17}} = 1$. Nørgaard et al. (2013) also suggested the overturning moment calculation as:

Eq. 2-21 $$\boldsymbol{Mh_{0.1\%}} = \left((\boldsymbol{A_c} - \boldsymbol{F_c}) + \frac{1}{2}\boldsymbol{y_{eff}}\mathbf{0.40}\right)\boldsymbol{a}_{\text{Eq.2-17}}\sqrt{\frac{\boldsymbol{L_{0m}}}{\boldsymbol{G_c}}}\left(\boldsymbol{p_m}\cdot\boldsymbol{y_{eff}}\cdot\mathbf{1}\right)+$$

$$+\frac{\mathbf{1}}{\mathbf{2}}(\boldsymbol{A_c} - \boldsymbol{F_c})\frac{\mathbf{1}}{\mathbf{2}}\boldsymbol{a}_{\text{Eq.2-17}}\sqrt{\frac{\boldsymbol{L_{0m}}}{\boldsymbol{G_c}}}(\boldsymbol{p_m}\boldsymbol{V}(\boldsymbol{A_c} - \boldsymbol{F_c}))\mathbf{0.95}$$

The range of application of the formula given by Nørgaard et al. (2013) is listed in Table 2-5.

Rc-Ac =0	**Rc-Ac>0**
$2.3< \xi_{0m} < 4.9$	$3.31< \xi_{0m} < 4.64$
$0.5<H_s/A_c<1.63$	$0.52<H_s/A_c<1.14$
$0.78<R_c/A_c<1$	$1<R_c/A_c<1.7$
$0.58<A_c/G_c<1.21$	$0.58<A_c/G_c<1.21$
$0.19<H_{m0}/h<0.55$	$0.19<H_{m0}/h<0.55$
$0.018<H_{m0}/ L_{0m}<0.073$	$0.02<H_{m0}/ L_{0m}<0.041$

Table 2-5. Range of application of formula given by Nørgaard et al. (2013).

Avaneendran et al. (2013) analyzed the influence of KOLOS (modification of the Dolos) and derived different formulas for horizontal and uplift pressures. Negro et al. (2013) conducted a revision of the state-of-the-art of crown wall design, discussing the applicability of each formula. Different formulas were applied and discussed for the Mutriku and Barcelona breakwaters to calculate the sliding and overturning failures, obtaining a high dispersion in the results. They proposed to create a new formula based on wave energy considerations. Due to the high dispersion of results, Negro et al. (2013) recommended using more than one method during the design stage as well as physical model tests to confirm the final design. Polvorinos (2013) proposed a methodology based on real crown walls, evaluating the influence of a high number of dimensionless variables on crown wall geometry. Instead of calculating the forces, Polvorinos (2013) calculated the crown wall geometry based on wave characteristics and the freeboard obtained from overtopping calculations: A_c and R_c. Negro et al. (2014) suggested the force percentile be associated to each formula to obtain comparable results.

2.3 Specific research conducted in this thesis

Different values of the roughness factor for the same armor unit arose during the literature review, indicating that the roughness factor depends not only on the armor porosity and permeability but also on the overtopping estimator and database. For that reason, Molines and Medina (2015) developed and applied a methodology to calibrate the roughness factor for a concrete armor unit. The methodology is discussed in detail in Chapter 4 and published in Molines and Medina (2015).

Molines and Medina (2015) also highlighted the superior performance of the CLASH NN compared to other simple wave overtopping estimators. Moreover, the CLASH NN allows for the calculation of trends to determine how specific changes in variables would affect wave overtopping. For both reasons, a new empirical formula which emulates the CLASH NN behavior for mound breakwaters in non-breaking conditions was developed in Chapter 5 for the present thesis.

In this research, the results from Molines (2011) for crown stability are reanalyzed, and it was found that none of the existing models used to calculate wave loads on crown walls worked satisfactorily with his experimental data. The influence of the type of armor

on wave loads attacking the crown walls is negligible for authors such as Pedersen (1996) or introduced through fitted empirical coefficients such as Martin et al. (1999) affecting run-up or Berenguer and Baonza (2006) affecting forces. However, wave forces on crown walls are closely related to run-up and overtopping processes: in this thesis, the concept of roughness factor is taken from wave overtopping and applied to wave loads on crown walls. The influence of the foundation level on wave loads attacking the crown walls is analyzed using experimental data.

Chapter 3.
Experimental data

In coastal engineering, small-scale tests are vital to analyze the interaction wave-structure and to create new empirical/numerical models or validate existing ones. In this research, two datasets were used:

- Tests by Smolka et al. (2009) for crown wall stability and wave overtopping on Cubipod armors.
- Tests extracted from the CLASH database for wave overtopping on mound breakwaters.

This chapter describes the tests used in the following Chapters.

3.1 Crown wall stability and overtopping tests (Smolka et al., 2009)

Smolka et al. (2009) conducted small-scale tests in the wind and wave flume of the Laboratory of Ports and Coasts at the *Universitat Politècnica de València* (LPC-UPV). The size of the flume is 1.2x1.2x30m and there is a piston wave maker with AWACS system.

The tested model consisted of cube- and Cubipod-armored mound breakwaters in non-breaking conditions with a crown wall, cotα=1:1.5, G_c[Cubipod armors]=3D_n, G_c[Cube armors]=2D_n and without toe berm (B_t=0). Two water depths were tested in the model zone, 50 and 55 cm. Two crown walls were tested with 20 and 26 cm in height and 882 and 1031N/m in weight, respectively. The model was designed to avoid

significant damage to the armor layer. Three armor layers with ρ(kg/m^3)≈2.15 were tested: conventional double-layer cube armor of *Dn* (mm) = 60 with ϕ=1.26 , and single- and double-layer Cubipod armor of *Dn* (mm) = 38.2 with ϕ=0.61 and 1.18, respectively (see Figure 3-1 and Figure 3-2). Table 3-1 summarizes the material sizes. Vertically measured wave loads in small scale model tests are influenced by scale effects due to the non [illegible] turbulent flow through the model core while in pro the tests described herein, core material was slightly oversized compared to the Froude scaling (~3mm) to better represent the turbulent flow according to Burcharth et al. (1999). Recently, Wolters et al. (2014) studied wave damping and permeability scaling in rubble mound breakwaters, concluding that the core should not be larger than Froude scaling size if $D_{n50,core,Froude}$(mm)>~7 (where D_{n50} is the nominal diameter exceeded by 50 % of the material).

Core	Filter	Cube	Cubipod
D_{n50}(mm)=7	D_{n50}(mm)=17.5	D_n(mm)=60	D_n(mm)=38.2

Table 3-1. Material sizes used in model tests.

A total of 209 irregular tests of double-layer cube armors and single- and double-layer Cubipod armors were used in the present thesis.

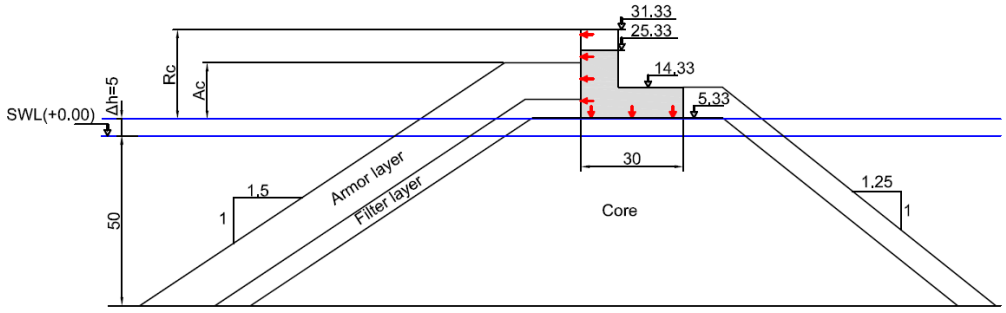

Figure 3-1. Tested cross-section. Levels in centimeters.

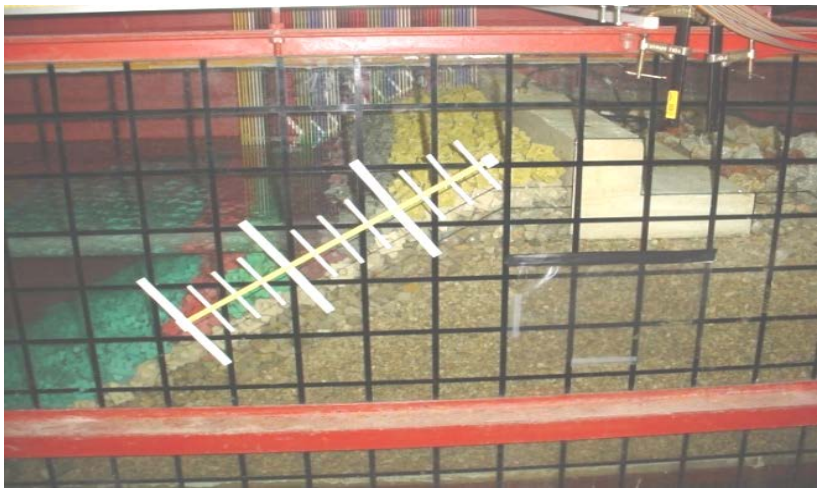

Figure 3-2. Double-layer Cubipod armor with Rc=20.33 cm.

During the tests, run-up, wave overtopping, crown wall stability and armor layer damage were analyzed. To collect the data necessary for a global analysis, the following gauges were used: 8 level sensors, 2 run-up sensors, a 10 cm rectangular pipeline ending in a scale for overtopping and 7 pressure sensors Drück PDCR 1830 (3 on the base and 4 on the vertical wall). All the gauges sampled at 20 Hz except the scale, which sampled at 5 Hz. The model was tested with regular and irregular incident waves while maintaining approximately constant the Iribarren number (ξ=2.0, 2.5, 3.0, 3.5 and 4.0) until armor damage or massive overtopping occurred. For irregular waves, Iribarren's number was calculated based on H_s at the toe and local wavelength based on mean period. Irregular waves were generated with 1000 waves following the JOSNWAP spectrum with γ=3.3, f_{min}=0.6*1/T_p and f_{max}=2.5*1/T_p.

The LASA-V method (Figueres and Medina, 2004) was applied to separate the incident and reflected waves. The LASA-V (Figueres and Medina, 2004) method was used because it provides wave separation in the time domain using an approximated model of non-linear Stokes-V waves with simulated annealing processes. To this end, wave gauges were separated in L/4 and L/8 in the generation area and in the area near the model. Figure 3-3 illustrates the cross-section of the flume during tests.

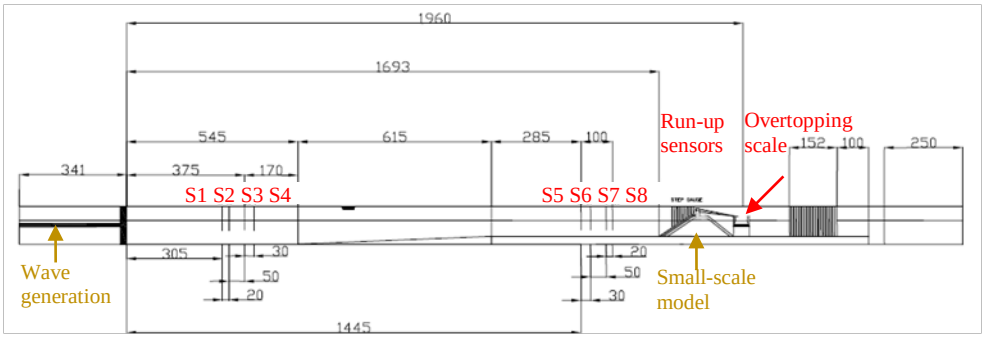

Figure 3-3. Cross-section of the wind and wave flume of the LPC-UPV. Levels in meters.

Wave loads on the crown wall were calculated assuming that each point of the crown wall takes the pressure value of the nearest pressure sensor. Figure 3-4 shows the location of the pressure sensors on the crown wall. The result is a wave force calculation based on a rectangular integration of the wave pressures.

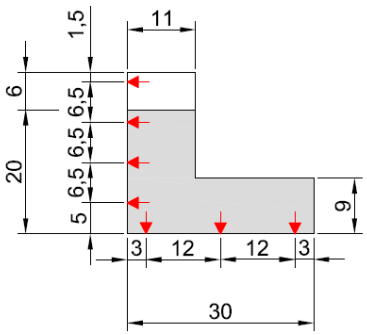

Figure 3-4. Pressure sensors placed in the crown wall. Levels in centimeters.

Pressure sensors placed in dry positions showed noise in some cases which was eliminated using running average techniques, as common procedure in time series treatments.

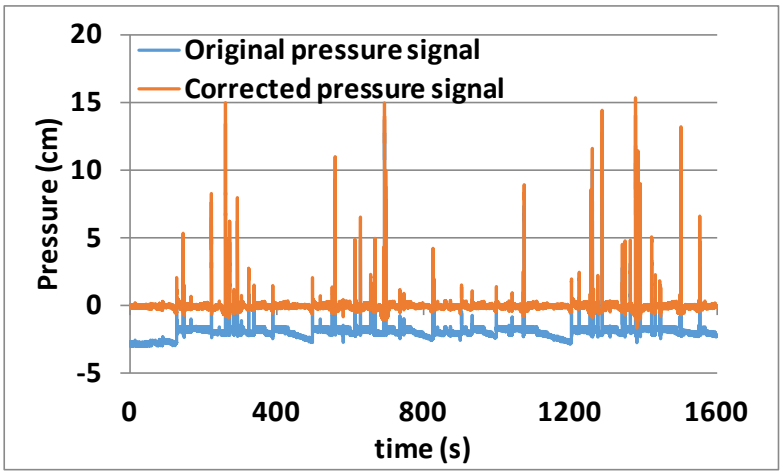

Figure 3-5. Original and corrected pressure signals.

3.2 Overtopping tests extracted from CLASH database

Two sets of data corresponding to conventional mound breakwaters were extracted from the CLASH database (http://www.clash.ugent.be/ [Accessed: December 2014]) depending if β=0 or β>0.

For perpendicular wave attack (β=0), to select the data corresponding to conventional mound breakwaters, the following data filters were applied to the CLASH database: β= 0, $\cot\alpha_d = \cot\alpha_u = \cot\alpha$, $1.19 \leq \cot\alpha \leq 4$, B = 0, $\tan\alpha_b = 0$, $h_b = 0$, RF (Reliability Factor) ≤ 2, CF (Complexity Factor) = 1, non-breaking conditions ($1.8H_{m0toe} < 0.8h$ and/or $\xi_{0p} = T_p/\cot\alpha[2\pi H_{m0toe}/g]^{0.5} > 2$ to ensure no wave breaking) and $Q \geq 10^{-6}$. Justification for these filters is given below.

The CLASH database was created to describe all kind of structures considering 11 hydraulic parameters, 17 structural parameters and 2 parameters to quantify the complexity of the cross-section (Complexity Factor, CF) and the reliability of each test (Reliability Factor, RF). Detailed information for both CF and RF is given in Van der Meer et al. (2009) and Verhaegue (2005).

The complexity factor CF ($1 \leq CF \leq 4$) gives an indication of the complexity of the overtopping structure. This factor refers to the degree of approximation which is obtained by describing a test structure using structural parameters in the database. Van der Meer et al. (2009) in page 111, described CF=1 as "simple section: the structural parameters describe the section exactly or as good as exactly". Conventional mound breakwaters considered in the present thesis consist of a toe berm, a straight slope and a top usually with a crown wall. As depicted in Figure 2-1, conventional mound breakwaters can be

described with 8 instead of 17 structural parameters used in the CLASH database (Van der Meer et al., 2009), so the complexity factor of this structures is CF=1.

The reliability factor RF ($1 \leq RF \leq 4$) indicates the reliability of the overtopping test. Van der Meer et al. (2009) described in page 110 RF=1 as "very reliable test (all needed information is available, measurements and analysis were performed in a reliable way)" and RF=2 as "reliable test (some estimations/calculations had to be made and/or some uncertainties about measurements/analysis exist, but the overall test can be classified as 'reliable')". Tests with RF=3 are "less reliable tests" and with RF=4 are "unreliable". In the present thesis, only the most reliable tests were selected: RF≤2.

EurOtop (2007) in chapter 6 reported that rubble mound structures often have steep slopes of about 1:1.5, leading to $\xi_{0p} > 2$ (non-breaking conditions) and hence, as seen in the previous section, EurOtop (2007) proposed calculating the overtopping rates using the non-breaking formula for dikes. The same considerations have been taken in the present thesis.

Furthermore, tests with remarks and/or without references were removed so as to identify singularities in the cross-section such as masonry walls on the core, which may affect wave overtopping. The CLASH database (Accessed in December, 2014 at http://www.clash.ugent.be/) identified the armor type using the values of γ_f listed by Bruce et al. (2006). For cases in which one value of γ_f identified two or more armor units, it was necessary to check the reference to correctly identify the tests corresponding to each armor unit. Test data provided by Stewart et al. (2002), corresponding to tightly packed rock armor, were removed given the divergence between the roughness factor found in the CLASH database, $\gamma_f = 0.40$, and $\gamma_f = 0.75$ proposed by Stewart et al. (2002). For smooth slopes, tests with R_c[m] = 0 were removed since they are not within the common range of conventional mound breakwaters. For Dolos, only 8 tests with references are available in the database, so all were used. After applying the filter described above, a total of 1,183 of 10,532 tests were selected from the CLASH database.

For oblique wave attack ($10 \leq \beta \leq 60$), 561 tests reported by Lykke-Andersen and Burcharth (2004, 2009) were used for this thesis since: (1) they were specifically conducted within the CLASH EU-Project to analyze the effect of oblique waves on overtopping on conventional mound breakwaters and (2) they constitute the 90% of tests with $\beta > 0$ on rough slopes in the CLASH database.

3.3 Summary of data on wave loads on crown walls

Table 3-2 specifies the characteristics of the data used to analyze wave forces on crown walls. It also specifies the applicability range of wave force estimators developed in Chapter 6.

Armor type	Datasets	No. data	H_s [m]	T_{01} [s]	R_c [m]	A_c [m]	G_c [m]	cot α	h_t [m]	h [m]	B_t [m]
Cube (2L, random)	Smolka et al. (2009)	46	0.078-0.162	0.947-2.330	0.203-0.263	0.19-0.240	0.120	1.50	0.500-0.550	0.500-0.550	0.000
Cubipod (2L)	Smolka et al. (2009)	90	0.055-0.149	0.871-2.366	0.203-0.263	0.150-0.200	0.120	1.50	0.500-0.550	0.500-0.550	0.000
Cubipod (1L)	Smolka et al. (2009)	73	0.064-0.152	0.881-2.351	0.203-0.263	0.110-0.160	0.120	1.50	0.500-0.550	0.500-0.550	0.000

Table 3-2. Wave loads on crown walls data

3.4 Summary of data on overtopping

Table 3-3 and Table 3-4 specify the characteristics of the overtopping tests extracted from the CLASH database and Smolka et al. (2009). Table 3-3 also specifies the applicability range of the roughness factors derived in this study. Table 3-3 and Table 3-4 list as well the applicability range of the overtopping estimator developed in Chapter 5. Given a specific armor unit, selecting the same dataset for all the overtopping formulas allows for the direct comparison of the results.

In the present study, CLdata refers to the 1,307 measured overtopping discharges of tests with $\beta=0^o$ given in Table 3-3 and NNdata to the 1,307 predicted overtopping discharges by the CLASH NN of tests with $\beta=0^o$.

Armor type	Datasets	No. data	H_{m0} [m]	$T_{-1,0}$ [s]	R_c [m]	A_c [m]	G_c [m]	cot α	h_t [m]	h [m]	B_t [m]
Smooth	30, 35, 42, 102, 103, 218, 220, 221, 222, 226, 227, 703	226	0.027-0.203	0.679-3.647	0.040-0.55	0.040-0.55	0.000	1.19-4.00	0.080-0.720	0.160-0.720	0.000-0.800
Rock (2L)	32, 35, 331, 510, 701, 702, 705, 954, 958	555	0.051-0.203	0.800-2.560	0.062-0.370	0.010-0.300	0.000-0.360	1.33-4.00	0.087-0.730	0.138-0.730	0.000-0.140
Cubes (2L, random)	331, 510, 702, 705	171	0.041-0.177	0.747-2.854	0.070-0.263	0.070-0.240	0.089-0.351	1.33-2.50	0.405-0.722	0.405-0.722	0.000-0.130
Cubes (2L, flat)	510	28	0.044-0.102	0.751-1.542	0.071-0.118	0.071-0.116	0.089	1.50-2.00	0.677-0.724	0.677-0.724	0.000
Cubes (1L, flat)	510	16	0.045-0.097	0.795-1.540	0.071-0.116	0.071-0.116	0.089	1.50	0.678-0.721	0.678-0.721	0.000
Antifer (2L)	379, 510	25	0.048-0.136	0.791-2.191	0.079-0.180	0.079-0.180	0.099-0.150	1.50	0.400-0.725	0.400-0.725	0.000
Haro^R (2L)	510	15	0.044-0.101	0.751-1.540	0.071-0.118	0.071-0.118	0.078-0.089	1.50	0.678-0.724	0.678-0.724	0.000
Tetrapod (2L)	331, 379, 510	86	0.079-0.136	0.952-2.191	0.081-0.024	0.081-0.180	0.105-0.351	1.33-2.00	0.400-0.731	0.400-0.731	0.000
Accropode (1L)	510	14	0.069-0.118	0.948-1.640	0.086-0.139	0.086-0.139	0.095	1.50	0.674-0.727	0.674-0.727	0.000
Core-Loc (1L)	379, 510	27	0.060-0.136	0.951-2.191	0.086-0.181	0.086-0.181	0.089-0.150	1.50	0.400-0.727	0.400-0.727	0.000
Xbloc (1L)	510	12	0.075-0.115	0.952-1.642	0.090-0.142	0.090-0.142	0.090	1.50	0.673-0.728	0.673-0.728	0.000
Dolos (2L)	702	8	0.122-0.177	1.091-2.000	0.200-0.240	0.110-0.150	0.180	2.50	0.550-0.590	0.550-0.590	0.000
Cubipod (2L)	Smolka et al. (2009)	65	0.089-0.157	1.045-2.780	0.203-0.263	0.150-0.200	0.120	1.50	0.500-0.550	0.500-0.550	0.000
Cubipod (1L)	Smolka et al. (2009)	59	0.075-0.158	0.978-2.683	0.203-0.263	0.110-0.160	0.120	1.50	0.500-0.550	0.500-0.550	0.000

Table 3-3. Overtopping data with β=0.

Armor type	Datasets	No. data	H_{m0} [m]	$T_{-1,0}$ [s]	R_c [m]	A_c [m]	G_c [m]	cot α	h_t [m]	h [m]	B_t [m]
Rock (2L)	705	312	0.052-0.1560.	0.865-1.970	0.070-0.160	0.070-0.160	0.130	2.00	0.425-0.515	0.455-0.545	0.130
Cubes (2L, random)	705	249	0.048-0.164	0.909-1.796	0.070-0.160	0.070-0.160	0.130	2.00	0.425-0.515	0.455-0.545	0.130

Table 3-4. Overtopping data with β>0.

3.5 Error calculation: relative mean squared error (rMSE)

In this thesis, the relative Mean Squared Error (*rMSE*) is used to measure the quality of the estimator "e" when applied to a group of target or observed data "o" (i=1,2,….,N). The rMSE corresponding to estimator "e" and observations "o" is given by Eq. 3-1:

Eq. 3-1

$$rMSE_e(o) = \frac{MSE_e(o)}{Var(o)} = \frac{\sum_{i=1}^{N} WF_i (e_i - o_i)^2}{\left(\sum_{i=1}^{N} WF_i\right) \cdot Var(o)}$$

where N is the total number of data; i is the data index; WF is the weight factor; e_i and o_i are the estimated and target variables using estimator "e" and target data "o". $0\%<rMSE_e(o)<100\%$ indicates the proportion of variance of the data not explained by the estimator "e". The lower the *rMSE*, the better.

For overtopping estimations (Chapter 4 and Chapter 5), e_i and o_i are the dimensionless mean overtopping discharges $logQe_i$ and $logQo_i$, respectively (with $Q=q/(gH_{m0}^3)^{1/2}$). *WF* is given in Table 3-5 from CLASH (see Van Gent et al., 2007).

RF	***WF***
1	9
2	6

Table 3-5. Weight Factor depending on the Reliability Factor.

For wave loads on the crown wall (Chapter 6), e_i and o_i are the wave loads on the crown wall Fe_i and Fo_i, respectively. F makes reference to the horizontal or up-lift force. In this case, WF=1.

Chapter 4.

Influence of rough slopes on wave overtopping

One of the structural characteristics introduced in overtopping estimators is the roughness factor (γ_f). It is accepted by the engineering community that the higher the γ_f, the higher the overtopping discharges. However, as pointed out in Chapter 2, there is no consensus as to the roughness factor value for a given armor unit. Given an overtopping estimator and the same armor unit, two authors may decide on different values for γ_f because their experimental layouts are not exactly the same and vice versa. Molines and Medina (2015) indicated that simple overtopping estimators with few variables allow the γ_f to implicitly absorb information not provided by the explanatory variables. These authors also noted that the roughness factor is not only dependent on the type of armor and permeability but also on the overtopping estimator and dataset used for calibration. In this thesis, the methodology provided by Molines and Medina (2015) to calibrate the roughness factor with data given in Table 3-3 is described.

4.1 Methodology to estimate the roughness factor

Considering a specific overtopping predictor and a given dataset, it is possible to estimate the optimum γ_f which minimizes *rMSE*. However, no information is obtained regarding the uncertainty of this γ_f. In order to overcome the uncertainty when estimating γ_f, a bootstrap resampling technique is used in this study following Van Gent et al. (2007). A bootstrap resample is a random selection of N datum taken from the N original dataset, with the probability 1/N that a particular datum is selected each time. As a result, some data are selected once or more than once, while other data may be absent in a resample.

In this research, 1000 resamples were made for each type of armor and overtopping predictor. For each resample, the γ_f was varied around the value given by Coeveld et al. (2005) and the *rMSE* was calculated for each γ_f. Thus, 1000 values for the roughness factor which minimized the *rMSE* were obtained and used to statistically characterize the γ_f to be considered for each type of armor and overtopping predictor. The γ_f was characterized by the percentiles 10% (γ_{f10}), 50% (γ_{f50}) and 90% (γ_{f90}) of the discrete histogram. The calculated-values of γ_{f10}, $\gamma_{f50}$and γ_{f90} were used in combination with data given in Table 3-3 to obtain the expected *rMSE* given in Table 4-1.

4.2 Example of application: cubes (2L, random)

Once the tests were selected from the CLASH database and the 1000 resamples were created by bootstrapping, each formula was applied to each resample to optimize the roughness factor. Figure 4-1 shows the *rMSE* corresponding to different γ_f for three specific resamples using the different overtopping estimators given in Chapter 2. Other types of armors show similar graphs; each has a different *rMSE* for a different value of γ_f.

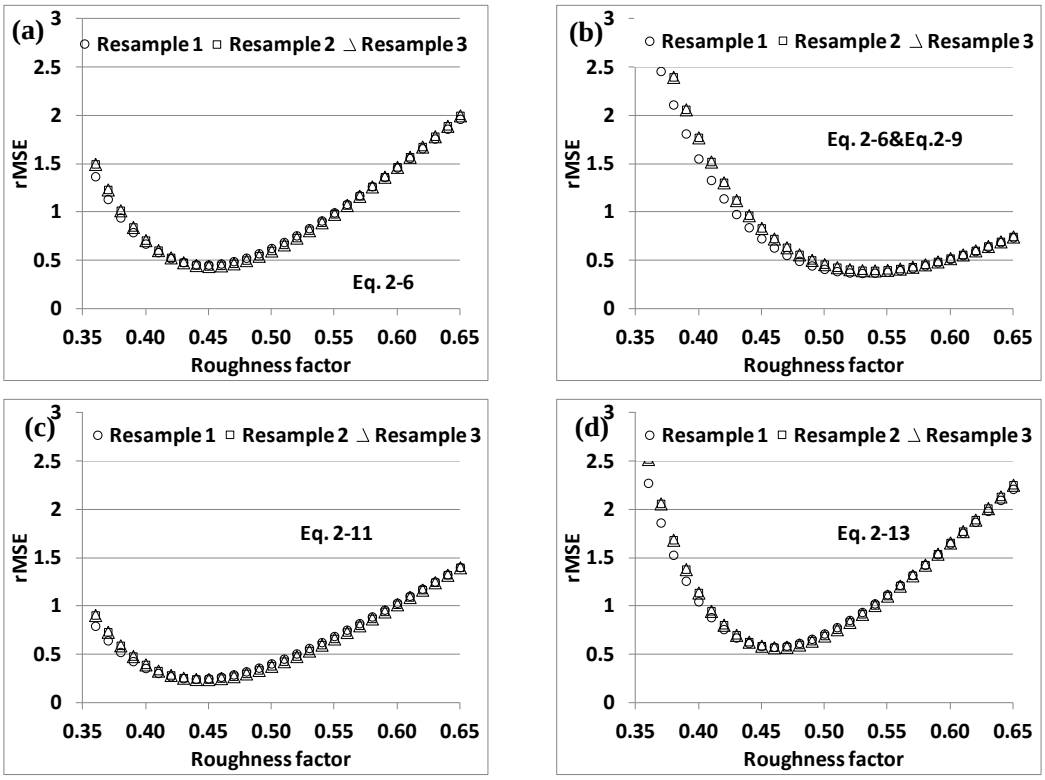

Figure 4-1. Roughness factor and rMSE for different overtopping estimators and cubes (2L, random).

Considering a specific overtopping predictor, the γ_f which minimized the *rMSE* of each resample was used to define a discrete frequency histogram (see Figure 4-2), characterized by the 10%, 50% and 90% percentiles: γ_{f10}, γ_{f50}, and γ_{f90}. In this study, the value of γ_f was obtained with two figures.

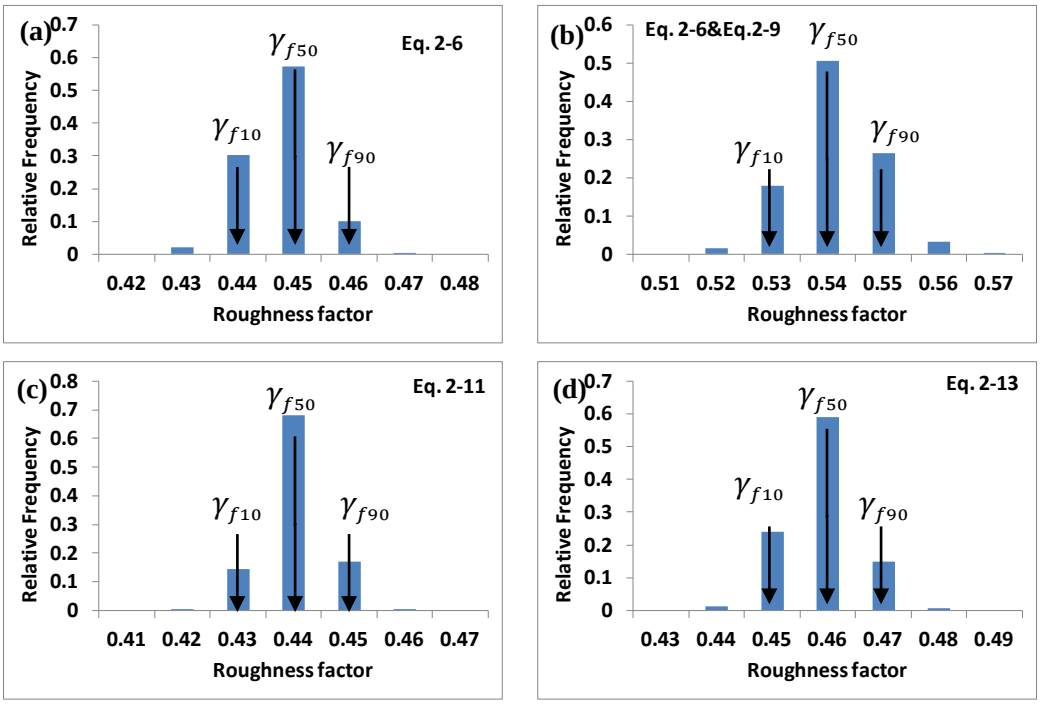

Figure 4-2. Roughness factor frequency histogram corresponding to cubes (2L random) using different overtopping estimators.

Figure 4-3 illustrates the cross-validation graph of the estimated overtopping using the γ_{f50} of each estimator in comparison to the measured overtopping.

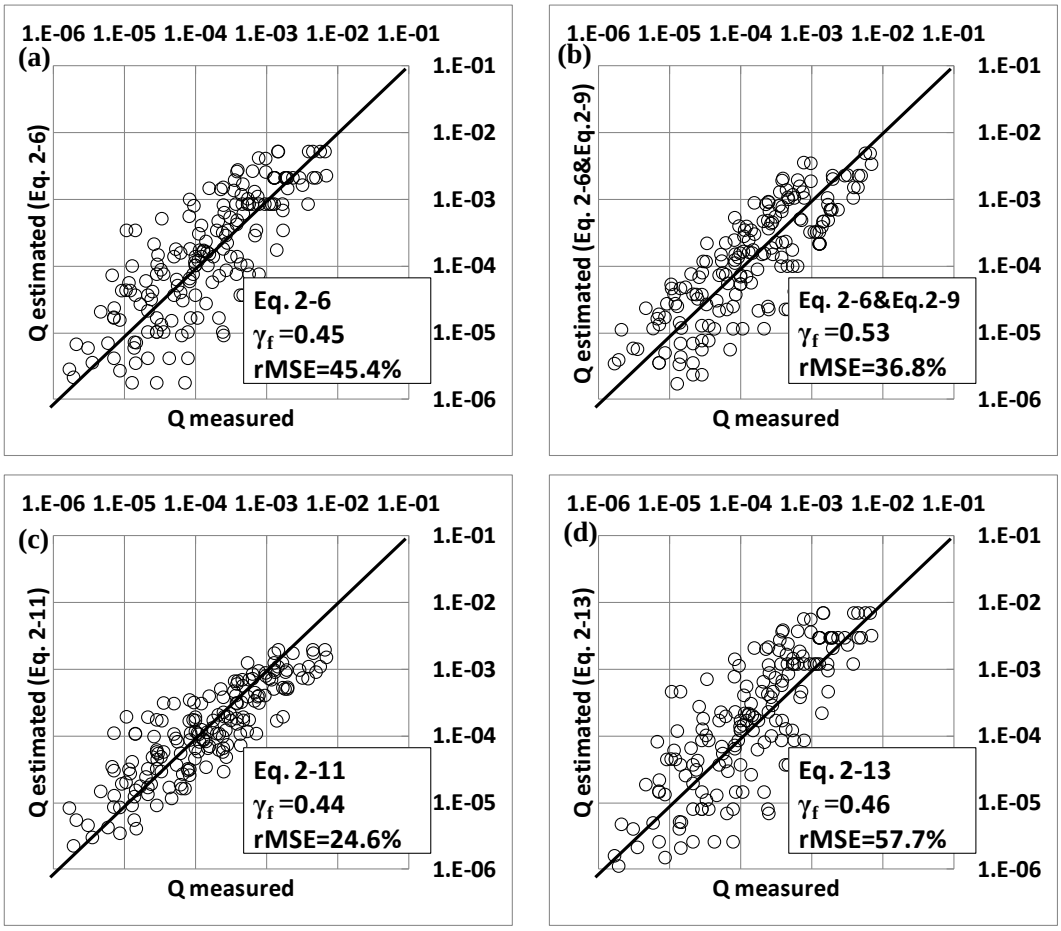

Figure 4-3. Measured versus estimated overtopping rates of cubes (2L random) using different overtopping estimators.

4.3 New calibrated roughness factors

Table 4-1 summarizes the results of γ_{f10}, γ_{f50}, and γ_{f90} as well as the associated rMSE for different armors. The CLASH NN gave the lowest rMSE for all cases except for Dolos, where a slightly lower *rMSE* for γ_{f50} was given by Smolka et al. (2009). For smooth slopes, the CLASH NN gives no prediction if γ_f>1.00 because the γ_f-value is internally limited by the CLASH NN to $0.30<\gamma_f\leq1.00$. The first column shows the roughness factors proposed by Coeveld et al. (2005) used for the CLASH NN and the roughness factors calculated by Smolka et al. (2009) for Cubipod armors. Both studies found γ_f=0.50 for cube armors (2L, random).

Table 4-1 shows the variability of the optimum roughness factor for each type of armor and formula. There is a range of roughness factors which leads to almost the same *rMSE* (see Figure 4-1) for each concrete armor unit. Therefore, the roughness factors shown in Table 4-1 may change in the future if additional tests are added to the dataset used for calibration.

The selected overtopping formulas clearly improved their prediction when increasing the number of variables, except Eq. 2-13 which gives less accurate predictions than Eq. **2-6** in most cases. One should take into consideration that selected CLASH tests for calibration (see Table 3-3) have $0.5<R_c/H_{m0}<3.5$; therefore, using Eq. 2-13 does not take advantage of its better performance for zero and low crest freeboard cases.

The CLASH NN shows the minimum *rMSE* and avoids the influence of certain structural variables on the estimation of the roughness factor. Thus, the CLASH NN is recommended to compare the influence of a given type of armor on overtopping discharges with different cross sections. Simple formulas such as those given by EurOtop (2007) can be applied considering the wave conditions and structural geometry which were used to obtain the roughness factors.

The armor placement did not significantly influence the overtopping discharges on cube armors. This result is consistent with the conclusions drawn by Bruce et al. (2009), and may change in the future when increasing the number of data for 2L-flat cubes (28 in this study) to be compared with the 171 tests of 2L-random cubes. Cubes and Cubipods were analyzed in single- and double- layer armors. In both cases, the single-layer system presented higher roughness factors, and hence higher overtopping discharges are expected.

Only eight tests using Dolos conducted by Pedersen (1996) were selected from CLASH database ($\cot\alpha=2.5$) with small overtopping discharges. Thus, variations in the roughness factors for Dolos listed in Table 4-1 are expected when more overtopping data are included.

Single- and double-layer Cubipod armors were tested with $A_c/R_c<1$; therefore, Eq. **2-6**, Eq. **2-6** with Eq. 2-9 and Eq. 2-13 which do not include A_c as an input variable give unrealistic values of γ_f for Cubipod armors compared to those given by the CLASH NN and Eq. 2-11, which includes A_c/R_c as an input variable. Thus, the formula in Smolka et al. (2009) or the CLASH NN are recommended to properly estimate wave overtopping on Cubipod armored breakwaters.

Armor type		Overtopping estimator									
		CLASH NN		Q_{VMJ} (1994)		$Q_{EurOtop}$(2007)		Q_{SZM}(2009)		Q_{VMB} (2014)	
Coeveld et al. (2005) Smolka et al. (2009)		(2007)		Eq. 2-6		Eq. 2-6&Eq. 2-9		Eq. 2-11		Eq. 2-13	
γ_f	γ_{fx}	γ_f	rMSE	γ_f	rMSE	γ_f	rMSE	γ_f	rMSE	γ_f	rMSE
Smooth	γ_{f10}	0.99	*5.0*	1.02	*11.1*	1.02	*11.1*	1.18	*16.9*	1.00	*9.9*
	$\boldsymbol{\gamma_{f50}}$	**1.00**	***4.9***	**1.03**	***11.1***	**1.03**	***11.1***	**1.21**	***16.8***	**1.01**	***9.8***
1.00	γ_{f90}	1.00	-	1.05	*11.2*	1.05	*11.2*	1.24	*16.9*	1.03	*9.9*
Rock (2L)	γ_{f10}	0.48	*14.6*	0.45	*59.5*	0.52	*51.9*	0.43	*32.8*	0.46	*80.8*
	$\boldsymbol{\gamma_{f50}}$	**0.49**	***14.4***	**0.45**	***59.5***	**0.53**	***51.5***	**0.44**	***32.6***	**0.47**	***79.9***
0.50	γ_{f90}	0.50	*14.6*	0.46	*59.9*	0.54	*51.8*	0.44	*32.6*	0.48	*80.9*
Cube (2L,	γ_{f10}	0.52	*10.2*	0.44	*45.8*	0.52	*37.3*	0.43	*25.2*	0.45	*58.5*
	$\boldsymbol{\gamma_{f50}}$	**0.53**	***10.0***	**0.45**	***45.4***	**0.53**	***36.8***	**0.44**	***24.6***	**0.46**	***57.7***
random)	γ_{f90}	0.53	*10.0*	0.46	*46.6*	0.54	*37.0*	0.45	*25.1*	0.47	*58.8*
Cube (2L, flat)	γ_{f10}	0.52	*7.5*	0.46	*29.5*	0.52	*17.5*	0.49	*24.0*	0.46	*36.1*
	$\boldsymbol{\gamma_{f50}}$	**0.53**	**6.9**	**0.48**	***27.4***	**0.53**	***16.8***	**0.51**	***22.6***	**0.48**	***32.3***
-	γ_{f90}	0.54	7.1	0.50	*29.6*	0.55	*17.5*	0.53	*23.5*	0.50	*34.3*
Cube (1L, flat)	γ_{f10}	0.53	*3.3*	0.49	*15.2*	0.56	*10.3*	0.50	*12.0*	0.50	*20.8*
	$\boldsymbol{\gamma_{f50}}$	**0.54**	***3.1***	**0.52**	***12.7***	**0.59**	***8.2***	**0.53**	***10.8***	**0.53**	***16.9***
-	γ_{f90}	0.55	*3.3*	0.54	*14.0*	0.62	*9.2*	0.55	*11.8*	0.56	*19.7*
Antifer (2L)	γ_{f10}	0.51	*9.8*	0.48	*34.3*	0.54	*25.9*	0.48	*33.6*	0.48	*38.9*
	$\boldsymbol{\gamma_{f50}}$	**0.52**	***9.3***	**0.50**	***32.2***	**0.57**	***23.7***	**0.51**	***31.6***	**0.50**	***35.8***
0.50	γ_{f90}	0.53	*9.9*	0.52	*33.9*	0.59	*25.1*	0.54	*34.8*	0.52	*37.5*
Haro (2L)	γ_{f10}	0.51	*2.4*	0.47	*19.6*	0.52	*8.5*	0.48	*18.6*	0.47	*21.3*
	$\boldsymbol{\gamma_{f50}}$	**0.52**	***2.3***	**0.49**	***17.6***	**0.54**	***7.8***	**0.50**	***17.4***	**0.49**	***17.9***
0.47	γ_{f90}	0.53	*2.9*	0.52	*20.7*	0.56	*9.3*	0.53	*19.5*	0.52	*21.3*

Continue next page

Armor type		Overtopping estimator									
Coeveld et al. (2005) Smolka et al. (2009)		*CLASH NN* (2007)		Q_{VMJ} (1994) Eq. 2-6		$Q_{EurOtop}$(2007) Eq. 2-6&Eq. 2-9		Q_{SZM}(2009) Eq. 2-11		Q_{VMB} (2014) Eq. 2-13	
γ_f	γ_{fx}	γ_f	rMSE	γ_f	rMSE	γ_f	rMSE	γ_f	rMSE	γ_f	rMSE
Tetrapod (2L)	γ_{f10}	0.41	*17.7*	0.42	*28.8*	0.50	*30.1*	0.38	*25.8*	0.43	*37.7*
	$\boldsymbol{\gamma_{f50}}$	**0.42**	***17.5***	**0.43**	***28.5***	**0.52**	***29.2***	**0.39**	***24.9***	**0.43**	***37.7***
0.40	γ_{f90}	0.43	*17.6*	0.43	*28.5*	0.53	*29.8*	0.40	*25.5*	0.44	*37.7*
Accropode (1L)	γ_{f10}	0.47	*3.9*	0.46	*15.5*	0.50	*10.1*	0.48	*9.9*	0.47	*19.7*
	$\boldsymbol{\gamma_{f50}}$	**0.48**	***3.7***	**0.48**	***13.0***	**0.51**	***9.2***	**0.49**	***9.4***	**0.49**	***16.9***
0.49	γ_{f90}	0.49	*4.7*	0.50	*14.8*	0.53	*10.1*	0.51	*10.4*	0.50	*17.7*
Core-Loc (1L)	γ_{f10}	0.45	*6.1*	0.44	*23.9*	0.48	*18.4*	0.44	*20.7*	0.45	*24.4*
	$\boldsymbol{\gamma_{f50}}$	**0.46**	***6.0***	**0.46**	***22.2***	**0.49**	***17.8***	**0.46**	***19.6***	**0.46**	***23.2***
0.47	γ_{f90}	0.47	*7.1*	0.47	*23.0*	0.51	*19.1*	0.48	*21.4*	0.48	*25.2*
Xbloc (1L)	γ_{f10}	0.49	*10.6*	0.44	*44.0*	0.46	*33.5*	0.46	*26.7*	0.44	*54.0*
	$\boldsymbol{\gamma_{f50}}$	**0.51**	***8.6***	**0.47**	***37.7***	**0.49**	***27.9***	**0.48**	***24.5***	**0.47**	***44.3***
0.49	γ_{f90}	0.52	*10.1*	0.49	*41.2*	0.51	*30.8*	0.51	*27.7*	0.49	*48.3*
Dolos (2L)	γ_{f10}	0.31	*22.3*	0.39	*37.9*	0.42	*39.4*	0.35	*28.0*	0.41	*33.3*
	$\boldsymbol{\gamma_{f50}}$	**0.32**	***22.3***	**0.41**	***30.0***	**0.45**	***31.8***	**0.37**	***22.0***	**0.43**	***29.1***
0.43	γ_{f90}	0.43	*26.0*	0.43	*35.0*	0.47	*38.0*	0.38	*24.2*	0.44	*33.0*
Cubipod (2L)	γ_{f10}	0.44	*18.5*	0.54	*47.7*	0.56	*46.3*	0.45	*23.7*	0.56	*53.5*
	$\boldsymbol{\gamma_{f50}}$	**0.45**	***18.1***	**0.55**	***46.8***	**0.57**	***44.7***	**0.45**	***23.7***	**0.57**	***5***
0.44	γ_{f90}	0.46	*18.3*	0.56	*47.7*	0.59	*46.1*	0.46	*23.8*	0.58	*54.1*
Cubipod (1L)	γ_{f10}	0.47	*15.0*	0.57	*33.4*	0.60	*32.6*	0.45	*18.2*	0.60	*40.4*
	$\boldsymbol{\gamma_{f50}}$	**0.48**	***14.8***	**0.58**	***32.4***	**0.61**	***31.4***	**0.46**	***16.8***	**0.61**	***40.3***
0.46	γ_{f90}	0.50	*15.5*	0.59	*33.2*	0.63	*33.2*	0.47	*18.4*	0.62	*42.3*

Table 4-1. Roughess factors and rMSE (%).

4.4 Influence of packing density and armor roughness on overtopping

None of the overtopping formulas given in the literature explicitly introduces armor porosity or packing density as input variables. In the present thesis, test data reported by Pearson et al. (2004) were selected from the CLASH database for all types of armor except Dolos and Cubipods. Thus, packing densities given by Pearson et al. (2004), which are the same as those considered by Bruce et al. (2006), were assumed here to represent the selected data for the different types of armor. For Dolos armors, Pedersen's (1996) overtopping data were used here but this author did not provide the packing density. For Cubipod tests, packing densities were taken from Smolka et al. (2009). The recommended values of packing densities for each type of armor are given in Table 2-4.

The γ_{f50}-calibrated roughness factors from the CLASH NN were used here to study the influence of packing density (ϕ) and armor roughness (γ_f) on overtopping, given that the CLASH NN showed the lowest *rMSE*. Figure 4-4 illustrates the influence of armor porosity ($p=1-\phi/n$) on the roughness factor. In both single- and double-layer armors, armor units placed with higher porosity tend to have a lower roughness factor. Given an armor unit, an armor porosity above recommended values decreases the concrete consumption but also decreases the hydraulic stability (see Medina et al., 2014), affecting the breakwater performance during lifetime.

The straight line drawn in Figure 4-4 represents the influence of armor porosity on the roughness factor without considering the armor unit geometry or number of layers. The linear model $\gamma_f = 1 - 1.25p$ shown in Figure 4-4 fits reasonably well all cases (CV=$\left|\gamma_f - \gamma_{f50}\right|/\gamma_f$<15%) except for that of the double-layer rock armor, which has a lower than expected roughness factor.

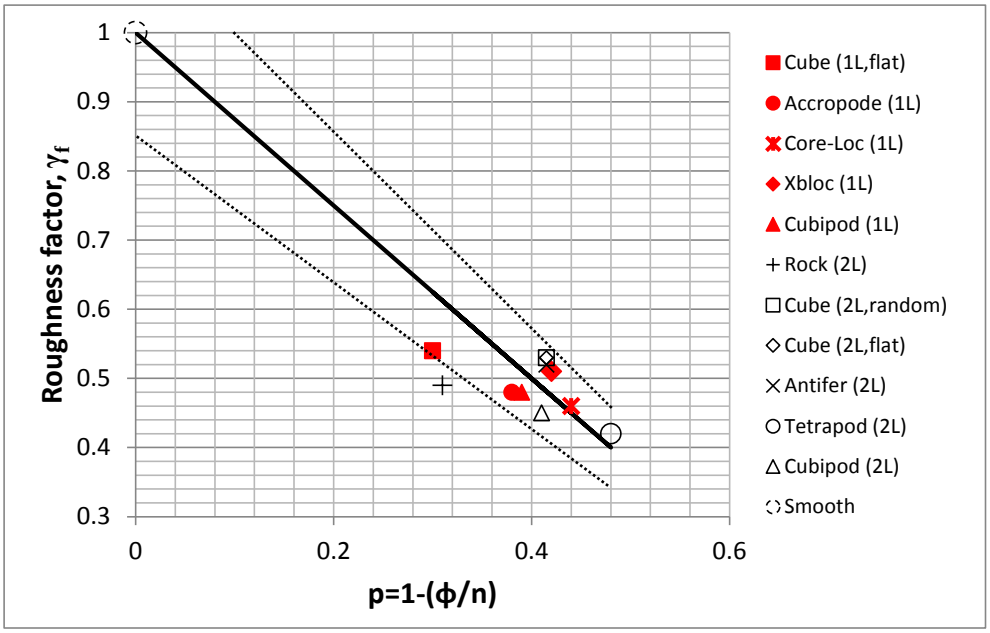

Figure 4-4. γ_{f50}-calibrated roughness factors of the CLASH NN and armor porosity.

4.5 Sensitivity of overtopping rates depending on the roughness factor

An analytical study of the influence of small variations in the roughness factor on overtopping is discussed in this section. Only formulas with a topology similar to that of Eq. **2-1** are considered here to analytically compare the different variables involved in the overtopping process. Eq. **4-1** summarizes the partial derivative of Eq. **2-6** and Eq. 2-11.

Eq. 4-1
$$\frac{\partial Q_e}{\partial \gamma_f} = -K\left(\frac{R_c}{H_{m0}}\right) Q_e \left(-\frac{1}{\gamma_f^2}\right)$$

where K is a positive constant, and $Q_e = q_e/\sqrt{gH_{m0}^3}$ is the estimated dimensionless overtopping rate. Eq. **4-1** can be rewritten as:

Eq. 4-2
$$\frac{\partial Q_e}{Q_e} = \left(\frac{\partial \gamma_f}{\gamma_f}\right)\left(\frac{K}{\gamma_f}\right)\left(\frac{R_c}{H_{m0}}\right)$$

Considering Eq. **2-6** and Eq. **4-2**, a slight variation in the roughness factor, say $\Delta\gamma_f/\gamma_f$ = +0.01/0.50 = +2%, generates a 15% increase in the estimated overtopping rates with R_c/H_{m0}=1.5. For lower values of R_c/H_{m0}, overtopping rates are less sensitive to variations in the roughness factor. Thus, the relative crest freeboard, R_c/H_{m0}, affects the sensitivity of overtopping to variations in the roughness factor; the higher the R_c/H_{m0}, the greater the influence of variations in γ_f on the estimated overtopping discharges. The

values for γ_{f10}, γ_{f50}, and γ_{f90} shown in Table 4-1 indicate that overtopping estimations using γ_{f50} may easily change in the future from 10% to 25% if the dataset is significantly enlarged with additional tests.

The relative increases in overtopping rates, $\Delta Q/Q_e$, are directly proportional to the relative increase in the roughness factor, $\Delta\gamma_f/\gamma_f$, the relative crest freeboard, R_c/H_{m0}, and indirectly proportional to the roughness factor, γ_f.

Chapter 5.

Explicit wave overtopping estimator on mound breakwaters

Molines and Medina (2015) compared different overtopping estimators and found that the CLASH NN performed better in comparison to other estimators; however, it is a “black-box” which does not clarify how overtopping is affected by specific explanatory variables. EurOtop (2007) noted that the CLASH NN provides the possibility to calculate trends by varying each input instead of only one calculation: the CLASH NN is able to calculate up to 15 trends corresponding to each of the 15 inputs. Figure 5-1 illustrates the good agreement of the CLASH NN predictions compared to CLdata.

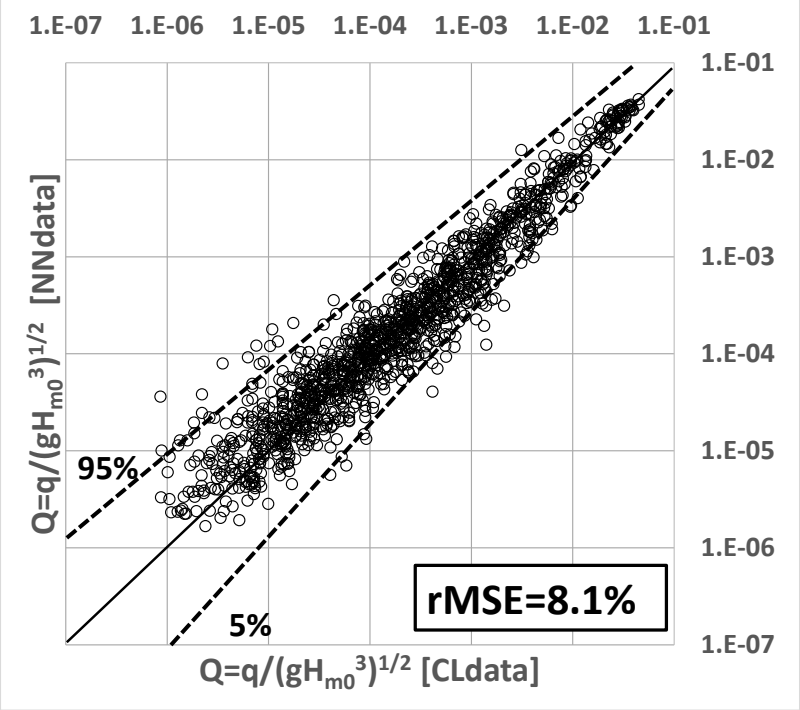

Figure 5-1. Measured overtopping rate (CLdata) compared to predicted overtopping rate using the CLASH NN.

The present thesis describes a methodology (which is an accepted paper in Journal of Waterway, Port, Coastal and Ocean Engineering by Molines and Medina) to build-up a new and explicit overtopping formula which can provide predictions for conventional mound breakwaters in non-breaking conditions. The new formula given by Eq. 5-8 estimates overtopping almost as well as the CLASH NN, but without being a "black-box". Eq. 5-8 provides explicit descriptions of the relationships between input variables and the overtopping rate on conventional mound breakwaters while allowing for a better understanding of how specific structural and wave characteristics influence wave overtopping. The formula was obtained from systematic simulations using the CLASH NN, and it was validated with the test results of the CLASH database and Smolka et al. (2009) corresponding to the conventional mound breakwaters typology (see Table 3-3).

5.1 Methodology to build-up the new overtopping estimator

The methodology described herein was used to obtain an explicit formula from the CLASH NN model, which is similar to that used by both Medina et al. (2002) to predict overtopping, and Garrido and Medina (2012) to estimate the coefficient of reflection of Jarlan-type breakwaters. The methodology does not guarantee exactly the same result

when using the same database and explanatory variable list, but it does provide an explicit formula to emulate the neural network "black-box" estimator. It is an intrinsic characteristic of Artificial Intelligence methods as pointed by Koza (1992).

Table 5-1 provides the flow chart to summarize the methodology used for this study. The new neural network-derived explicit formula was built-up by consecutively introducing each dimensionless variable X_j (j=1, 2, etc.) that may influence overtopping. The overtopping estimator after introducing each variable was referred to as $Qj = Q(X_1, X_2,\ldots, X_j)$.

The process of building-up the formula started by selecting the candidate variables that may influence overtopping discharges, X_j (j=1, 2, etc.). After that, the first overtopping predictor $Q1 = Q(X_1)$ was selected given by Eq. **5-1**. Then, overtopping simulations were carried out with the CLASH NN varying X_2 and using constant values of X_1 and X_3 to X_7. The qualitative analysis of a graphic representation of the neural network overtopping simulations (Q_{CLNN}) allowed for the recommendation of an estimator $Q2 = Q(X_1, X_2)$. Parameters were calibrated to minimize (1) $rMSE_{Q2}$ (CLdata), (2) $rMSE_{Q2}$ (NNdata) and (3) the number of significant figures. Variables X_3, X_4, and so on were considered similarly to build-up estimators *Q3*, *Q4*, and so on. The simulations of the CLASH NN served as a base to build-up the new overtopping predictor Q6, which was validated using all the conventional mound breakwater cases selected from the CLASH database described in Chapter 3. The following sections describe the process step by step.

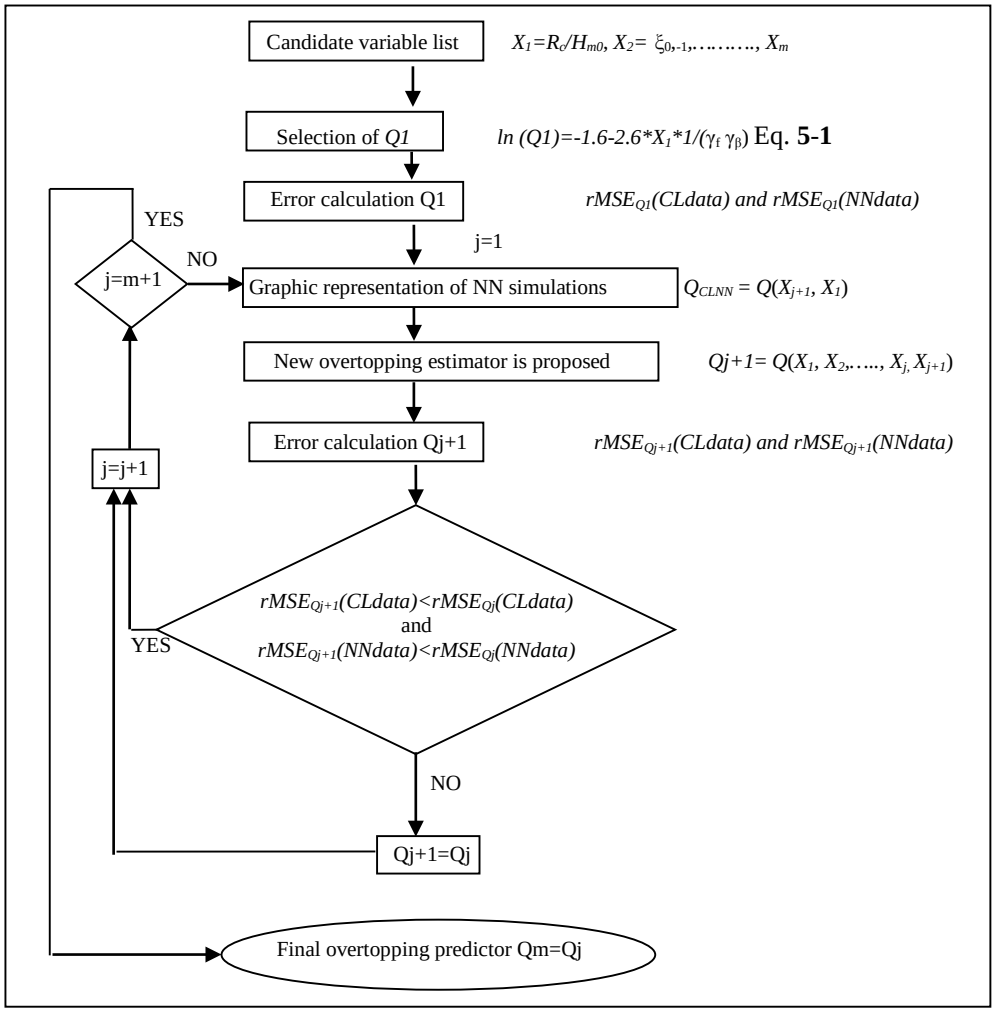

Table 5-1. Flow chart describing the methodology to build-up Q6.

5.1.1. Explanatory variables affecting overtopping on conventional mound breakwaters

In this thesis, the 11 input variables from the CLASH NN were considered for conventional mound breakwaters (Figure 2-1) and 7 dimensionless variables were selected as candidates which may significantly influence overtopping discharge on conventional mound breakwaters:

1. R_c/H_{m0} (dimensionless crown wall freeboard) is the most common and widely accepted dimensionless variable which mainly governs the overtopping discharge. The effects of roughness slope and oblique waves are usually considered using the

roughness factor ($\gamma_f \leq 1.0$) and obliquity factor ($\gamma_\beta \leq 1.0$), respectively; γ_f and γ_β, are used as reduction factors in the significant wave height as $R_c/(\gamma_f \gamma_\beta H_{m0})$.

2. $\xi_{0,-1} = tan\alpha/[2\pi H_{m0}/gT^2_{-1,0}]^{1/2}$ (Iribarren's number or breaker parameter using H_{m0} and $T_{-1,0}$ at the toe of the structure) is a variable widely used in coastal engineering. $\xi_{0,-1}$ takes into account the influence of wave steepness and structure slope angle, determining the type of wave breaking on the slope. The influence of wave steepness, slope angle or $\xi_{0,-1}$ on overtopping was reported by Pedersen (1996), Hebsgaard et al. (1998) and Medina et al. (2002), among others. Bruce et al. (2009) concluded that γ_f increases with $\xi_{0,-1}$ and thus $\xi_{0,-1}$ affects the overtopping rates. In the present study, wave steepness and slope angle were analyzed separately to determine if $\xi_{0,-1}$ reasonably integrates the influence of both variables on the overtopping discharge.
3. *Rc/h* (relative water depth) is a variable which relates the crown wall freeboard with the water depth. It was used by Molines et al. (2012) to study wave overtopping on conventional mound breakwaters during construction. This variable includes the information about the water depth, which can be valuable for overtopping estimations of conventional mound breakwaters with deep armors, such as those existing during the construction phase.
4. G_c/H_{m0} (relative armor crest berm width) is a variable which considers the armor crest berm width of the breakwater. It was used by Besley (1999) and recommended by EurOtop (2007) in the reduction factor *Cr* given by Eq. 2-9. Wide crest berms lead to high energy dissipation and hence a low overtopping discharge.
5. A_c/R_c (relative armor crest freeboard) is a variable to relate the armor crest freeboard with the crown wall freeboard [used by Smolka et al. (2009)]. High values for Ac mean high crests which lead to high energy dissipation and thus a low overtopping rate.
6. B_t/H_{m0} (relative toe berm width) is a variable describing the toe berm width, which may influence overtopping discharge.
7. h_t/H_{m0} (relative toe depth) is a variable used in the mound breakwater design rules given by Grau (2008). This dimensionless variable is related to the depth of the toe berm, which may influence overtopping discharge.

Simulations were conducted using the following indicative constant values of the variables: R_c/H_{m0}=0.80,1.00,1.20,1.50,2.00 (five values); $\xi_{0,-1}$=3.50; R_c/h=0.25; G_c/H_{m0}=1.00; A_c/R_c=1.00; B_t/H_{m0}=0.00 and $h/H_{m0}=h_t/H_{m0}$ (no toe berm); γ_f = 0.47 and, $\beta=0^o$. The ranges of the variables aforementioned in tests given in Chapter 3 are specified in Table 5-2.

Order (j)	Variable (X_j)	Range
1	R_c/H_{m0}	$0.52 \leq R_c/H_{m0} \leq 3.75$
2	$Ir=\xi_{0,-1}$	$1.65 \leq \xi_{0,-1} \leq 7.21$
3	R_c/h	$0.09 \leq R_c/h \leq 1.34$
4	G_c/H_{m0}	$0.00 \leq G_c/H_{m0} \leq 3.50$
5	A_c/R_c	$0.38 \leq A_c/R_c \leq 1.38$
6	B_t/H_{m0}	$0.00;\ 0.70 \leq B_t/H_{m0} \leq 15.9$
7	h_t/H_{m0}	$1.45 \leq h_t/H_{m0} \leq 17.5$

Table 5-2. Range of the variables of overtopping tests given in section 3.4.

5.1.2. Dimensionless crown wall freeboard, $X_1= R_c/H_{m0}$. Initial formula Q1

It is widely accepted in the literature that $X_1=R_c/H_{m0}$ is the main variable governing overtopping phenomenon. Eq. **2-6** may be rewritten as follows:

Eq. 5-1
$$\mathbf{\ln Q1} = \boldsymbol{ln}\left(\frac{q}{\sqrt{gH_{m0}^3}}\right) = \mathbf{-1.6 - 2.6}\frac{R_c}{H_{m0}}\frac{1}{\gamma_f\gamma_\beta}$$

The roughness factor was taken initially as the best fitted value for the CLASH NN model given in Chapter 4 (section 4.3), so for the final estimator Q6, the γ_f was then derived specifically following the methodology given in section 4.1.

The obliquity factor given by Lykke-Andersen and Burcharth (2009) in Eq. 2-10 was applied in this thesis for the final estimator Q6 on the 561 tests selected from the CLASH database with $10^o \leq \beta \leq 60^o$ given in Table 3-4.

Figure 5-2 compares the overtopping rate in CLdata with estimations $Q1=Q(X_1)$; the general trend is well defined by Eq. **5-1**. Thus, Eq. **5-1**, equivalent to Eq. **2-6**, was considered in the initial formula to predict mean overtopping discharge on conventional mound breakwaters; $rMSE_{Q1}$ (CLdata) = 41.2% and $rMSE_{Q1}$ (NNdata) = 42.2%.

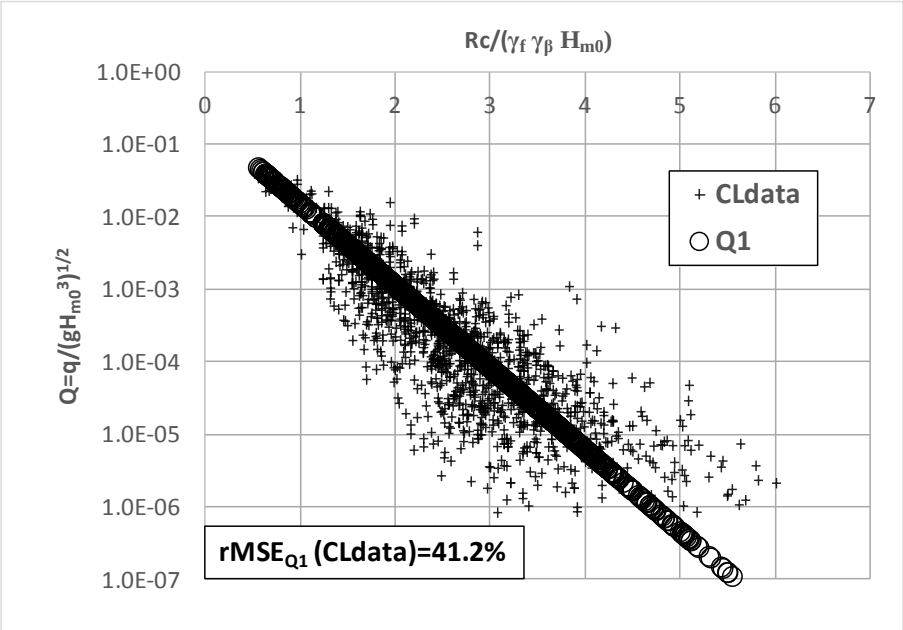

Figure 5-2. Overtopping rate in CLdata compared to that predicted by Q1.

Each new variable X_j (j=2 to 7) was added as a new explanatory term for Eq. **5-1**. The general structure of the overtopping formula is expressed in Eq. 5-2:

Eq. 5-2
$$\ln Q j = (\lambda_2 \cdot \lambda_3 \ldots\ldots \lambda_j) \cdot [\ln Q1]$$

where λ_j is the j-th explanatory term corresponding to the variable X_j (j=2 to 7). The predicted overtopping discharge increases if λ_j<1 (ln(*Q1*)<0).

5.1.3. Iribarren's number, X_2= $\xi_{0,-1}$=Ir

Iribarren's number or the breaker parameter, $\xi_{0,-1}=\tan\alpha/[2\pi H_{m0}/gT^2_{-1,0}]^{1/2}$, depends on two independent dimensionless variables: (1) armor slope angle (α) and (2) deep water wave steepness ($H_{m0}/L_{0,-1}= [2\pi H_{m0}/ gT^2_{-1,0}]$) with H_{m0} and $T_{-1,0}$ measured at the breakwater toe. To determine the influence of each variable, two sets of simulations were considered: one varying the wave steepness (Figure 5-3.a) and the other varying slope angle (Figure 5-3.b).

Figure 5-3 shows that both armor slope ($\cot\alpha$) and wave steepness ($H_{m0}/L_{0,-1}$) significantly influence overtopping rates. Thus, Iribarren's number ($\xi_{0,-1}$) seems to be a reasonable variable to account for the influence of armor slope and wave steepness simultaneously.

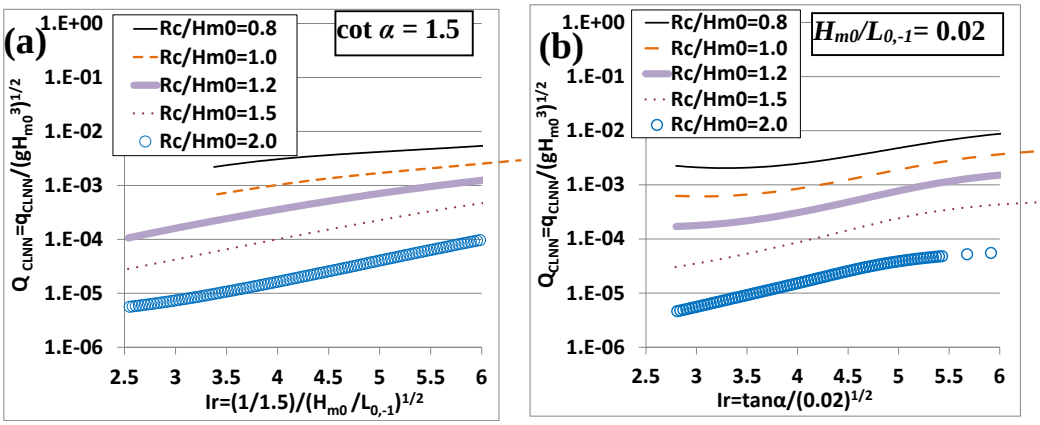

Figure 5-3. Influence of Ir on log Q if (a) slope angle or (b) wave steepness are constant.

The interaction between $X_1=R_c/H_{m0}$ and $X_2=\xi_{0,-1}$ was analyzed to improve the explanatory term using only two parameters. The explanatory term using the variable $\xi_{0,-1}\,[R_c/H_{m0}]^{1/2}$ (Figure 5-4.b) was found to be a better descriptor than that obtained using only $\xi_{0,-1}$ (Figure 5-4.a).

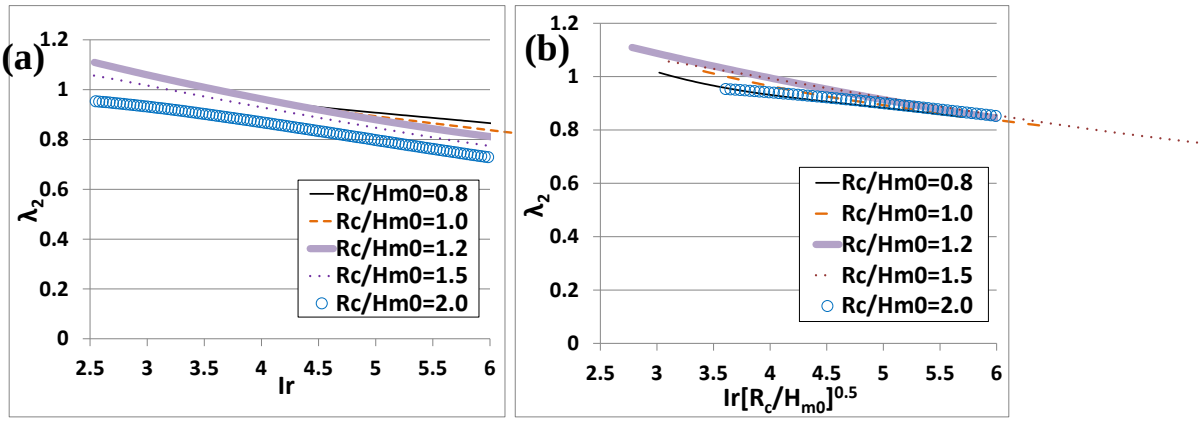

Figure 5-4. Explanatory term λ_2 as function of (a) $\xi_{0,-1}$ or (b) $\xi_{0,-1}[R_c/H_{m0}]^{1/2}$.

The overtopping prediction of Q2 is given by:

Eq. 5-3 $$\ln Q2 = \lambda_2 \ln Q1 = \left[1.20 - 0.05\left(\xi_{0,-1}\sqrt{R_c/H_{m0}}\right)\right]\ln Q1$$

with $rMSE_{Q2}$ (CLdata) = 26.1% << 41.2% = $rMSE_{Q1}$ (CLdata) and $rMSE_{Q2}$ (NNdata) = 21.8% << 42.2% = $rMSE_{Q1}$ (NNdata). Eq. **5-3** clearly improves the overtopping prediction given by Eq. **5-1**. Iribarren's number ($\xi_{0,-1}=\tan\alpha/[2\pi H_{m0}/gT^2_{-1,0}]^{1/2}$) is a relevant variable to explain the mean overtopping discharge on conventional

mound breakwaters; the higher the $\xi_{0,-1}$, the higher the overtopping discharge. The predicted overtopping discharge increases if λ_2<1 (ln(*Q1*)<0).

5.1.4. Dimensionless water depth, $X_3=R_c/h$

Figure 5-5.a is a graphic representation of overtopping simulations using the CLASH NN. The lower the $X_3=R_c/h$, the greater the impact on overtopping. The explanatory term λ_3 is represented in Figure 5-5.b.

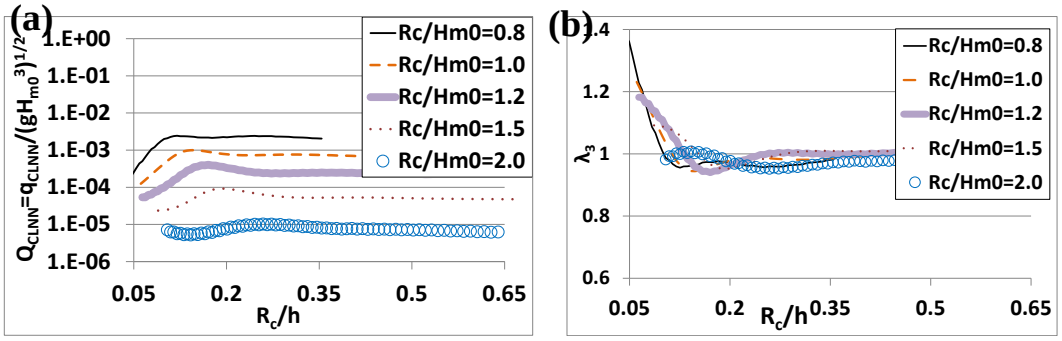

Figure 5-5. Influence of R_c/h on overtopping: (a) CLASH NN model and (b) λ_3 term.

The overtopping prediction of *Q3* is given by:

Eq. 5-4 $$\ln Q3 = \lambda_3 lnQ2 = [1.0 + 2.0exp(-35\,R_c/h)]lnQ2$$

with $rMSE_{Q3}$ (CLdata) = 24.7% < 26.1% = $rMSE_{Q2}$ (CLdata) and $rMSE_{Q3}$ (NNdata) = 20.4% < 21.8% = $rMSE_{Q2}$ (NNdata). Eq. **5-4** improves the overtopping prediction of Eq. **5-3** significantly when 0.09 < R_c/h < 0.13; however, its effect is not significant *(Q3≈Q2)* if R_c/h>0.13. Only 10 % of the CLdata fall in the range 0.09 < $X_3=R_c/h$ < 0.13. In the final formula, $X_3=R_c/h$ was considered because it significantly decreased $rMSE_{Q2}$ (CLdata) and $rMSE_{Q2}$ (NNdata). The predicted overtopping discharge increases if λ_3<1 (ln(*Q1*)<0).

5.1.5. Dimensionless armor crest berm width, $X_4 = G_c/H_{m0}$

Figure 5-6.a is a graphic representation of overtopping simulations using the CLASH NN. The higher the $X_4=G_c/H_{m0}$, the greater the impact on overtopping. The explanatory term λ_4 is represented in Figure 5-6.b.

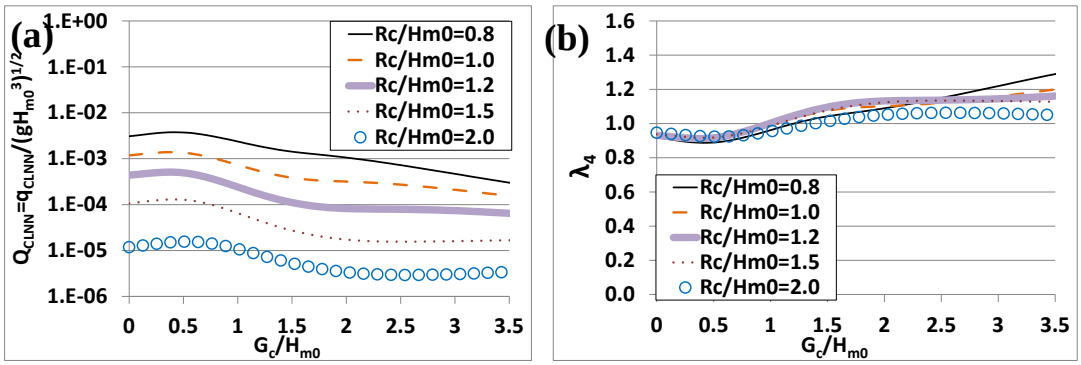

Figure 5-6. Influence of G_c/H_{m0} on overtopping: (a) CLASH NN model and (b) λ_4 term.

Eq. **5-5** gives the overtopping prediction of *Q4*, which considers the influence of the relative armor crest berm width:

Eq. 5-5 $$\ln Q4 = \lambda_4 lnQ3 = max[0.95; (0.85 + 0.13\, G_c/H_{m0})]lnQ3$$

with $rMSE_{Q4}$ (CLdata) = 21.4% < 24.7% = $rMSE_{Q3}$ (CLdata) and $rMSE_{Q4}$ (NNdata) = 16.2% < 20.4% = $rMSE_{Q3}$ (NNdata). Eq. (11) Eq. **5-5** significantly improves the overtopping prediction of Eq. **5-4**. $X_4 = G_c/H_{m0}$ is a relevant variable to explain the mean overtopping discharge on conventional mound breakwaters; when $G_c/H_{m0}>0.75$, the higher the ratio G_c/H_{m0}, the lower the overtopping. The predicted overtopping discharge increases if $\lambda_4<1$ ($\ln(Q1)<0$).

5.1.6. Dimensionless armor crest freeboard, $X_5 = A_c/R_c$

Figure 5-7.a is a graphic representation of overtopping simulations using the CLASH NN. The higher the $X_5=A_c/R_c$, the greater the impact on overtopping. The explanatory term λ_5 is represented in Figure 5-7.b.

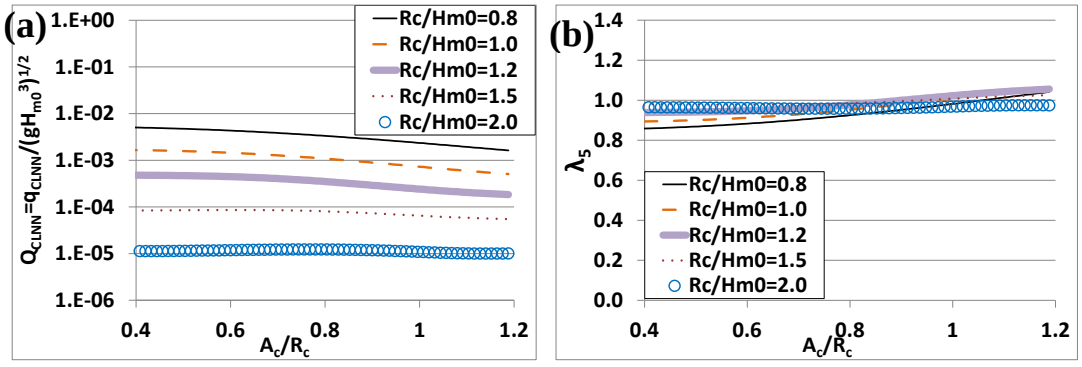

Figure 5-7. Influence of A_c/R_c on overtopping: (a) CLASH NN model and (b) λ_5 term.

Eq. **5-6** gives the overtopping prediction of *Q5*, which considers the influence of the relative armor crest freeboard:

Eq. 5-6 $$\mathbf{ln}\, \boldsymbol{Q5} = \boldsymbol{\lambda_5 lnQ4} = (\mathbf{0.85} + \mathbf{0.15}\, \boldsymbol{A_c/R_c})\boldsymbol{lnQ4}$$

with $rMSE_{Q5}$ (CLdata) = 16.9% < 21.4% $rMSE_{Q4}$ (CLdata) and $rMSE_{Q5}$ (NNdata) = 10.6% < 16.2% = $rMSE_{Q4}$ (NNdata). Eq. **5-6** improves the overtopping prediction given by Eq. **5-5**. $X_5 = A_c/R_c$ is a relevant variable to explain the mean overtopping discharge on conventional mound breakwaters; the higher the ratio A_c/R_c, the lower the overtopping. The predicted overtopping discharge increases if $\lambda_5<1$ ($\ln(Q1)<0$).

5.1.7. Dimensionless toe berm: $X_6 = B_t/H_{m0}$ and $X_7 = h_t/H_{m0}$

The conventional mound breakwater with concrete armor units usually has a toe berm with $X_7 = h_t/H_{m0}$ around 1.5 (see Grau, 2008). In the CLASH database, toe berms are controlled by B_t and h_t: if there is no toe berm, $B_t = 0$ and $h_t = h$. Two sets of simulations were conducted varying $X_6 = B_t/H_{m0}$ and $X_7 = h_t/H_{m0}$, respectively. The CLASH NN predictions were sensitive to the presence of a toe berm ($B_t>0$). In the CLdata, 80% of the data represented conventional mound breakwaters without a toe berm ($B_t=0$).

Figure 5-8.a is a graphic representation of overtopping simulations using the CLASH NN varying $X_7=h_t/H_{m0}$ with R_c/h=0.2. It is clear that the CLASH NN predictions detected the presence of a toe berm. Similar graphs were obtained for other values of R_c/h. The explanatory term λ_6 is represented in Figure 5-8.b.

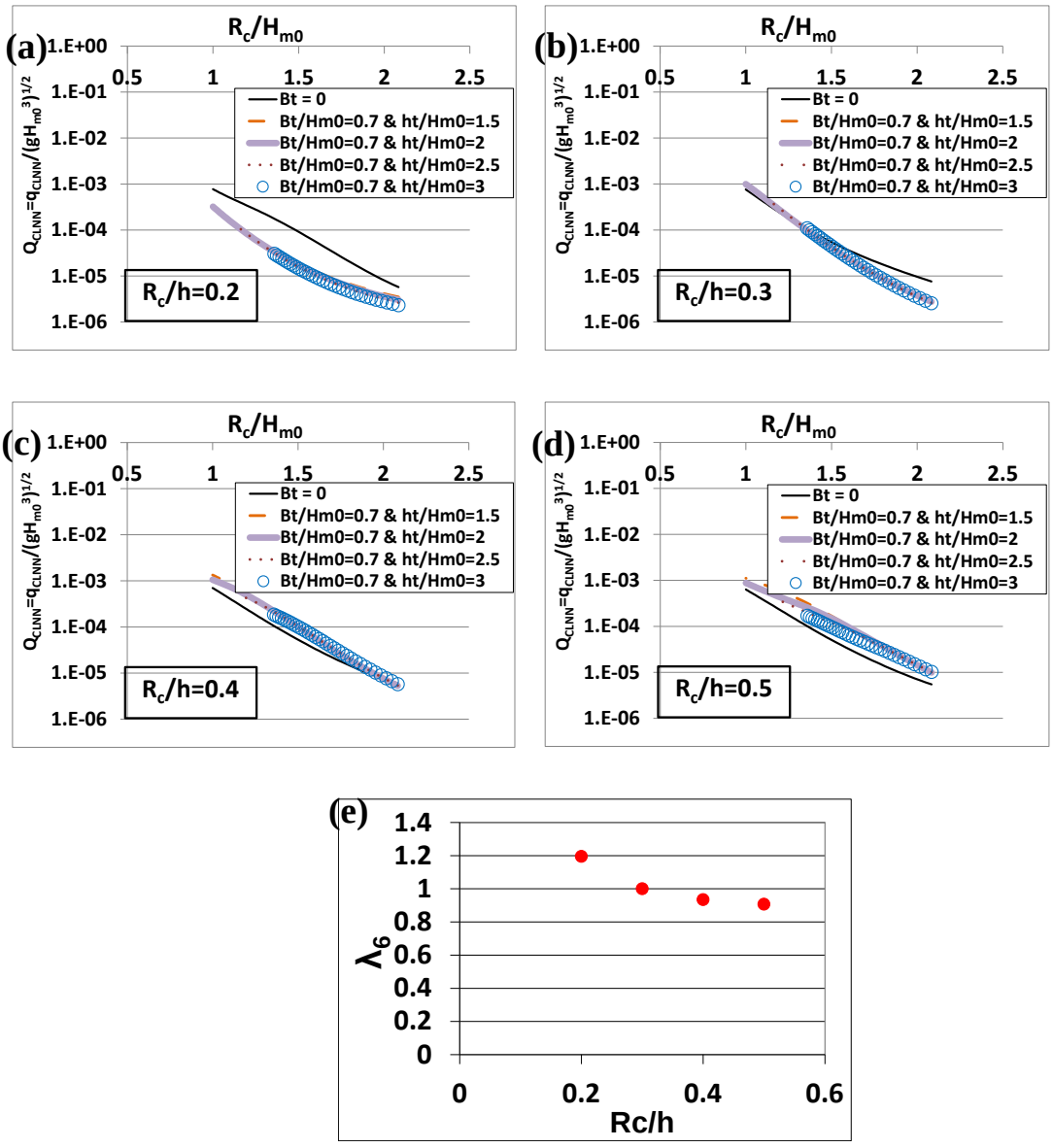

Figure 5-8. Influence of h_t/H_{m0} on overtopping: (a), (b), (c), (d) CLASH NN model and (e) λ_6 term.

If there is a toe berm (B_t >0), $X_3=R_c/h$ is a relevant variable to explain the overtopping prediction of the CLASH NN. The influence of the toe berm is described by:

Eq. 5-7 $$\ln Q6 = \lambda_6 lnQ5 = \begin{cases} max[1;(1.2-0.5\,R_c/h)]lnQ5 & if\ B_t > 0 \\ 1 \cdot lnQ5 & if\ B_t = 0 \end{cases}$$

with $rMSE_{Q6}$ (CLdata) = 13.6% < 16.9% = $rMSE_{Q5}$ (CLdata) and $rMSE_{Q6}$ (NNdata) = 6.9% < 10.6% = $rMSE_{Q5}$ (NNdata). Eq. **5-7** improves the overtopping prediction of Eq. **5-6**. A toe berm slightly reduces the overtopping discharge. The predicted overtopping discharge increases if λ_6<1 (ln(*Q1*)<0).

5.2 Explicit overtopping formula for conventional mound breakwaters

Eq. **5-1** to Eq. **5-7** can be used to define an explicit overtopping formula valid for conventional mound breakwaters in the ranges specified in Table 5-2. Eq. 5-8 integrates Eq. **5-1** to Eq. **5-7**. The predicted overtopping discharge increases if λ_j<1 (ln(*Q1*)<0).

Eq. 5-8.a $$Q = \left(\frac{q}{\sqrt{g \cdot H_{m0}^3}} \right) = Q6 = \exp\left(\lambda_2 \cdot \lambda_3 . \lambda_4 \cdot \lambda_5 \cdot \lambda_6 \left[-1.6 - 2.6 \cdot \frac{R_c}{H_{m0}} \cdot \frac{1}{\gamma_f \gamma_\beta} \right] \right)$$

where:

Eq. 5-8.b $$\lambda_2 = \left[1.20 - 0.05\left(\xi_{0,-1}\sqrt{R_c/H_{m0}}\right)\right]$$

Eq. 5-8.c $$\lambda_3 = [1.0 + 2.0 exp(-35\,R_c/h)]$$

Eq. 5-8.d $$\lambda_4 = max[0.95;(0.85 + 0.13\,G_c/H_{m0})]$$

Eq. 5-8.e $$\lambda_5 = (0.85 + 0.15\,A_c/R_c)$$

Eq. 5-8.f $$\lambda_6 = \begin{cases} max[1;(1.2-0.5\,R_c/h)] & if\ B_t > 0 \\ 1 & if\ B_t = 0 \end{cases}$$

Eq. 5-8.g $$\gamma_\beta = \begin{cases} 1 - 0.0077|\beta| & for\ long-crested\ waves \\ 1 - 0.0058|\beta| & for\ short-crested\ waves \end{cases}$$ valid for $\beta \leq 60^o$

The influence of oblique wave attack was introduced using the obliquity factor γ_β given by Lykke-Andersen and Burcharth (2009) for rough slopes and validated in section 5.2.1. For single-peaked wave energy spectra with a spectral shape similar to JONSWAP spectra, $T_p \approx 1.1 * T_{-1,0}$.

According to Molines and Medina (2015) and the methodology described in Chapter 4, each formula must provide a list of roughness factors, since γ_f depends on the formula and the database used to calibrate the parameters. Table 5-3 gives the optimum roughness factors for Eq. 5-8 and CLdata following the methodology described in Chapter 4. Using the γ_f given in Table 5-3, $rMSE_{Q6}$ (CLdata) = 12.1% and $rMSE_{Q6}$ (NNdata) = 5.1% are slightly different from the values 13.6% and 6.9% obtained using the best fitted γ_f for the CLASH NN model reported by Molines and Medina (2015).

Armor type (2L: 2 Layers) (1L: 1 Layer)	**Overtopping estimator**						
	Q_{VMJ}	**$Q_{EurOtop}$**	**Q_{SZM}**	**Q_{JE}**	**Q_{VMB}**	**Q6**	**CLASH NN**
	γ_f	γ_f	γ_f	γ_f	γ_f	γ_f	γ_f
Smooth	1.03	1.03	1.21	1.25	1.01	0.95	1.00
Rock (2L)	0.45	0.53	0.44	0.38	0.47	0.48	0.49
Cube (2L, random)	0.45	0.53	0.44	0.42	0.46	0.51	0.53
Cube (2L, flat)	0.48	0.53	0.51	0.46	0.48	0.52	0.53
Cube (1L, flat)	0.52	0.59	0.53	0.46	0.53	0.55	0.54
Antifer (2L)	0.50	0.57	0.51	0.44	0.50	0.52	0.52
Haro ^{R} (2L)	0.49	0.54	0.50	0.44	0.49	0.51	0.52
Tetrapod (2L)	0.43	0.52	0.39	0.37	0.43	0.45	0.42
Accropode (1L)	0.48	0.51	0.49	0.42	0.49	0.48	0.48
Core-Loc (1L)	0.46	0.49	0.46	0.36	0.46	0.45	0.46
Xbloc (1L)	0.47	0.49	0.48	0.42	0.47	0.46	0.51
Dolos (2L)	0.41	0.45	0.37	0.36	0.43	0.42	0.32
Cubipod (2L)	0.55	0.57	0.45	0.36	0.57	0.47	0.45
Cubipod (1L)	0.58	0.61	0.46	0.41	0.61	0.48	0.48

Table 5-3. Roughness factor (γ_f) for different overtopping estimators.

Eq. 5-8 has 16 parameters plus 14 roughness factors calibrated with 1,307 data (CLdata). In order to determine the uncertainty associated when using Eq. 5-8, it is convenient to calculate the final prediction error (FPE). The FPE takes into account not only MSE, but also the number of independent parameters used in the formula and the number of data for calibration. According to Barron (1984), the final prediction error is FPE = MSE(1+2P/(N-P)), where N is the number of data used for calibration and P is the number of calibrated parameters. In this case, N=1,307 and P=(16+14)=30. The relative final prediction error (rFPE) is given by:

Eq. 5-9

$$rFPE = \frac{FPE}{Var(\log Qo)} = rMSE\left(1+\frac{2P}{N-P}\right)$$

where rMSE is the relative mean squared error given by Eq. 3-1; *P* is the number of calibrated parameters, and *N* is the number of data used for calibration. Therefore, one should expect rMSE to be similar to rFPE = 12.1%*(1+2*30/(1,307-30)) = 12.7% when applying Eq. 5-8 to any new data not included in CLdata, i.e. data not used to calibrate parameters.

In contrast, the CLASH NN is a "black-box" with 500 neural networks having 320 parameters each and trained with 8,372 data (extracted from the CLASH database). The complexity of the neural network structure makes it difficult to determine the rFPE. It is not possible to apply Eq. 5-9 to the CLASH NN to estimate rFPE because bootstrapping was used to develop the neural network model, and the neural network parameters may be correlated.

5.2.1. Confidence intervals for the overtopping formula

The confidence intervals for the overtopping formula Q6 given by Eq. 5-8 were calculated from CLdata. Owen (1980) as well as Victor and Troch (2012) assumed that the logarithm of dimensionless overtopping discharge follows a Gaussian distribution with constant variance. In this study, the variance was not considered as constant. To characterize the variance, it was necessary to analyze the errors (ε^2=WF(ln*Q6*-ln*Q*[CLdata])^2) of the overtopping predictions from Eq. 5-8, where WF is the weighting factor given in Table 3-5. Assuming a Gaussian error distribution, the errors were ordered from the lowest to the highest value and grouped into sets of consecutive 50 data. To characterize the variance of the errors, the FPE=MSE*(1+2*30/(1,307-30)) for each 50 data group was calculated, resulting in higher FPE when ln *Q6* decreased. Thus, the error (ε) may be considered Gaussian-distributed with zero mean and variance estimated by FPE:

Eq. 5-10 $$FPE = \sigma^2(\varepsilon) = -0.15 lnQ6 - 0.51$$

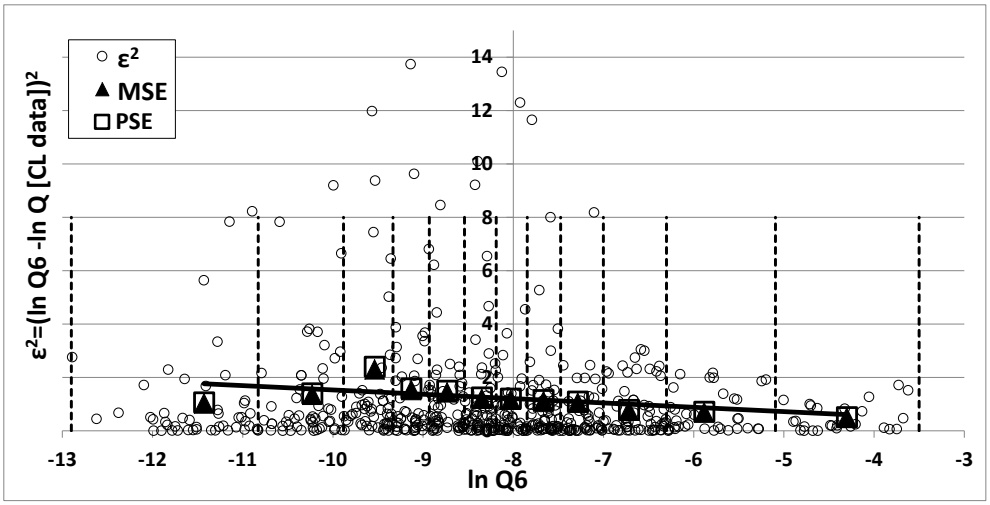

Figure 5-9. Overtopping squared errors, MSE and PSE of data groups.

The 5% and 95% percentiles for the Q6 overtopping estimator, given by Eq. 5-8, may be obtained by:

Eq. 5-11

$$\ln Q\Big|_{5\%}^{95\%} = \ln Q6 \pm 1.65 \cdot \sqrt{-0.15 \cdot \ln Q6 - 0.51}$$

Figure 5-10.a shows the 90% confidence interval for the overtopping estimator *Q6* compared to 1,307 CLdata (black circles, $\beta=0^0$) and 561 CLASH oblique wave data (crosses, $10^0 \leq \beta \leq 60^0$). Figure 5-10.b compares the overtopping estimator Q6 to 1,307 NNdata (circles, $\beta=0^0$) and 561 CLASH oblique wave data (crosses, $10^0 \leq \beta \leq 60^0$).

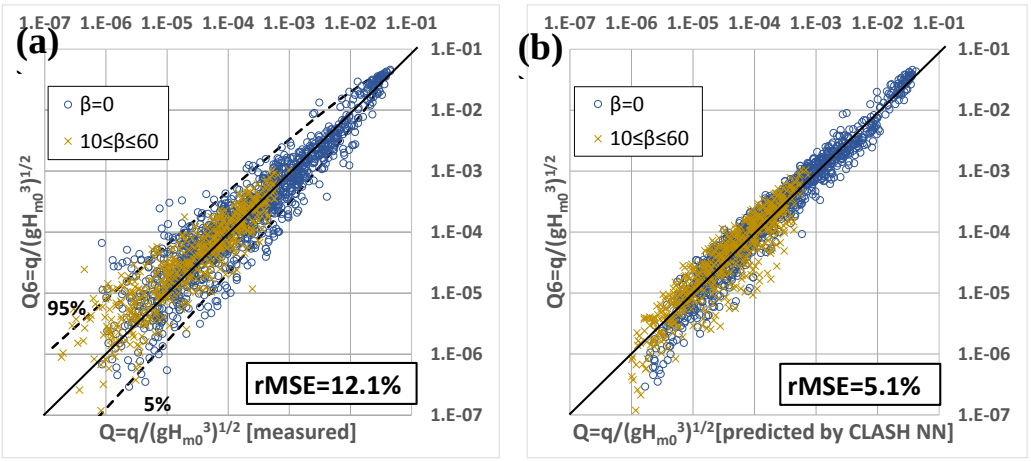

Figure 5-10. Q6 overtopping estimation and 90% confidence interval compared to (a) measured overtopping in CLASH, and (b) predicted overtopping by the CLASH NN.

The predictions of the overtopping estimator Q6 are accurate, especially in the range of high overtopping discharges, with a narrow 90% confidence interval. When applying Q6 with γ_f given in Table 5-3 and γ_β given by Eq. 5-8.g, Figure 5-10.a shows good agreement for both perpendicular and oblique wave attack. One should note that oblique wave data were not used to build-up or calibrate Q6; however, Lykke-Andersen and Burcharth (2009) did use these data to calibrate γ_β given by Eq. 5-8.g.

5.3 Sensitivity analysis and applications of Q6

The influence of the explanatory terms λ_i (X_i), i=2 to 6, given in Eq. 5-8, on the original CLdata are analyzed here. Table 5-4 shows the maximum, minimum and coefficient of variation for each λ_i (X_i), i=2 to 6. The λ_2 ($\xi_{0,-1}$) and λ_4 (G_c/H_{m0toe}) have a greater influence on the overtopping rate than λ_3 (R_c/h), λ_5 (A_c/R_c) and λ_6 (toe berm). The influence of λ_3 (R_c/h) is the lowest because its effect is only significant for deep armors (during construction phase).

λ_i (X_i), i=2 to 6	*Min*	*Max*	$CV(\%)=\sigma/\bar{\lambda_i}$
λ_2 ($\xi_{0,-1}$)	0.64	1.13	6.5
λ_3 (R_c/h)	1.00	1.10	1.6
λ_4 (G_c/H_{m0})	0.95	1.30	6.7
λ_5 (A_c/R_c)	0.86	1.06	3.2
λ_6 (toe berm)	1.00	1.14	3.2

Table 5-4. Ranges of the explanatory terms in CLdata used in Q6 given by Eq. 5-8.

Burcharth et al. (2014) presented examples of how coastal defense structures can be upgraded to withstand increased loads caused by climate change. Q6 can be used in the preliminary design stage to quantify the influence on overtopping when alternative geometrical modifications are made to existing conventional mound breakwaters. Analyzing a case similar to that described by EurOtop (2007), with parameters (see Figure 2-1): $\beta=0^o$; H_{m0}(m)=5; $T_{-1,0}$(s)=9; R_c(m)=5; A_c(m)=4; G_c(m)=5; cotα=1.5; γ_f [cube, 2Layers, randomly-placed] =0.51 and h(m)=12 with toe berm (B_t (m)=4 and h_t(m)=9), the predicted overtopping discharge is *q(l/s/m)*=49. Four scenarios are considered in Figure 5-11 to reduce overtopping discharge in the initial design: (1) higher structure freeboard (both R_c and A_c); (2) higher crown wall freeboard (R_c); (3) higher armor crest freeboard (A_c) and (4) wider armor crest berm (G_c). Figure 5-11 illustrates the effectiveness of each scenario, being the most effective an increase in the structure freeboard (R_c and A_c) followed by increasing only the crown wall freeboard (R_c).

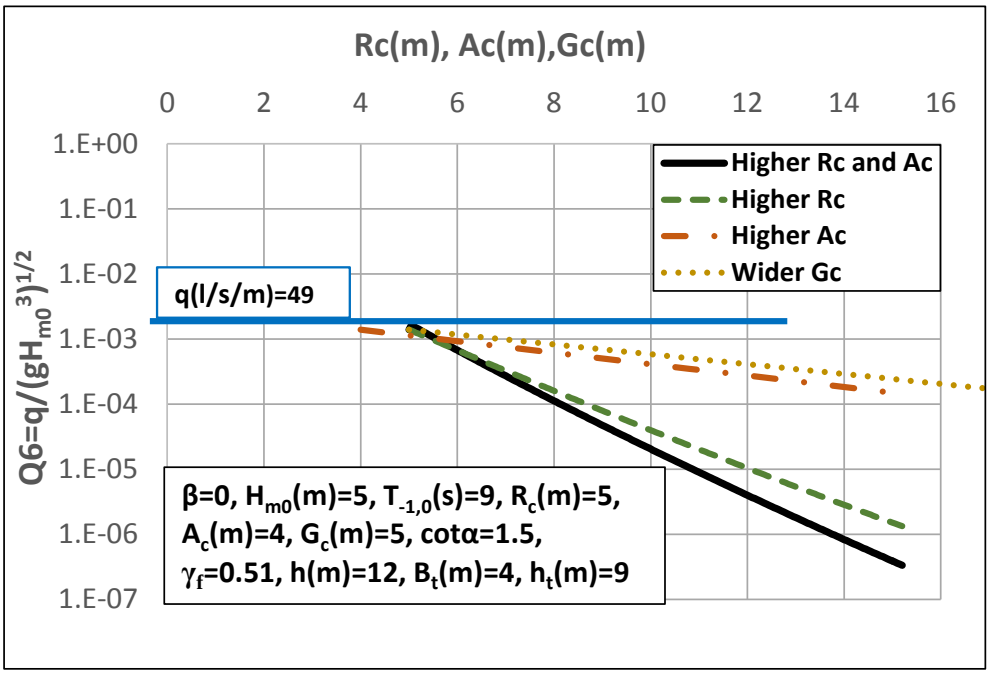

Figure 5-11. Sensitivity of conventional mound breakwaters geometrical changes to overtopping rates.

The effectiveness for each scenario given in the previous analysis does not take into account the cost of each geometrical change. A cost-effective change would require considering simultaneously the overtopping-reduction effectivity and the cost associated with each alternative, which would be dependent on the construction site and logistical constraints.

5.4 Comparison to overtopping estimators given in the literature

Wave overtopping predictors were compared using the same CLdata and NNdata. Each estimator was used with the optimum roughness factor, γ_f, derived by Molines and Medina (2015) and Chapter 4. Table 5-5 indicates the reference, overtopping model, number of parameters, explanatory variables, rMSE calculated using Eq. 3-1 on CLdata and NNdata and rFPE calculated using Eq. 5-9 on CLdata.

rMSE measures the goodness of fit of overtopping estimators to the target data. However, when comparing different overtopping estimators, it is better to use rFPE, which measures the expected error for new data not used during calibration. rFPE considers the rMSE, the number of parameters of each estimator and the number of data used for calibration.

Considering the results given in Table 5-5, *Q6* shows a behavior similar to the CLASH NN, but provides explicit relationships between explanatory variables and overtopping. Q6 has the lowest rFPE and hence it is the best estimator. Eq. 2-13 provided the highest rFPE, but one should take into consideration that the CLASH tests selected for this study (CLdata ranges given in Table 5-2) fall in the range $0.52<R_c/H_{m0}<3.75$. Therefore, using Eq. 2-13 does not take advantage of its better performance for zero and low crown wall freeboard cases ($0.00<R_c/H_{m0}<0.50$).

Reference (year)	Overtopping model	No. parameters	Explanatory variables	rMSE (CLdata)	rFPE (CLdata)	rMSE (NNdata)
Van der Meer and Janssen (1994)	Eq. 2-6	2	γ_f , γ_β, X_1	27.4%	28.1%	22.9%
EurOtop (2007)	Eq. 2-6&Eq. 2-9	5	γ_f , γ_β, X_1, X_4	23.7%	24.4%	17.9%
Smolka et al. (2009)	Eq. 2-11	4	γ_f , X_1, X_2, X_5	17.5%	18.0%	10.1%
Van der Meer and Bruce (2014)	Eq. 2-13	3	γ_f , γ_β, X_1	34.9%	35.8%	33.4%
Jafari and Etemad-Shahidi (2012)	Eq. **2-12**	11	γ_f, γ_β, X_1, X_2, X_4 tanα	23.7%	24.6%	16.2%
This thesis	Q6	16	γ_f , γ_β, X_1 to X_7	12.1%	12.7%	5.1%
Van Gent et al. (2007)	CLASH NN	500 x 320	γ_f, R_c, A_c, G_c, cotα_u, cotα_d, B_t, B, h_B, cotα_b, h, h_t, H_{m0}, $T_{-1,0}$, β	8.1%	-	0%

Table 5-5. Comparison of overtopping estimators using CLdata and NNdata.

Chapter 6.
Crown wall stability

Tests detailed in Chapter 3 focused on crown wall stability were analyzed by Molines (2010 and 2011) and will be reanalyzed in this chapter. Since tests were run using 1000 waves, the maximum force is equivalent to the force exceeded by 0.1% of the waves ($F_{h0.1\%}$). In the following analysis, the crown wall was considered to fail when an event larger than the resistance force occurs, no matter the duration of the event, being then on the safe side. The analysis focuses on horizontal and up-lift forces.

In this thesis, the forces were calculated considering that the pressure at each point of the crown wall takes the value from the nearest pressure sensor. This calculation does not assume any specific pressure distribution, since there are many rectangular distributions as pressure sensors. For the application of the forthcoming equations, it is necessary for the waves to not directly break onto the crown wall, which would produce impact forces not considered in the present method.

Molines (2010 and 2011) proposed calculating the maximum horizontal force $Fh_{0.1\%}$ and the up-lift force $Fv(Fh_{0.1\%})$ associated to the wave that caused $Fh_{0.1\%}$ (Figure 6-1). These actions, although separated some tenths of a second, were considered to occur at the same time thus being on the safe side.

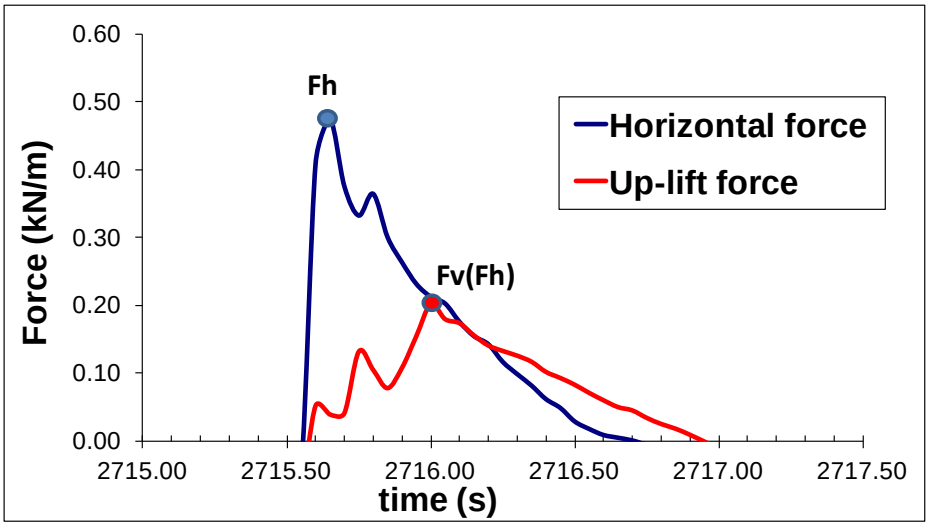

Figure 6-1. Time record of wave impact. Definition of Fh and Fv(Fh).

6.1 Analysis of test results. Representativeness of the design using $Fh_{0.1\%}$ and $Fv(Fh_{0.1\%})$

Molines (2010 and 2011) applied different formulas and concluded that none satisfactorily fit to the tests for horizontal and up-lift forces simultaneously, ($Fh_{0.1\%}$, $Fv(Fh_{0.1\%})$). Figure 6-2 illustrates the performance of formulas given by Pedersen (1996), Martin et al. (1999), Berenguer and Baonza (2006) and Nørgaard et al. (2013) on the reanalyzed experimental data. The estimation of the horizontal forces using existing formulas agrees quite well with the experimental data (especially forces lower than 400 N/m); however, the up-lift forces are clearly overestimated. The formulas were applied with the following considerations:

- All the formulas were applied even when did not exactly fulfil the ranges of application. In formulas which include the type of armor, the coefficients for cubes were used for cube and Cubipod armors.

- Jensen (1984) was applied using $a_{\text{Eq.2-16}}$ =-0.026 and $b_{\text{Eq.2-16}}$=0.051 given by USACE (2002) for a cube armored breakwater with a crown wall and toe berm.

- Günback and Göcke (1984) was used with the measured values of H_{max} and T_{Hmax} (wave period associated to H_{max}) to obtain the maximum wave loads assuming the equivalence hypothesis.

- The formula by Martin et al. (1999) was developed using regular waves. In the present thesis, it was applied using the measured values of H_{max} and T_{Hmax} to obtain the maximum wave loads instead of generating synthetic time series from the spectrum, analogously to Nørgaard et al. (2013). Martin et al. (1999) was applied using

$a_{\text{Eq.2-18}}$=0.296, $b_{\text{Eq.2-18}}$=0.073, $c_{\text{Eq.2-18}}$=383.1, A_u=1.2 and B_u=-0.7 (best fitted values for cubes from Martin et al., 1999).

- The formula by Berenguer and Baonza (2006) was applied with the coefficients $a1_{\text{Eq.2-20}}$, $a2_{\text{Eq.2-20}}$, $a3_{\text{Eq.2-20}}$, $b1_{\text{Eq.2-20}}$, $b2_{\text{Eq.2-20}}$, $b3_{\text{Eq.2-20}}$ for cubes when there is no armor damage.

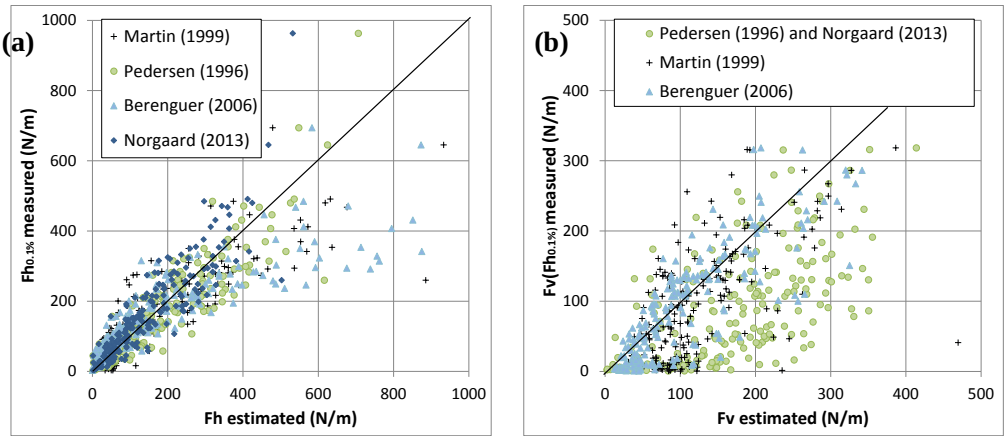

Figure 6-2. Comparison between estimated and measured (a) horizontal forces and (b) uplift forces.

The rMSE of the formulas detailed in Chapter 2 is given in Table 6-1.

Model estimator	**rMSE($Fh_{0.1\%}$) (%)**	**rMSE($Fv(Fh_{0.1\%})$) (%)**
Jensen (1984)	89.5	115.9
Günback and Göcke (1984)	70.8	281.4
Pedersen (1996)	22.4	123.0
Martin et al. (1999)	40.6	51.1
Berenguer and Baonza (2006)	132.7	22.0
Nørgaard et al. (2013)	23.7	123.0

Table 6-1. rMSE (%) of existing formulas to estimate wave loads on crown walls on experimental data given in Chapter 3.

In this thesis, a set of new formulas was proposed to fit the experimental data given in Chapter 3. First, the representativeness of the design with ($Fh_{0.1\%}$, $Fv(Fh_{0.1\%})$) is analyzed. Second, a list of candidate variables that may influence forces on crown walls is defined. Third, new formulas are derived using statistical techniques. Finally, the results are discussed.

In order to characterize the representativeness of the design with ($Fh_{0.1\%}$, $Fv(Fh_{0.1\%})$), the crown wall stability against sliding considering only wave loads was analyzed for each test as follows:

- The failure function was calculated for each time step of 0.05 seconds as:

Eq. 6-1 $$S(t)=(W-Fv(t))\mu-Fh(t)$$

where $S(t)$ is the failure function at each time step, W is the crown wall weight, $Fv(t)$ is the up-lift wave force at each time step, μ is the friction coefficient between rock and concrete and $Fh(t)$ is the horizontal wave force at each time step. $S(t)\geq 0$ indicates the safety region.

- $S(t)$ values were ordered from greater to lower, thus obtaining the most unfavorable case for the test, i.e. the smallest $S(t)$ from now on referred to as Sd.
- On the other hand, the experimental values for $Fh_{0.1\%}$ and $Fv(Fh_{0.1\%})$ were obtained, and the failure function $S_1=(W-Fv(Fh_{0.1\%}))\mu-Fh_{0.1\%}$ was calculated.
- Therefore, the parameter $(Sd-S_1)/Fh_{0.1\%}$ was obtained. If $(Sd-S_1)/Fh_{0.1\%}\geq 0$, then the ($Fh_{0.1\%}$, $Fv(Fh_{0.1\%})$) estimator pair is on the safety side, since $S_1 < Sd$. This would indicate that during the tests there are at least one force pair ($Fh(t)$, $Fv(t)$) worse than ($Fh_{0.1\%}$, $Fv(Fh_{0.1\%})$).

The formulation of the sliding failure mode is very sensitive to the friction coefficient μ, a parameter that presents a great variability and which is also influenced by the constructive process. For this reason, different values of μ were analyzed to cover the most typical range of values (0.50, 0.55, 0.60, 0.65, 0.70).

Table 6-2 illustrates the probability of having $(Sd-S_1)/Fh_{0.1\%}\geq 0$ depending on the type of armor and μ after reanalyzing Molines (2011) data. Since at least in 91.9% of the tests the estimator was on the safety side, it is reasonable to obtain the forces $Fh_{0.1\%}$ and $Fv(Fh_{0.1\%})$.

μ	**Probability $(Sd-S_1)/Fh_{0.1\%}\geq 0$**
0.50	93.8%
0.55	92.8%
0.60	92.8%
0.65	91.9%
0.70	97.1%

Table 6-2. Probability that the design with ($Fh_{0.1\%}$, $Fv(Fh_{0.1\%})$) is the least favourable case.

6.2 Explanatory variables affecting crown wall stability

In this thesis, the following variables were considered as candidates that may influence crown wall stability (see Figure 6-3):

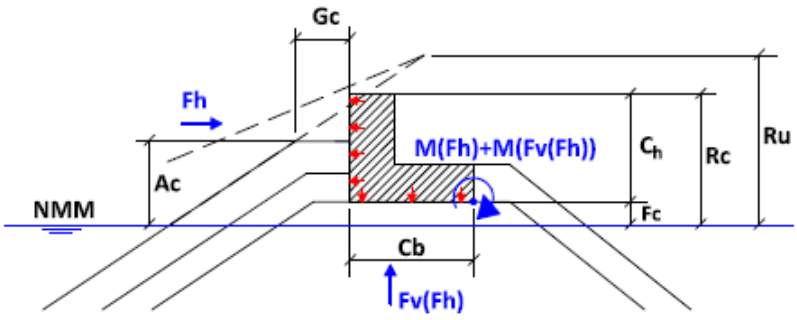

Figure 6-3. Variables affecting wave forces on crown walls.

- $\gamma_f R_{u0.1\%}/R_c$ relates the run-up level with the crown wall freeboard. It indicates if overtopping takes place and the higher level of water that reaches the crown wall. Similar variables are used by Pedersen (1996) or Martin et al. (1999) to consider the influence of the type of armor using the roughness factors derived by Smolka et al. (2009) as reduction factors on the run-up height. In this thesis, the approximation for run-up by Van der Meer and Stam (1992) was used.
- $(R_c\text{-}A_c)/C_h$ represents the crown wall area which is not protected by the crest berm. It is accepted in the literature that the area protected by the crest berm receives lower forces than unprotected areas. When $(R_c\text{-}A_c)/h_f=0$, the crown wall is completely protected by the armor units in the crest berm.
- $\sqrt{L_m/G_c}$ represents the relationship between the local wavelength using T_{01} and the crest berm width, similar to Pedersen (1996). Higher crest berms will lead to lower forces on the crown wall because more energy is dissipated in the holes.
- F_c/C_h represents the foundation level of the crown wall, which is similar to that included in Berenguer and Baonza (2006). Higher foundation levels will mean lower forces since the crown wall is farther from the sea water level. However, as the crest freeboard R_c is usually previously fixed to deal with overtopping requirements, higher F_c will also lead to a reduction in the crown wall height and hence a reduction in weight.

The forces were made dimensionless as follows:

- $Fh_{0.1\%}/(0.5\rho g C_h^2)$, dimensionless horizontal force.
- $Fv(Fh_{0.1\%})/(0.5\rho g C_h C_b)$, dimensionless horizontal force.

6.3 New formulas to estimate wave loads on crown walls

Figure 6-4.a and Figure 6-4.b illustrate the influence of $\gamma_f R_{u0.1\%}/R_c$ comparing cube and Cubipod armors with similar $(R_c\text{-}A_c)/C_h$. Both figures show that both R_u/R_c and the type of armor have an influence on the horizontal force: the higher the roughness factor, the greater the forces. Figure 6-4.c and Figure 6-4.d illustrate how wider crest berms lead to decreased forces on crown walls. The variables $(R_c\text{-}A_c)/C_h$ and F_c/C_h were not

continuous (only six values of $(R_c\text{-}A_c)/C_h$ and two values of F_c/C_h were tested) but it was observed that the higher the F_c/C_h or the lower the $(R_c\text{-}A_c)/C_h$, the lower the wave forces.

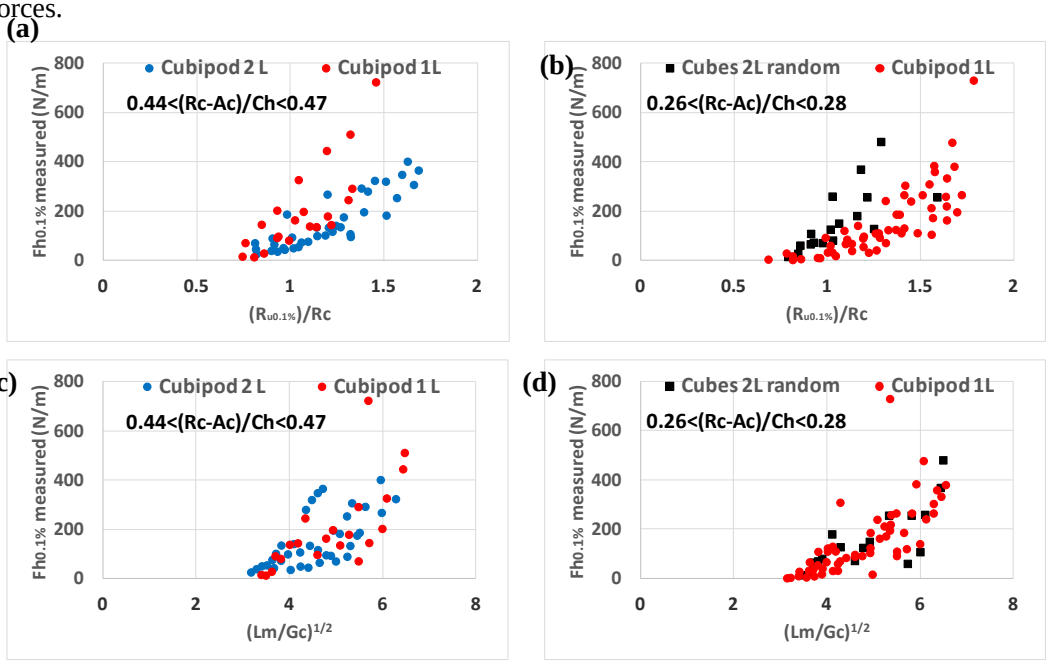

Figure 6-4. Influence of run-up, type of armor and crest berm width on horizontal forces.

The initial model proposed by Molines (2011) for horizontal and up-lift forces was based on the linear model given by:

Eq.6-2 $$\frac{Fh_{0.1\%}}{(0.5\rho g C_h^2)} = a_{\text{Eq.6-2}} + b_{\text{Eq.6-2}}\frac{\gamma_f R_{u0.1\%}}{R_c} + c_{\text{Eq.6-2}}\frac{(R_c-A_c)}{C_h} + d_{\text{Eq.6-2}}\sqrt{\frac{L_m}{G_c}} + e_{\text{Eq.6-2}}\frac{F_c}{C_h}$$

Eq.6-3 $$\frac{Fv(Fh_{0.1\%})}{(0.5\rho g C_h\, C_b)} = a_{\text{Eq.6-3}} + b_{\text{Eq.6-3}}\frac{\gamma_f R_{u0.1\%}}{R_c} + c_{\text{Eq.6-3}}\frac{(R_c-A_c)}{C_h} + d_{\text{Eq.6-3}}\sqrt{\frac{L_m}{G_c}} + e_{\text{Eq.6-3}}\frac{F_c}{C_h}$$

Molines (2010 and 2011) analyzed Eq.6-2 and Eq.**6-3** using the t-student test (5% significance error) to eliminate variables (only the variable F_c/C_h was eliminated from Eq.6-2). The result after the t-student test was used together with each dimensionless variable as input in a pruned neural network model (see Medina et al., 2002). The prediction of the pruned neural network model showed a quadratic relationship instead of the linear model defined in Eq.6-2 and Eq.**6-3**. After analyzing this again and using the same final topology as Molines (2010 and 2011), Eq. **6-4** and Figure 6-5 describe the central estimation of $Fh_{0.1\%}$ and $Fv(Fh_{0.1\%})$.

Eq. 6-4.a $$\frac{Fh_{0.1\%}}{(0.5\rho g C_h^2)} = \left(-1.29 + 1.80\frac{\gamma_f R_{u0.1\%}}{R_c} + 0.93\frac{(R_c-A_c)}{C_h} + 0.16\sqrt{\frac{L_m}{G_c}}\right)^2$$

Eq. 6-4.b $$\frac{Fv(Fh_{0.1\%})}{(0.5\rho g C_h\, C_b)} = \left(-0.86 + 0.75\frac{\gamma_f R_{u0.1\%}}{R_c} + 0.41\frac{(R_c - A_c)}{C_h} + 0.17\sqrt{\frac{L_m}{G_c}} - 0.9\frac{F_c}{C_h}\right)^2$$

Eq. 6-4.c $$R_{u0.1\%} = \begin{cases} 1.12 H_s \xi_{0m} & \xi_{0m} \le 1.5 \\ 1.34 H_s \xi_{0m}^{0.55} & \xi_{0m} \ge 1.5 \end{cases}$$ with a maximum $\frac{R_{u0.1\%}}{H_s} \le 2.58$

In Eq. **6-4**, γ_f [cube, 2 Layers randomly-placed] =0.50; γ_f [Cubipod, 1 Layer] =0.46 and γ_f [Cubipod, 2 Layers] =0.44, T_m was taken as T_{01}, $\xi_{0m} = tan\alpha/\sqrt{2\pi H_s/(gT_m{}^2)}$) and $L_m = \frac{gT_m{}^2}{2\pi} tanh\left(\frac{2\pi h}{L_m}\right)$. For single-peaked wave energy spectra with a spectral shape similar to JONSWAP spectra, $T_p \approx 1.2 * T_m$. Assuming a Gaussian error distribution, the confidence intervals of Eq. 6-4 can be estimated by:

Eq. 6-5.a $$\left.\frac{Fh_{0.1\%}}{(0.5\rho g C_h^2)}\right|_{5\%}^{95\%} = \left.\frac{Fh_{0.1\%}}{(0.5\rho g C_h^2)}\right|_{\text{Eq.6-4.}a} \pm 1.65\sqrt{MSE} = \left.\frac{Fh_{0.1\%}}{(0.5\rho g C_h^2)}\right|_{\text{Eq.6-4.}a} \pm 0.46$$

Eq. 6-5.b $$\left.\frac{Fv(Fh_{0.1\%})}{(0.5\rho g C_h\, C_b)}\right|_{5\%}^{95\%} = \left.\frac{Fv(Fh_{0.1\%})}{(0.5\rho g C_h\, C_b)}\right|_{\text{Eq.6-4.}b} \pm 1.65\sqrt{MSE} = \left.\frac{Fv(Fh_{0.1\%})}{(0.5\rho g C_h\, C_b)}\right|_{\text{Eq.6-4.}b} \pm 0.14$$

Figure 6-5 illustrates the cross-validation graph of Eq. 6-4 for the horizontal and up-lift forces. Table 6-3 gives the range of application of Eq. 6-4.

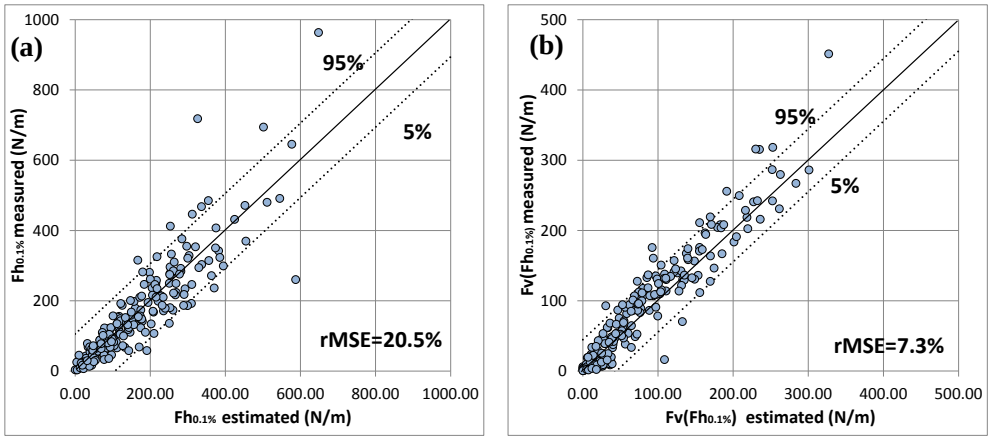

Figure 6-5. Cross-validation graphs with 90% confidence intervals of Eq. 6-4**.**

$$0.314 < \frac{\gamma_f R_{u0.1\%}}{R_c} < 0.938$$

$$0.067 < \frac{(R_c - A_c)}{C_h} < 0.589$$

$$3.134 < \sqrt{\frac{L_m}{G_c}} < 6.539$$

$$0.013 < \frac{F_c}{C_h} < 0.267$$

Table 6-3. Range of application of Eq. 6-4**.**

Although sliding is the most common type of failure for crown walls, to estimate the overturning moments the following considerations are proposed in this study:

- Overturning moments due to $Fh_{0.1\%}$: since the formula by Pedersen (1996) gives almost the same rMSE as Eq. **6-4**, it is assumed that the horizontal pressure distribution given by Pedersen (1996) should be representative of Eq. **6-4**. Thus, the methodology developed by Pedersen (1996) to calculate the overturning moments due to $Fh_{0.1\%}$ given by Eq. **2-17** is proposed here to estimate the overturning moments of $Fh_{0.1\%}$ calculated using Eq. **6-4**.
- Overturning moments due to $Fv(Fh_{0.1\%})$: a triangular up-lift pressure distribution is widely accepted in the literature. The same assumption is made here, so the overturning moment due to $Fv(Fh_{0.1\%})$ can be calculated as $2/3 * C_b * Fv(Fh_{0.1\%})$.

6.4 Methodology to design crown walls

To design the crown wall using Eq. 6-4, a general methodology is proposed. It may change depending on the specific constraints of each project:

- A_c, R_c and G_c are calculated to achieve the overtopping requirements. Eq. 5-8 can be used to estimate wave overtopping.
- Crown wall height (C_h), base width (C_b) and foundation level (F_c) are proposed depending on factors such as previous experience or sea water level.
- With the previous values and wave characteristics at the breakwater toe, horizontal and up-lift wave forces can be calculated using Eq. 6-4. Eq. 6-4 does not include hydrostatic pressure, which must be determined separately.
- Active and passive earth pressure of the armor units adjacent to the crown wall can be calculated using methods such as Rankine or Coulomb.
- Once the forces are calculated, the minimum weight of the crown wall can be obtained using Eq. 2-14 and Eq. 2-15 to evaluate the sliding and overturning failure modes, respectively. The safety factors required by the corresponding standards should be considered.

- The weight obtained in the previous step must be compared to the weight obtained with the initial crown wall geometry. If the initial geometry does not provide the required weight, the design process is started over but increasing C_h and/or C_b.
- Finally, the load transmitted from the crown wall to the foundation is checked to make sure it does not surpass the earth bearing capacity obtained, for example, with Brinch Hansen's formula.

The previous methodology assumes that a crown wall can be considered as monolithic. However, due to construction processes the crown wall may not be monolithic. In this case, different failure sections would appear and each rigid body would have to be independently analyzed (shear stress should not exceed material resistance in the concrete joint). Moreover, the global sliding failure through the breakwater core should be checked.

6.5 Discussion

The new formulas are easy to apply and are based on statistical analysis of dimensionless variables. Eq. 6-4 gives the best estimation on horizontal and up-lift forces at the same time. The fitted coefficients may differ if run-up estimators different from that specified by Van der Meer and Stam (1992) were used. Horizontal forces on crown walls agree quite well using formulas given in the literature. However, up-lift forces are influenced by parameters such as the permeability of the material below the foundation and the foundation level. Substantial differences are observed when estimating up-lift forces in Figure 6-2, usually skewed to higher values than those measured.

It is common practice to assume that the distribution of the up-lift pressures is triangular varying from a value different from zero at the seaward side to a zero value at the leeward side. The pressure at the seaward side is usually considered to be equal to the horizontal pressure at the lower edge of the vertical wall (pressure continuity law). Camus and Flores (2004) studied Alicante, Ferrol and Coruña breakwaters and reported that the previous hypothesis was conservative in some cases and the opposite in others. Nørgaard (2013) reported that higher up-lift forces than those measured are predicted when assuming the continuity law. For these authors the tests in which the triangular assumption highly overestimated the measurements, a high foundation level was also considered. Figure 6-6 illustrates that estimating the up-lift force assuming a triangular distribution with the pressure at the lower edge of the vertical wall highly overestimates the measured up-lift force in cases where $F_c/C_h \approx 0.26$. In those cases the measured up-lift force was almost three times lower than the estimated one. The foundation level significantly influences the up-lift forces and therefore, it must be explicitly considered as an input variable in prediction formulas. Eq. **6-4** explicitly includes the influence of the foundation level on the up-lift forces. Increasing SWL due to climate change can thus be very critical not only for horizontal forces but also for up-lift forces.

The crown wall weight is increased after force calculation to achieve the required safety factors against sliding and overturning failure modes. Hence, overestimating the up-lift forces certainly provides an extra safety margin but may lead to overly conservative designs. The method proposed in this research does not consider the continuity law but the measurements of up-lift forces. Due to the high dispersion in the results of up-lift forces, using the upper band of the confidence interval given by Eq. **6-5** is recommended for prior sizing of crown walls.

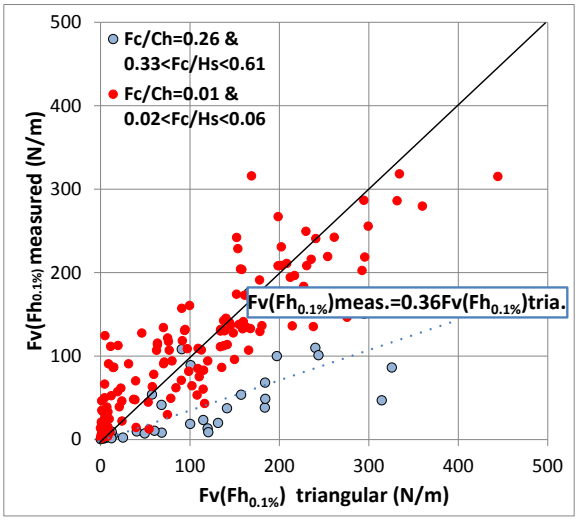

Figure 6-6. Comparison between measured and calculated up-lift force assuming triangular distribution with pressure at the seaward side is equal to the horizontal pressure at the lower edge of the vertical wall

Figure 6-7 compares the measured maximum up-lift force and the measured $Fv(Fh_{0.1\%})$, showing that values were similar in all tests.

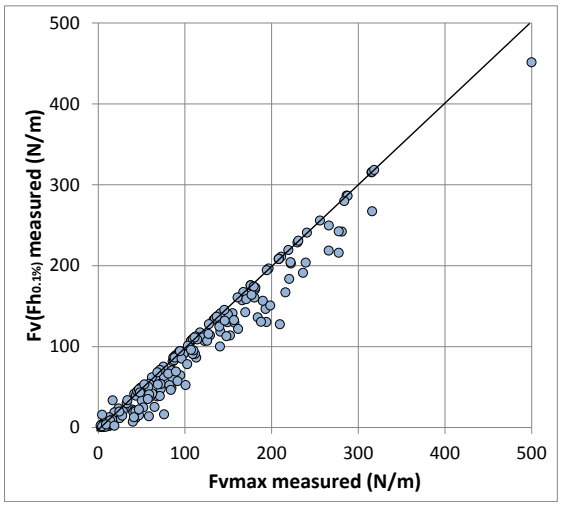

Figure 6-7. Comparison between maximum and Fv($Fh_{0.1\%}$) measured up-lift force.

The influence of the type of armor on wave loads on crown walls depicted in Figure 6-3 was included in Eq. **6-4** as a reduction factor of run-up. Figure 6-4 shows that higher forces are expected for cube armors than for Cubipod armors, which is consistent with overtopping behavior: the higher the roughness factor, the higher the forces on crown walls. If data for other type of armors were available, the methodology described in Chapter 4 may be applied to calibrate the roughness factors affecting the wave loads on crown walls.

Each formula should be carefully applied considering the limitations in application and the force percentile which is being estimated. Moreover, due to the high dispersion in results observed in Figure 6-2 and as indicated by Negro et al. (2013), using more than one formula for prior sizing of the crown wall and to verify the design with small-scale tests is recommended.

Chapter 7. Conclusions

7.1 Influence of rough slopes on overtopping

The methodology described in Chapter 4 can be applied to accurately estimate the roughness factor to be used in new formulas which include the γ_f as an input variable to estimate wave overtopping. For practical design applications, the γ_{f50}-calibrated roughness factors given in Table 4-1 can be used together with their corresponding formula to estimate wave overtopping discharges on mound breakwaters. The best estimations are given by CLASH NN. Armor porosity affects not only armor roughness and overtopping, but also armor hydraulic stability; recommended packing densities should be followed to avoid changes in porosity during lifetime. Designing an armor with porosity values higher than the recommended may decrease the roughness factors and the economic costs, but significant settlements should be expected during lifetime, thus changing the initial armor porosity affecting the armor stability and increasing estimated overtopping rates.

Simple overtopping formulas with fewer input variables are easy to use but more information is implicitly absorbed by the roughness factor. The γ_f is highly dependent on the corresponding formula and the dataset used for calibration. For instance, single- and double-layer Cubipod armors were tested with $A_c/R_c < 1$; therefore, Eq. 2-6, Eq. 2-9 and Eq. 2-13 which do not include A_c as an input variable, give unrealistic values of γ_f

for Cubipod armors compared to those given by CLASH NN, Eq. 2-11 and Eq. 5-8, which do include A_c as an input variable. The formula proposed by Smolka et al. (2009), the CLASH NN or Eq. 5-8 are recommended here to estimate overtopping discharges on Cubipod armors. Very low and disperse values of roughness factor were obtained for Dolos armors because of the low number of Dolos results in the database; significant changes in Dolos roughness factors are expected when more overtopping data are available for calibration.

The EurOtop (2007) overtopping predictor given by Eq. 2-6 and Eq. 2-9 requires increasing the roughness factor given by Bruce et al. (2006) to effectively improve the mean overtopping prediction reducing rMSE. Generally speaking, the formula by Van der Meer and Bruce (2014) gave slightly higher rMSE than Eq. (1) in the range of data used in this study ($0.5 \leq R_c/H_{m0} \leq 3.5$) which do not include zero and low crest freeboard cases.

The roughness factors given in Table 4-1 correspond to armors with characteristics described in Table 3-3. Cubes and Cubipods were analyzed in single- and double-layer armors: one layer systems had higher roughness factors and hence higher overtopping discharges. Initially, higher armor porosity ($p= 1 - \phi/n$) leads to a lower roughness factor but also to lower hydraulic stability and a higher risk of settlements during lifetime. Designing an armor with porosity above the recommended values will tend to generate settlements during lifetime, thus decreasing the initial armor porosity, changing the roughness factor and increasing overtopping rates. Thus, each type of armor must be designed and constructed with its recommended armor porosity and placement technique to maintain the reliability of the overtopping estimations.

The values of γ_{f10}, γ_{f50}, and γ_{f90} given in Table 4-1 indicate that overtopping estimations using γ_{f50} may easily change in the future from 10% to 25% if the dataset is significantly enlarged with additional tests. The relative crest freeboard (R_c/H_{m0}) affects the sensitivity of overtopping estimations to variations in the roughness factor; the higher the R_c/H_{m0}, the greater the influence of the increase in γ_f on the estimated overtopping discharges.

When comparing the influence of a concrete armor unit on overtopping discharges with different cross sections, the CLASHNN or Eq. 5-8 are recommended. Both showed the minimum rMSE in this study and eliminated the influence of certain structural variables on the estimation of the roughness factor, not included in other formulas. To avoid misunderstandings, the experimental database and the roughness factor should be clearly specified when new overtopping formulas are published.

7.2 Explicit overtopping estimator Q6

Chapter 5 describes a methodology to build-up a CLASH neural network-derived formula and confidence intervals to estimate mean overtopping discharge on conventional mound breakwaters. The new formula explicitly includes seven

explanatory dimensionless variables: γ_f given in Table 5-3, R_c/H_{m0}, $\xi_{0,-1}$, R_c/h, G_c/H_{m0}, A_c/R_c and λ_6 to consider the presence of a toe berm.

The 16 parameters of the new overtopping estimator *Q6* given by Eq. 5-8 were calibrated to minimize: (1) rMSE corresponding to conventional mound breakwaters in the CLASH database (CLdata), (2) rMSE corresponding to the overtopping predictions given by the CLASH neural network (NNdata) and (3) the number of significant figures. The final result is a consistent and robust overtopping formula which reasonably emulates the CLASH neural network predictions for mound breakwaters, with $rFPE_{Q6}$ (CLdata) = 12.7%. The 90% confidence interval for the overtopping estimations of *Q6* is given by Eq. 5-11.

A sensitivity analysis was carried out to determine the effect of geometrical changes on overtopping discharge. Four different scenarios were considered for an initial design: (1) higher structure freeboard (R_c and A_c); (2) higher crown wall freeboard (R_c); (3) higher armor crest freeboard (A_c) and (4) wider armor crest berm (G_c). An increase in both R_c and A_c was most efficient to decrease overtopping discharge followed by increasing only the R_c. A cost analysis should be carried out for each specific mound breakwater to determine the most cost-effective geometrical change to reduce overtopping, because geometrical changes in different variables may lead to considerable differences in cost, depending on the construction site and logistical constraints. *Q6* describes explicit relationships between input variables and overtopping discharge and hence it can be used during the design phase to identify cost-effective designs and to quantify the influence of variations on wave and structural parameters.

Compared to other overtopping models, *Q6* provides excellent results using CLdata and NNdata. The predictions of *Q6* are reasonably accurate in the design phase. The new overtopping formula *Q6*, valid for conventional mound breakwaters in non-breaking conditions, provides overtopping predictions similar to those given by the CLASH neural network; $rMSE_{Q6}$ [NNdata] = 5.1%. The CLASH neural network does provide slightly better estimations; however, it is a "black-box". By contrast, the new formula explicitly describes the influence of the γ_f and the seven dimensionless variables (X_1 to X_7) on dimensionless overtopping (Q). Overtopping discharge on conventional mound breakwaters is greater if (1) R_c/H_{m0} decreases; (2) $\xi_{0,-1}$ increases; (3) R_c/h increases; (4) G_c/H_{m0} decreases, or (5) A_c/R_c decreases. The overtopping discharge is somewhat lower when placing a toe berm (B_t>0). Additionally, the higher the armor roughness (γ_f), the greater the overtopping discharge.

7.3 Crown wall stability

Chapter 6 describes the analysis of wave loads on crown walls. Two new formulas are derived with their confidence intervals to calculate horizontal and up-lift forces on crown walls of cube- and Cubipod-armored breakwaters. The formulas are developed to estimate the horizontal force exceeded by 1 out of 1000 waves ($Fh_{0.1\%}$) and the maximum up-lift force caused by the same wave $Fv(Fh_{0.1\%})$. The new estimators

explicitly include the effect of four dimensionless variables: (1) γ_f $R_{u0.1\%}/R_c$, (2) $(R_c-A_c)/C_h$, (3) $\sqrt{L_m/G_c}$ and (4) F_c/C_h.

The type of armor is introduced using the concept of roughness factor. Higher forces are expected for cube armors than for Cubipod armors, which is consistent with overtopping behavior: the higher the roughness factor, the higher the wave overtopping and forces on crown walls.

For each test, the sliding failure function was evaluated using the measured forces pair ($Fh_{0.1\%}$, $Fv(Fh_{0.1\%})$) and compared to the instantaneous sliding failure value. Since the sliding failure is very sensitive to the friction coefficient μ, five values were considered (0.50, 0.55, 0.60, 0.65, 0.70). At least in 91.9% of the tests, the design with ($Fh_{0.1\%}$, $Fv(Fh_{0.1\%})$) is on the safe side.

The new force estimators given by Eq. **6-4** are easy to apply and provide the lowest rMSE on both horizontal and up-lift forces. Since Pedersen (1996) formula gives an rMSE similar to Eq. **6-4** for $Fh_{0.1\%}$, the method given by Pedersen (1996) to evaluate the overturning moment due to horizontal forces is proposed here after calculating the horizontal force with Eq. **6-4**. To calculate the overturning moment due to up-lift forces, a triangular distribution is proposed as widely accepted in the literature.

The comparison of existing formulas to estimate wave loads on crown walls with 2D experimental data agreed quite well for horizontal forces but not for up-lift forces, usually skewed to larger values. Nørgaard (2013) pointed out that larger than measured up-lift forces are predicted if assuming the pressure continuity law between the vertical wall and base wall. The crown wall weight is increased after force calculation to achieve the required safety factors to prevent sliding and overturning failure modes, among others. Hence, overestimating the up-lift forces certainly provides an extra safety margin but may lead to overly conservative designs. The method proposed in this thesis does not consider the continuity law but the measurements of up-lift forces.

The foundation level has a significant influence on the up-lift forces and therefore, it should be explicitly considered as input variable in prediction formulas. Eq. **6-4** explicitly includes the influence of the foundation level on the up-lift forces. Increasing SWL due to climate change can thus be very critical not only for horizontal forces but also for up-lift forces.

Each formula should be carefully applied considering the limitations in their application and the force percentile which is being estimated. Moreover, due to the high dispersion in results and also as pointed out by Negro et al. (2013), using more than one formula for prior sizing of the crown wall and verify the design with small-scale tests is recommended. One should also consider that due to constructive process the crown wall may not be monolithic. In that case, different failure sections would appear and each rigid body should be independently analyzed.

7.4 Future research

Breaking waves are present in many coastal structures and must be carefully treated. Future research will help to extend and modify the formulas given in this thesis to breaking waves. Part of wave energy is dissipated during the breaking process, so it should be expected lower overtopping rates and wave forces on the crown wall. Both physical and numerical modelling will help to better understand the influence of wave breaking on wave hydrodynamics.

Although scaling the core to represent the flow characteristics inside the porous media (as usual procedure given by specific scaling laws), further research in larger scale tests is necessary to better assess the up-lift pressures on the crown wall base. The calculation of overturning moments due to forces proposed in this thesis should be verified as well.

The influence of the type of armor on wave loads on crown walls has been included using the roughness factor but more tests are necessary to extrapolate the findings to other concrete armor units. The methodology described in Chapter 4 using bootstrapping can be used to characterize the roughness factors corresponding to wave force formulas.

Earth pressure due to the armor layer on the crown wall is usually considered assuming geotechnical laws that are specifically developed for soil materials. However, armor units can be considered as individual rigid bodies which push or hit the crown wall. Armor units on the crest berm should be supported by the crown wall but they can get separated of the wall during lifetime and hit the crown wall as consequence of wave attack. Further research on the interaction between armor units and the crown wall considering the static and dynamic forces of each armor unit and using finite element methods will help to better understand their interaction.

Wave overtopping and wave forces on crown walls are consequence of the same physical phenomena, and hence both must be dependent on almost the same geometrical and wave conditions. The interaction between wave overtopping and wave loads can help to better understand the hydrodynamics of both phenomena. Using the formulas proposed in the present thesis, a deeper analysis can be conducted to correlate both phenomena.

References

Ahrens, J.P., and Heimbaugh, M.S., 1988. Seawall Overtopping Model, Proceedings of the 21st International Conference on Coastal Engineering, ASCE, pp. 795-806.

Aminti, P., and Franco, L., 1988. Wave overtopping on rubble mound breakwaters. Proceedings 21st International Conference on Coastal Engineering, ASCE, Vol. 1, pp. 770-781.

Avaneendran, A., Sannasiraj, S.A., and Vallam, S., 2013. Pressures on the Crown Wall of Breakwater Formed by New Armor Block KOLOS due to Regular Waves. Journal of Waterway, Port, Coastal and Ocean Engineering, 139, 518-526.

Barron, A., 1984. Predicted squared error. A criterion for automatic model selection. In S. Farlow (ed.), Self-Organizing Methods in Modelling, Marcel Dekker, 87-103.

Battjes, J.A., and Groenendijk, H.W., 2000. Wave height distributions on shallow foreshores. Coastal Engineering, 40, 161–182.

Berenguer, J.M., and Baonza, A., 2006. Diseño del espaldón de los diques rompeolas. Libro de ponencias del II Congreso Nacional de la Asociación Técnica de Puertos y Costas, pp. 35-56 (in Spanish).

Besley, P., 1999. Overtopping of sea-walls-design and assessment manual. R & D Technical Report 178, Environment Agency, Bristol, UK.

Bradbury, A.P., and Allsop, N.W.H., 1988. Hydraulic effects of breakwater crown walls. Design of Breakwaters, ICE, Thomas Telford, 385-396.

Bruce, T., Van der Meer, J.W., Franco, L., and Pearson, J.M., 2006. A comparison of overtopping performance of different rubble mound breakwater armour. Proceedings 30th International Conference on Coastal Engineering, World Scientific, Vol. 5, pp. 4567-4579.

Bruce, T., Van der Meer, J.W., Franco, L., and Pearson, J.M., 2009. Overtopping performance of different armour units for rubble mound breakwaters. Coastal Engineering, 56 (2), 166-179.

Burcharth, H.F., 1993. The design of breakwaters. Internal Report, Aalborg University.

Burcharth, H.F., Liu, Z., and Troch, P., 1999. Scaling of core material in rubble mound breakwater model tests. Proceedings COPEDEC V conference, pp. 1518-1528.

Burcharth, H. F., Andersen, L., and Lykke-Andersen, T., 2008. Analysis of Stability of Caisson Breakwaters on Rubble Foundation Exposed to Impulsive Loads. Proceedings 31st International Conference on Coastal Engineering, World Scientific, pp. 3606-3618.

Burcharth, H.F., Lykke-Andersen, T., and Lara, J.L., 2014. Upgrade of coastal defense structures against increased loadings caused by climate change: A first methodological approach. Coastal Engineering, 87, 112-121.

Camus, P., and Flores, J., 2004. Wave forces on crown walls: Evaluation of existing empirical formulae. Proceedings 29th International Conferences on Coastal Engineering, World Scientific, pp. 4087-4099.

Chini, N., and Stansby, P.K., 2012. Extreme values of coastal wave overtopping accounting for climate change and sea level rise. Coastal Engineering, 65, 27 -37

Coeveld, E.M., Van Gent, M.R.A., and Pozueta, B., 2005. Neural Network, Manual NN_OVERTOPPING 2.0, CLASH: Workpackage 8, http://nn-overtopping.deltares.nl/ (Accessed: July, 2013).

Crest Level Assessment of coastal Structures by full scale monitoring, neural network prediction and Hazard analysis on permissible wave overtopping, http://www.clash.ugent.be/ (Accessed: July, 2013).

Dupray, S., and Roberts, J., 2009. Review of the use of concrete in the manufacture of concrete armour units. Proceedings of Coasts, Marine Structures and Breakwaters 2009, ICE, Thomas Telford Ltd., Vol 1, 260-271 and 298-299.

Etemad-Shahidi, A., and Jafari, E. 2014. New formulae for prediction of wave overtopping at inclined structures with smooth impermeable surface. Ocean Engineering, 84, 124-132.

EurOtop, 2007. Wave Overtopping of Sea Defences and Related Structures: Assessment Manual (EurOtop Manual). Pullen, T., Allsop, N.W.H., Bruce, T., Kortenhaus, A., Schüttrumpf, H., Van der Meer, J.W. Environment Agency, UK/ENW Expertise Netwerk Waterkeren, NL/KFKI Kuratorium für Forschung im Küsteningenieurwesen, Germany, http:// www.overtopping-manual.com (Accessed: July, 2013).

Figueres, M., and Medina, J.R., 2004. Estimating incident and reflected waves using a fully nonlinear wave model. Proceedings 29th International Conference on Coastal Enigneering, World Scientific, pp. 594-603.

Garrido, J.M., and Medina, J.R., 2012. New neural-network derived empirical formulas for estimating wave reflection on Jarlan-type breakwaters. Coastal Engineering, 62 (1), 9-18.

Grau, J.I., 2008. Experiencias en obras portuarias. Recomendaciones para el diseño y la ejecución. III Congreso Nacional de la Asociación Técnica de Puertos y Costas, Puertos del Estado, pp. 13-60 (in Spanish).

Günback, A.R., and Göcke, T., 1984. Wave screen stability of rubble mound Breakwaters. International Symposium of Maritime Structure in the Meditarrean Sea, pp. 2099-2112.

Hamilton, D.G., and Hall K.R., 1992. Preliminary analysis of the stability of rubble mound breakwater crown walls. Proceedings 23rd International Conferences on Coastal Engineering, ASCE, pp. 1217-1230.

Hebsgaard, M., Sloth, P., and Juul, J., 1998. Wave overtopping of rubble mound breakwaters. Proceedings 26th International Conference on Coastal Engineering. ASCE, Vol. 3, pp. 2235-2248.

Hudson, R.Y., 1959. Laboratory investigations of rubble-mound breakwater. Journal of Waterways and Harbors Division, 89(WW3), 260-271.

IPCC, 2013. Climate Change 2013: The Physical Science Basis. Contribution of Working Group I to the Fifth Assessment Report of the Intergovernmental Panel on Climate Change [Stocker, T.F., D. Qin, G.-K. Plattner, M. Tignor, S.K. Allen, J. Boschung, A. Nauels, Y. Xia, V. Bex and P.M. Midgley (eds.)]. Cambridge University Press, Cambridge, United Kingdom and New York, NY, USA, 1535 pp.

Iribarren, R., and Nogales, C., 1954. Obras Marítimas: Oleaje y Diques. Editorial Dossat Madrid, Spain (in Spanish).

Isobe, M., 2013. Impact of global warming on coastal structures in shallow water. Ocean Engineering, 71, 51-57.

Jafari, E., and Etemad-Shahidi, A., 2012. Derivation of a new model for prediction of wave overtopping at rubble mound structures. Journal of Waterway, Port, Coastal, and Ocean Engineering, 138 (1), 42-52.

Jensen, O. J., 1984. A monograph of rubble mound breakwaters. Danish Hydraulic Institute, Hórsholm, Denmark.

Kobayashi, N., de los Santos, F.J., and Kearney, P.G., 2008. Time-averaged probabilistic model for irregular wave runup on permeable slopes. Journal of Waterway, Port, Coastal and Ocean Engineering, 134 (2), 88–96.

Kortenhaus, A., Vloebergh, H., Weymeis, M., De Rouck, J., Gallach-Sánchez, D., and Troch, P., 2014. Improved understanding of stability and overtopping performance of single layer Haro blocks on rubble mound breakwaters. Proceedings 5th International Conference on the Application of Physical Modelling to Port and Coastal Protection, Vol. 1, pp. 279-288.

Koza, J.R., 1992. Genetic Programming: On the programming of computers by means of natural selection, MIT Press. ISBN: 0-262-11189-6.

Lykke-Andersen, T., and Burcharth, H.F., 2004. D24 Report on additional tests Part A: Effect of obliqueness, short-crested waves and directional spreading. CLASH: Workpackage 4, http://www.clash.ugent.be/ (Accessed: December 2014).

Lykke-Andersen, T., and Burcharth, H.F., 2009. Three-dimensional investigations of wave overtopping on rubble mound structures. Coastal Engineering, 56, 180-189.

Martín, F. L., Vidal, C., Losada, M.A., and Medina, R., 1995. Un método para el cálculo de las acciones del oleaje sobre los espaldones de los diques rompeolas. Ingeniería del agua, 2(3), 37-52.

Martín, F. L., Losada, M. A., and Medina, R., 1999. Wave loads on rubble mound breakwater crown walls. Coastal Engineering, 37, 149-174.

Medina, J.R., González-Escrivá, J.A., Garrido, J.M., and de Rouck, J., 2002. Overtopping analysis using neural networks. Proceedings 28th International Conference on Coastal Engineering, World Scientific, Vol. 2, pp. 2165-2177.

Medina, J.R., Molines, J., and Gómez-Martín, M.E., 2014. Influence of Armour Porosity on the Hydraulic Stability of Cube Armour Layers. Ocean Engineering, 88, 289-297.

Molines, J., and Medina J.R., 2010. Overtopping and Wave Forces on Crown Walls of Cube and Cubipod Armoured Breakwaters, Proceedings 3rd International Conference on the Application of Physical Modelling to Port and Coastal Protection, p. 8 Paper No. 24/ structures.

Molines, J., 2011. Stability of Mound Breakwater Crown Walls armoured with Cubes and Cubipods, PIANC e-Magazine On Course 143, 29-41.

Molines, J., Pérez, T.J., Zarranz, G., and Medina, J.R., 2012. Influence of cube and Cubipod® armor porosities on overtopping. Proceedings 33rd International Conference on Coastal Engineering, Coastal Engineering Research Council (ASCE), Paper No. 43/structures (Online).

Molines, J., and Medina, J.R., 2015. Calibration of overtopping roughness factors for concrete armor units in non-breaking conditions using the CLASH database. Coastal Engineering, 96, 62-70.

Molines, J., and Medina, J.R., accepted. Explicit wave overtopping formula for mound breakwaters with crown walls using CLASH neural network-derived data. Journal of Waterway, Port, Coastal and Ocean Engineering, 10.1061/(ASCE)WW.1943-5460.0000322

Negro, V., López, J.S., and Polvorinos, J.I., 2013. Comparative study of breakwater crown wall-calculation methods. Maritime Engineering, 166, 25-41.

Negro, V., López, J.S., Polvorinos, J.I., Molines, J., 2014. Discussion: Comparative study of breakwater crown wall – calculation methods, Maritime Engineering, Proceedings of the ICE, 154-155.

Nørgaard, J.Q.H., Andersen, L.V., Andersen, T.L., and Burcharth, H.F., 2012. Displacement of monolithic rubble-mound breakwater crown-walls. Proceedings 33rd International Conference on Coastal Engineering, Coastal Engineering Research Council (ASCE), Paper No. 7/structures (Online).

Nørgaard, J.Q.H., 2013. Upgrade and design of coastal structures exposed to climate changes. Ph.D. Thesis. Aalborg University. Denmark.

Nørgaard, J.Q.H., Lykke-Andersen, T., and Burcharth, H.F., 2013. Wave loads on rubble mound breakwater crown walls in deep and shallow water conditions. Coastal Engineering, 80, 137-147.

Owen, M.W., 1980. Design of seawalls allowing for wave overtopping. HR Wallingford, Report EX 924.

Pearson, J., Bruce, T., Franco, L., Van der Meer, J., Falzacappa, M., and Molino, R., 2004. Report on additional tests, part B: Standard tests for roughness factors, CLASH WP4 report, University of Edinburgh, UK.

Pedersen, J., and Burchart, H.F., 1992. Wave Forces on Crown Walls. Proceedings 23rd International Conference on Coastal Engineering, ASCE, pp. 1489-1502.

Pedersen, J., 1996. Wave forces and overtopping on crown walls of rubble mound breakwaters. Series paper 12, Hydraulic and Coastal Engineering Laboratory, Department of Civil Engineering, Aalborg University, Denmark.

Polvorinos, J.I., 2013. Cálculo de espaldones en diques rompeolas. Estudio comparativo de las formulaciones actuales y propuesta de una nueva metodología. Ph.D. Thesis. Madrid Polytechnic University. Spain.

Silva, R., Govaere, G., and Martín F., 1998. A statistical tool for breakwater design. Proceedings 26th International Conference on Coastal Engineering, ASCE, pp. 1921-1933.

Smolka, E., Zarranz, G., and Medina, J.R., 2009. Estudio Experimental del Rebase de un Dique en Talud de Cubípodos. Libro de las X Jornadas Españolas de Costas y Puertos, Universidad de Cantabria-Adif Congresos, pp. 803-809 (in Spanish).

Stewart, T.P., Newberry, S.D., Simm, J.D., and Latham, J.P., 2002. The hydraulic performance of tightly packed rock armour layers. Proceedings 28th International Conference on Coastal Engineering. World Scientific, Vol. 2, pp. 1449–1471.

TAW, 2002. Technical report wave run-up and wave overtopping at dikes. Technical Advisory Committee on Water Defences in The Netherlands. Government Publishing Office, The Hague, The Netherlands.

U.S. Army Corps of Engineers. USACE, 2002. Coastal Engineering Manual. Engineer Manual 1110-2-1100. U.S. Army Corps of Engineers, Washington, D.C. (in 6 volumes).

Van der Meer, J.W., and Stam, C.J.M., 1992. Wave run-up on smooth and rock slopes. Journal of Waterway, Port, Coastal, and Ocean Engineering, 188 (5), 534–550.

Van der Meer, J.W., 1993. Conceptual design of rubble mound breakwaters, Report No. 483, Delft Hydraulics, The Netherlands.

Van der Meer, J.W., and Janssen, J.P.F.M., 1994. Wave Run-Up and Wave Overtopping at Dikes, Delft Hydraulics No. 485.

Van der Meer, J.W., Verhaeghe, H., and Steendam, G.J., 2009. The new wave overtopping database for coastal structures. Coastal Engineering, 56 (2), 108-120.

Van der Meer, J.W., and Bruce, T., 2014. New Physical Insights and Design Formulas on Wave Overtopping at Sloping and Vertical Structures. Journal of Waterway, Port, Coastal and Ocean Engineering, 140 (6), 04014025.

Van Doorslaer, K., De Rouck, J., Audenaert, S., and Duquet, V., 2015. Crest modifications to reduce wave overtopping of non-breaking waves over a smooth dike slope. Coastal Engineering, http://dx.doi.org/10.1016/j.coastaleng.2015.02.004 (in press).

Van Gent, M.R.A., Van den Boogaard, H.F.P., Pozueta, B., and Medina, J.R., 2007. Neural network modelling of wave overtopping at coastal structures. Coastal Engineering, 54 (8), 586–593.

Verhaeghe, H., Van der Meer, J.W., Steendam, G.J., Besley, P., Franco, L., and Van Gent, M.R.A., 2003. Wave overtopping database as the starting point for a neural network prediction method. Proceedings Coastal Structures 2003. ASCE, pp. 418–430.

Verhaegue, H., 2005. Neural Network Prediction of Wave Overtopping at Coastal Structures. Ph.D. Thesis. Gent University, Belgium.

Victor, L. and Troch, P., 2012. Wave overtopping at smooth impermeable steep slopes with low crest freeboards. Journal of Waterway, Port, Coastal, and Ocean Engineering, 138 (5), 372-385.

Wolters, G., Van Gent, M.R.A., Hofland, B., and Wellens, P., 2014. Wave damping and permeability scaling in rubble mound breakwaters. Proceedings 5th International Conference on the Application of Physical Modelling to Port and Coastal Protection, pp. 344-353.

Notations and acronyms

a_j = parameters used in formulas. i indicates number of the equation*;*

A_c = armor crest freeboard;

α = slope angle of the breakwater;

β = angle of wave attack;

b_j = parameters used in formulas. i indicates number of the equation*;*

B = width of the intermediate berm;

B_t = width of the toe berm;

c_j = parameters used in formulas. i indicates number of the equation*;*

cotα = slope of the breakwater without intermediate berm;

cotα_b = slope of the intermediate berm;

cotα_d = slope of the breakwater downward from the intermediate berm;

cotα_u = slope of the breakwater upward from the intermediate berm;

C_b = length of the crown wall base;

C_h = crown wall height;

Cr = reduction factor given by Besley (1999);

CF = complexity factor given in CLASH;

CV = coefficient of variation;

D_n = nominal diameter;

ϕ = packing density;

γ_f = roughness factor;

γ_β = obliquity factor;

$Fh_{0.1\%}$ = horizontal force exceeded by 1 out of 1000 waves;

$Fv(Fh_{0.1\%})$ = up-lift force from the wave that produces $Fh_{0.1\%}$;

F_c = foundation level;

g = gravity acceleration: g=9.81 m/s^2;

G_c = armor crest berm width;

h = water depth in front of the breakwater;

h_b = water depth on the intermediate berm;

h_t = water depth at the toe of the structure;

H_{m0} = significant wave height from spectral analysis: $H_{m0} = 4(m_0)^{1/2}$;

H_s = significant wave height;

$\xi_{0,-1}$ = Ir = Iribarren's number based on H_{m0} and $L_{0,-1}$: $\xi_{0,-1} = Ir = T_{-1,0}/\cot\alpha[2\pi H_{m0}/g]^{1/2}$;

ξ_{0p} = Iribarren's number based on H_{m0} and L_{0p} : $\xi_{0p} = T_p/\cot\alpha[2\pi H_{m0}/g]^{1/2}$;

ξ_{0m} = Iribarren's number based on H_{m0} and L_{0m} : $\xi_{0m} = T_m/\cot\alpha[2\pi H_{m0}/g]^{1/2}$;

ξ_0 = Iribarren's number for regular waves based on H and L_0: $\xi_0 = T/\cot\alpha[2\pi H/g]^{1/2}$;

λ_j = explanatory terms corresponding to the variables X_j (j=1 to 6);

L = local wavelength for regular waves;

L_m = local wavelength at the toe of the structure using T_m, $L_m = \frac{gT_m^2}{2\pi} tanh\left(\frac{2\pi h}{L_m}\right)$;

L_p = local wavelength at the toe of the structure using T_p, $L_p = \frac{gT_p^2}{2\pi} tanh\left(\frac{2\pi h}{L_p}\right)$;

L_{0m} = deep water wave length based on T_m: $L_{0m} = g\,T_m^2/(2\pi)$;

$L_{0,-1}$ = deep water wave length based on $T_{-1,0}$: $L_{0,-1} = g\,T_{-1,0}^2/(2\pi)$;

L_{0p} = deep water wave length based on T_p: $L_{0p} = g\,T_p^2/(2\pi)$;

μ = friction factor between concrete and rock;

m_i = ith spectral moment defined as $m_i = \int_0^\infty f^i S(f)df$ (i=1, 2, ….);

π = pi number: π =3.14159;

p = porosity;

q = mean overtopping discharge per meter of structure width;

Q_{CLNN} = overtopping estimations by the CLASH neural network to develop the explanatory terms in Chapter 5;

Qj = overtopping estimator after introducing each X_j; $Qj = Q(X_1,\ldots,X_j)$ with j=2 to 6;

$Q_{EurOtop}$ = dimensionless mean overtopping discharge given by EurOtop (2007), Eq. **2-6** and Eq. 2-9;

Q_{JE} = dimensionless mean overtopping discharge given by Jafari and Etemad-Shahidi (2012),Eq. **2-12**;

Q_{SZM} = dimensionless mean overtopping discharge given by Smolka et al. (2009), Eq. 2-11;

Q_{VMB} = dimensionless mean overtopping discharge given by Van der Meer and Bruce (2014), Eq. 2-13;

Q_{VMJ} = dimensionless mean overtopping discharge given by Van der Meer and Janssen (1994), Eq. **2-6**;

$rMSE_e$ *(o)* = relative mean squared error when using estimator "e" and a group of target data "o";

rFPE = relative final prediction error;

R_c = crown wall freeboard;

RF = reliability factor given in CLASH;

s = directional spreading;

$s_{0,-1}$ = wave steepness based on H_{m0} and $L_{0,-1}$;

s_{0p} = wave steepness based on H_{m0} and L_{0p};

s_{0m} = wave steepness based on H_{m0} and L_{0m};

T_{01} = mean spectral period defined as $T_{01} = m_0/m_1$;

$T_{-1,0}$ = energy spectral period defined as $T_{-1,0} = m_{-1}/m_0$;

T_p = peak period;

W = crown wall weight;

WF = weight factor used in error calculations;

X_j = dimensionless variables analyzed to create the overtopping estimator (j=1 to 7).

Acronyms

CLASH = EU-Project Crest Level Assessment of coastal Structures by full scale monitoring, neural network prediction and Hazard analysis on permissible wave overtopping;

CLASH NN = CLASH Neural Network given by Van Gent et al. (2007);

CLdata = measured overtopping discharges on selected datasets from CLASH database and Cubipod® data with $\beta=0^o$;

CMBW = conventional mound breakwater with crown wall (see Figure 2-1);

FPE = final prediction error;

MSE = mean squared error;

NNdata = predicted overtopping discharges on CLdata by the CLASH NN.

Figure list

Table list

Appendix 1: application example

Given a double-layer cube armored mound breakwater with toe berm (ht(m)=9 and Bt(m)=4), cotα=1.5, h(m)=12, ρ(kg/m^3)=1025 and the following wave conditions: β=0º; *Hs(m)*=H_{m0}(m)=4.5; $T_{-1,0}$(s)=9 and T_m*(s)=8.25* (see Figure 2-1 and Figure 6-3), the steps below are a possible workflow to estimate wave overtopping and wave forces on crown walls using the formulas developed in this thesis:

(1) Using Hudson's formula (1959), the armor size is given by W(t) = $(2.3*4.5^3)/(6*(2.3/1.025-1)^3*1.5) \approx 12$ with Dn(m)=1.74. As common procedure, three armor units are considered on the crest berm, Gc(m)=3*Dn=5.22.

(2) The crest freeboard is firstly considered as Rc(m)=1.5*Hs=6.75 as common practice when few overtopping is allowed. Moreover, the armor crest freeboard is considered as Ac(m)=Rc(m)=6.75 to reduce wave overtopping and protect the crown wall.

(3) Wave overtopping is calculated using Eq. 5-8 with $\xi_{0,-1}$*=3.53* and γ_f = 0.51 as $Q=q/(9.81*H_{m0}{}^3)^{0.5}=\exp(\lambda_2*\lambda_3*\lambda_4*\lambda_5*\lambda_6*(-1.6-2.6*6.75/(4.5*0.51))=$ $\exp(0.984*1.000*1.001*1.000*1.000*(-9.247))=1.115*10^{-4}$ and q(l/s/m)=3.333. If this discharge is under the tolerable overtopping discharge for the structure, step (4) can be followed. If not, wave overtopping should be reduced.

(4) Considering a foundation level of *Fc(m)*=1 to provide dry conditions during construction and a length of the crown wall base of *Cb(m)*=5, wave forces can be calculated using Eq. **6-4** and γ_f = 0.50. The values of the other variables are *Ch(m)=Rc(m)-Fc(m)*=5.75; *Lm(m)*=78.89 (local wavelength); ξ_{0m}=3.24 and $R_{u0.1\%}$*(m)*=11.51 (run-up). The central estimation of the forces is $Fh_{0.1\%}$*(kN/m)*= 124.92 and *Fv(*$Fh_{0.1\%}$*) (kN/m)*=11.66. As proposed in chapter 6 the upper

confidence interval of the up-lift force is proposed for prior sizing of the crown wall as $Fv(Fh_{0.1\%})]_{95\%}$ *(kN/m)=31.90.*

(5) Overturning moments are calculated as proposed in Chapter 6, $M(Fh_{0.1\%})$ *(kN*m/m)*=395.05 and $M(Fv(Fh_{0.1\%})]_{95\%})$ *(kN*m/m)*=106.31.

(6) Using the external forces and overturning moments (due to waves and earth pressure) and the stabilizing forces (due to crown wall weight defined by *Ch* and *Cb*), sliding and overturning safety factors can be calculated as given by Eq. 2-14 and Eq. 2-15. If the desired safety factors are not achieved, *Fc* and *Cb* can be modified to increase crown wall weight (step (4)) and/or variables such as *Rc*, *Ac* or *Gc* can be modified to reduce wave forces (and overtopping).

(7) Figure below illustrates the influence of increasing *Rc* on wave overtopping and wave forces: Eq. 5-8 and Eq. **6**-**4** can be used to analyze the influence of variations on specific variables.

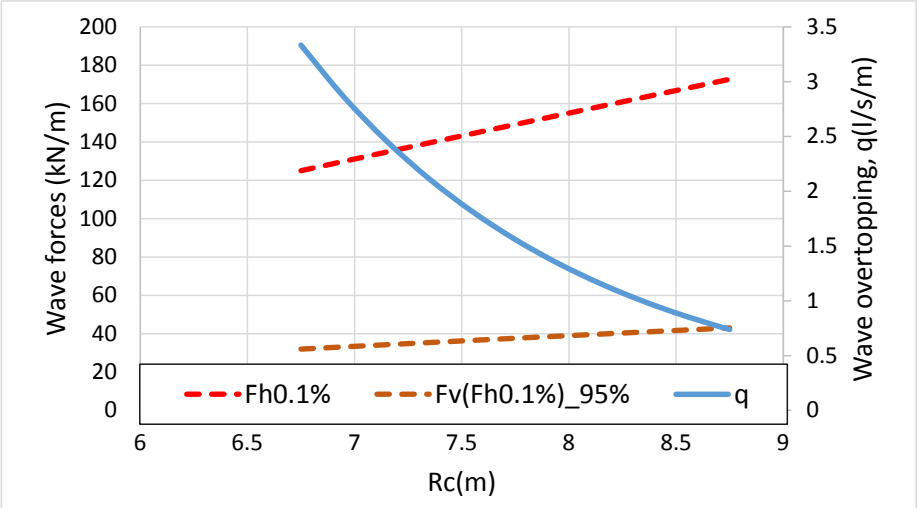

Figure A1-1. Influence of variations of *Rc* on wave overtopping and wave forces on crown walls.